University of Stavanger

FACULTY OF SCIENCE AND TECHNOLOGY

MASTER'S THESIS

Study programme/specialization: Petroleum Engineering/ Drilling Technology	Spring semester, 2018 Open
Author: Kim Huy Nguyen	…….. (Signature of author)
Programme coordinator: Supervisor(s): Mesfin Belayneh.	
Title of master's thesis: **Effect of 15nm SiO_2 Nanoparticles on Enhanced Oil Recovery and Drilling Fluid: Experimental and Simulation studies**	
Credits: 30	
Keywords: Drilling fluid EOR Silica nanoparticle (SiO_2) Rheological properties Tribology Viscoelasticity IFT Contact angle	Number of pages: 101 + Supplemental material/other: 18 Stavanger, 15 – 06 – 2018

ACKNOWLEDGEMENTS

First of all, I would like to give my deepest appreciation for the invaluable guidance from my supervisor of this thesis, Professor Mesfin Belayneh from the University of Stavanger. As the supervisor, he encouraged me to fulfil the project about improving oil recovery, as well as he personally and economically invested to allow the core flooding experiments to be executed at IRIS. Throughout the whole period of writing the thesis he was always available at the office, and even joined and advised the laboratory work.

At the occasion, I would also show my gratitude for the assistance and the cooperation to John Zuta at IRIS which supported me during the flooding of the sandstone core plugs.

Finally, I will thank the University of Stavanger to be able to use the laboratory and the associated equipment that has been presented and utilized for the experimental part of the thesis, as well as the necessary materials.

ABSTRACT

Nanotechnology is among the most remarkable technology in the modern science, and due to unique and unrevealed abilities the tiny size of particles possesses, this technology has also been questioned in order to be worthy. The implementations of nanotechnology have already been used in diverse industries, yet to be a part of the oil and gas industry. The lack of investigations, and trust may be the reason for not applying the technology to the current ordinary technologies and techniques.

However, there are numerous optimistic scientists who suggest integrating the nanoparticles as a part of either formulating the drilling fluids and cement, or the enhanced oil recovery, as the nanotechnology shows promising potential.

During the thesis, nanofluids of different SiO_2 concentrations were studied to influence in EOR to raise the recovery factor and the performance of the drilling fluids in terms of rheology and the desired functions. The following points present the highlighted observations:

- 0.075 wt.% SiO_2 NF gave the best value as reducing the IFT by 14,44% and increased the contact angle by 52,3% to change the wettability to water – wet.
- 0.050 wt.% SiO_2 NF gave an incremental of 2,42% in a tertiary recovery method, while 0.075 wt.% SiO_2 NF did not alter the recovery factor.
- PV and ECD was not found to be any noteworthy influenced by adding nanoparticles.
- Additional 6.20% extended drilling was achieved by using CMC + 0.025g SiO_2 DF in WellPlan.

TABLE OF CONTENT

LIST OF FIGURES

LIST OF TABLES

NOMENCLATURE

OBM	Oil Based Mud
WBM	Water Based Mud
DF	Drilling Fluid
NF	Nano Fluid
SBM	Synthetic Based Mud
NS	Nano Solution
WF	Water Flooding
PF	Polymer Flooding
NPF	Nano Polymer Flooding
PV	Plastic Viscosity, Pore Volume
LVER	Linear Viscoelastic Range
ECD	Equivalent Circulating Density
CMC	Carboxymethyl Cellulose
KCl	Potassium Chloride
SEM	Scanning Electron Microscope
EDS	Energy Dispersive Spectrograph
EOR	Enhanced Oil Recovery
IFT	Interfacial Tension
CA	Contact Angle
SW	Seawater
YS	Yield Stress
LSYS	Lower Shear Yield Stress
BF	Base Fluid
REF	Reference
HB	Herschel Bulkley
RS	Robertson and Stiff
NP	Nanoparticle

1. INTRODUCTION

The presentation of the thesis will at the majority of the time focuses on the effect of SiO_2 nanoparticles as implemented in drilling fluids and enhanced oil recovery techniques. In the course of the thesis, a stabilized SiO_2 nanofluid have been designed and characterized. The evaluation of the influence in terms of raising the oil recovery was highlighted with core flooding of Berea sandstones, reducing interfacial tension and changing the wettability. Further, the impact of nanoparticles was studied in drilling fluids as the objective is to achieve desired performance to improve the functions of drilling fluids.

1.1. BACKGROUND & MOTIVATION

There is no secret that the world's population has increased rapidly in the recent decades, and our modern lifestyles have altered the necessity of more energy. The demand for energy has been increased simultaneously with the years, and even though our scientists have been seeking for other options for energy, the oil and gas industry remains as the number one provider of energy. To be able to keep providing the demanding energy, the industry must seek for another solution than the current way of producing fossil fuel beneath the surface. Higher risks have been taken in form of expanding the exploration for the hydrocarbons, further challenges have been encountered as drilling wells have been found in environments with higher temperature and pressure, as well as the challenges due to drilling in the arctic. [1] [2]

Nanotechnology has been an exciting term within the modern technology and has highly potential to alter the current technology. In fact, industries as medicine, electronics and food science have already proved nanotechnology's worth in their respectively operations. [3]

Although numerous of positive impressions from precedingly researched reports, the fate for the Nano-sized materials have not been decided yet in the oil and gas industry, and the protentional application of nanotechnology in current methods have currently been left out.

The following subsections will briefly introduce the basic principle of conventional technology within enhanced oil recovery and drilling fluids, as well as the drawbacks.

1.1.1. ENHANCED OIL RECOVERY

As one of four major processes of oil and gas industry, the production process may be categorized into three main stages:

1. Primary recovery
2. Secondary recovery
3. Tertiary recovery (EOR)

In the first development of the production process, the major mechanism of oil recovery is namely the pressure differential. Higher pressure in the reservoir than in the recent drilled wellbore will make the hydrocarbons stream into the well and up to the surface. The combination of the pressure differential, pumps and the assistance of lift techniques is the characterization of the primary recovery stage. [4]

In the next stage of the recovery process, the objective is to maintain the reservoir pressure to keep it from reaching the bubble point pressure and avoid further gas production. To be able to achieve the maintenance of the reservoir pressure, secondary recovery has to be made, and it consist of injection of either water or gas to displace the oil. During the secondary recovery, the oil recovery of the original oil in place can be predicted to be between 20 – 40%. [5] [6]

The final stage of the production process is called for tertiary recovery, but rather known as enhanced oil recovery due to all application of any further method to increase the recovery percentage from the reservoirs which alters from the primary and secondary recovery. At the moment, there exists three leading enhanced oil recovery techniques which should increase the ultimately oil recovery further to 30 – 60%: [6]

1. Thermal recovery
2. Gas injection
3. Chemical injection

The diagram below presents an overview of the distribution of oil fields and resources on the Norwegian Continental Shelf graphically. As it shows both produced and remaining oil reserves, a report achieved by the NPD states the current recovery factor to be an average on 47%. In fact, the report implies that even higher recovery factor can be achieved. [7]

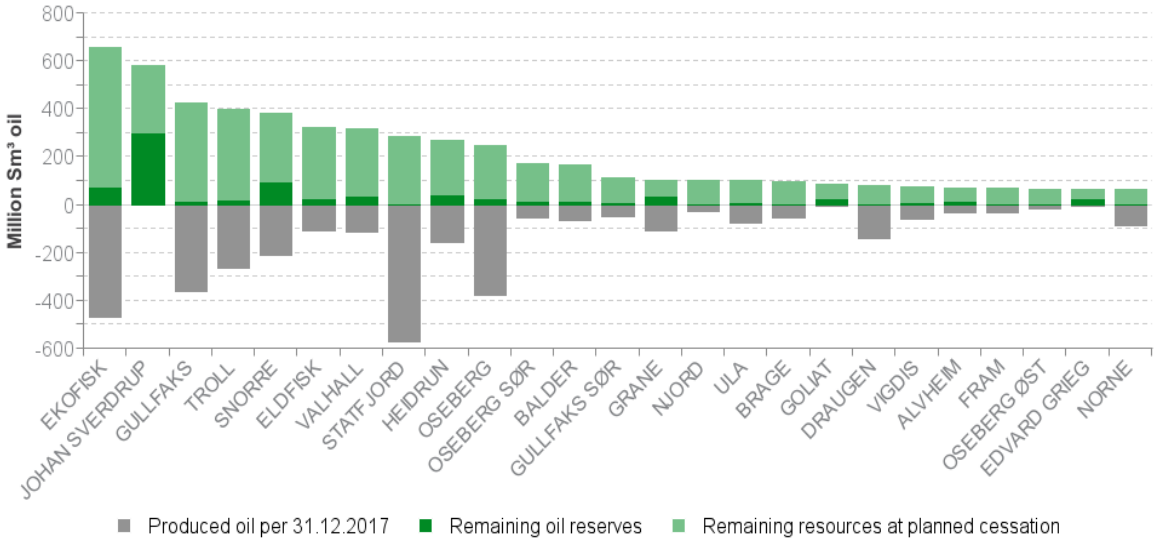

Figure 1 A graphical overview of the distribution of oil fields and resources on NCS per 31.12.2017. [1]

1.1.2. DRILLING FLUID

The drilling fluid plays a crucial part of any drilling operation. Among many functions, drilling fluids are mainly used to transport cuttings to surface and maintain well pressure. Besides the mentioned functions, cooling, cleaning and lubricating the drill bit are also importance to avoid damaging the bit. [8]

The ordinary types of drilling fluid can be classified into fluid systems such as oil-based mud (OBM), water-based mud (WBM) and synthetic based mud (SBM). The right pick of drilling fluids relies on handful factors such as technical performance, cost and environmental impacts. [9]

If drilling fluids are formulated below par, the consequences may lead to drilling related problems such as formation damage, mud loss, drill string sticking, clay swelling, high torque and drag and insufficient hole cleaning and hydraulic performances. [10] [11]

According to reports, 75% of drilling formations consist of shale where the occurrence of well instability has been recorded to be a major issue. Usually, oil-based drilling fluid is better than water-based drilling fluid regarding swelling control of shales, and additional due to higher lubricity result in better torque-drag performance. However, it is expensive and environment unfriendly compared to water-based mud. [11]

Consequently, to avoid the drilling issues which occurs due to drilling of shale formations, the development of water-based mud with the equal performance of oil-based mud is decisive for the future drilling operations, as well as to be more concern about the environmental aspect. [12] [13]

1.2. FORMULATION OF THE PROBLEM

It has been previously shown that conventional technologies regarding EOR and drilling fluids have shortcomings. Successful solutions have been documented in the literature in terms of utilizing the nanotechnology in oil and gas industry. However, both the research and development are still at an early stage.

This thesis will therefore address issues such as:

- How nanofluid of SiO_2 in brine systems can have an impact on oil/rock surface energy to improve oil recovery?
- How nanoparticles of SiO_2 can have an impact on drilling fluid properties?

1.3. OBJECTIVE

The foremost objectives of this thesis are to formulate SiO_2 Nano-fluid, characterize, and as well to test the performances of the nanofluids in drilling fluid and EOR.

The activities are:

- Review applications of nanotechnology in EOR and drilling fluids
- Experimental investigation
- Simulation of the performance

1.4. METHOD OF RESEARCH

The methods of research for the thesis can be categorized into three major parts. The figure 2 presents these parts, as well as the highlighted sections for their respectively major parts. The first major part introduces the extensive literature study for the relevant theories utilized in the work of this thesis, information for the chemical additives and the applications of nanoparticles in terms of EOR.

The second part deals with the experimental work of the influence nanoparticles in EOR and drilling fluids, where the formulation, characterization and tests will be found. While, the last part presents the simulation of the modelling for the drilling fluids.

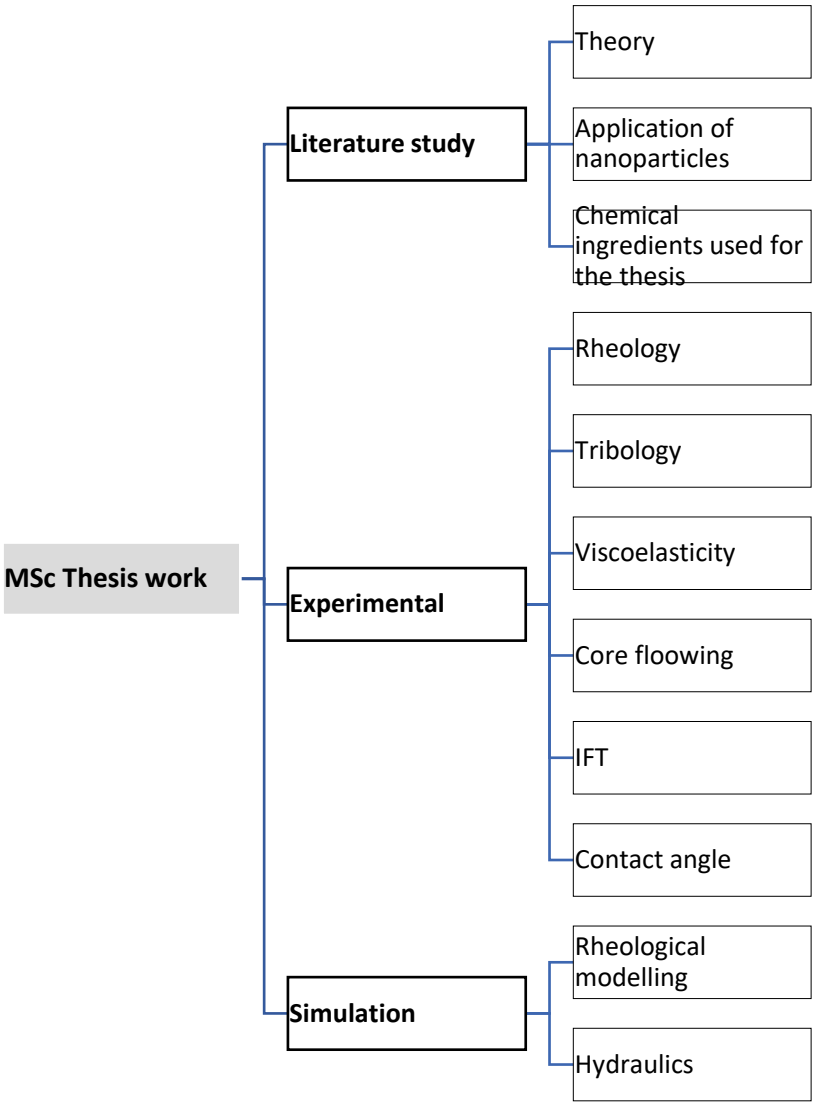

Figure 2 Method of Research

2. LITERATURE STUDY

Nanotechnology as a term, as well as a few applications of nanotechnology in the oil and gas industry will be presented in the following sections.

2.1. NANOTECHNOLOGY

The term nanotechnology is primary engineering of functional systems at the scale of molecular. Strictly speaking, the definition of nanotechnology can be smoother described as the science, technology and engineering to manipulate at a nanoscale. The range of a nanoscale is approximately within 1 – 100 nanometres.

Unlike most things, the range of nanoscale does not relate to us humans, as it may be difficult to imagine as well. A nanometer is in fact a billionth of a meter, and in a more mathematically way is equivalent to 10^{-9} of a meter.

The following figure 3 will give the idea of how tiny the scale is related with other objects.

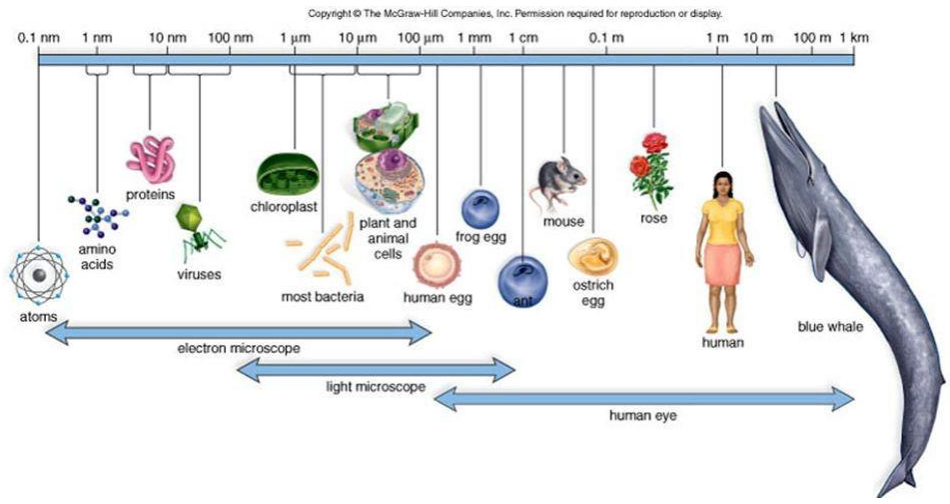

Figure 3 Logarithmic scale of sizes of living things [14]

The greatest remarked advantage by applying nanoparticles rather than materials at macroscale, is the high ratio of surface to volume. In other words, this implies that particles within the nanoscale could be applied at a sufficient lower concentration and still have greater interactions due to the greater area. Successfully applications of nanotechnology can already be found in such as medicine – and electronic industry. [15] [3]

2.2. APPLICATIONS OF NANOTECHNOLOGY

The major investigation of the thesis work is highlighted in this section as the potential applications of nanotechnology are under scope. As mentioned earlier, nanotechnology have been adapted in several other sectors such as electronics, pharmaceutical and food science. The extensive study focuses mainly on enhancing the oil recovery.

Reference	NPs / Basefluid	Oil type	Rock type	% Additional Ultimate Oil Recovery	Effect factor
Elgibaly	SiO_2 / Brine	Black oil	Sandstone	12,7 %	NP concentration
Kharrat	SiO_2 / Brine	Heavy crude oil	Glass	26 %	Wettability concentration
Jafari	SiO_2 / Polymer	N/A	Glass micromodel	18,37 %	Wettability Sweep efficiency
Tarek	Al_2O_3 + Fe_2O_3 + SiO_2	Mineral oil	Sandstone	20 %	Concentration Sweep efficiency (Fe_2O_3)
Ehtesabi	TiO_2	N/A	Carbonate	31 %	Wettability Concentration
Torsæter	SiO_2 / Brine	Light Crude oil	Berea SS	12 %	IFT Contact angle Concentration
Roustei	SiO_2 / Brine	N/A	Carbonate	25 %	Wettability
Wang	SiO_2 / Brine	N – Decane	Calcite	-	Wettability concentration

Table 1 Summary of all applications of Nanotechnology

Elgibaly et al. (2017) presents the influence of commercial hydrophilic mono dispersed silica (SiO_2) nanoparticles in enhanced oil recovery. The nanoparticles were 20 nm in size, and where tested in different aspects to affect oil recovery as a whole.

The authors of the papers acknowledge that nanoparticles have several mechanisms to improve oil recovery such as disjoining pressure mechanism and wettability alteration mechanism which is addressed in Section 4.7.

The experimental work conducted by Elgibaly et al. (2017) compared the efficiency of adapting Nano silica in either secondary – or tertiary recovery technique, as well as investigating the optimum concentration of nanoparticles. The oil recovery percentage increases simultaneously with increasing concentration of silica nanoparticles up to 0.1 wt% which was found as the optimum concentration and gave an additional 12,7% oil recovery. [16]

Due to minimal difference in secondary and tertiary recovery by using SiO_2, waterflooding may still be the best option to secondary recovery since it is the most reliable and economic compared to Nano silica.

Additionally, the authors address permeability impairment is an issue, and in this paper, both injection rate of the nanofluid and the concentration of the fluid show to have a direct effect of permeability impairment.

While, Ogolo et al. (2012) compares the impact of nine diverse oxide nanoparticles such as Aluminium oxide, Nickel oxide, Magnesium oxide, Iron oxide, Zinc oxide, Zirconium oxide, Tin oxide, Silicon oxide treated with silane and hydrophobic Silicone oxide. In order to evaluate the beneficence of applying nanoparticles for the total oil recovery, the various oxide nanoparticles were tested with different dispersing agents (distilled water, ethanol, brine and diesel). [17]

The methods of core flooding were set into either to apply nanofluids to flush a pre-injected pack of sand with brine and oil, or was to additionally soak the preinjected pack of sand with nanofluids for 60 days which gave the least best result among these methods.

The authors made two quite important observations:

Firstly, distilled water gave poorly recover overall, even with nanoparticles involved. Secondly, often the presence of nanoparticles with ethanol or brine did not enhance the oil recovery if compared to same respectively fluids without nanoparticles.

Overall, according to the authors, Aluminium oxide in brine and Silicone oxide in ethanol were both promising candidates for enhancing the oil recovery. While ethanol may be used singly to improve the total oil recovery.

Nano silica is popular as the nanoparticles have shown to be a great potential EOR agent, and Jafari et al. (2015) have included a polymer in a solution containing Nano silica. To be able to fully reveal the influence of the nanoparticle on wettability alternation of the porous medium, three flooding tests including water flooding (WF), polymer flooding (PF) and Nano – polymer flooding (NPF) were conducted. [18]

As shown in the following table 2, both the polymer and NS improves the oil recovery about 10% and 20%, respectively, compared to water itself.

The reason is the higher viscosity of the injected fluid that improves the oil displacement, and additionally it is obtained that NS can alter the wettability of the medium from oil – wet condition to water – wet. For this reason, Nano silica has the ability to lower the thickness of oil layer which allows the polymer to adsorb on pore walls and higher sweep efficiency has been achieved.

Test	Breakthrough time [min]	Ultimate recovery [%]	Viscosity of the injected fluid [cP]
WF	42	16.63	1
PF	64	26.32	8
NPF	84	35.00	35

Table 2 Results of flooding tests obtained by Jafari et al. (2015) [18]

The performance of a potential mixture of several nanoparticles to enhance the oil recovery rather than solely one nanoparticle was studied thoroughly by Tarek et al. (2015) from Cairo University. [19]

The author chose to base the alternatives of nanoparticles by two main criteria:

- The increased amount of oil recovery
- The mechanism of the nanoparticle which is responsible for the enhanced oil recovery

Former papers suggest both Aluminium Oxide and Iron Oxide as good candidates for the mixture of nanofluid due to their significant oil recovery ability.

Silica Oxide is another candidate to join the mixture of this investigation due to be proven to alter the wettability to water wet formation. Oil wet formation is by far poorer than water wet formation in regards of production, and additionally, SiO_2 forms a wedge – layer between the surface of the rock and the particular oil droplet. [19]

In this investigation, core flooding was the major part of the experimental work and the ratios of different nanoparticles are shown in the following table 3.

Mixture	Al_2O_3	Fe_2O_3	SiO_2
1	40 %	20 %	40 %
2	33.33 %	33.33 %	33.33 %
3	35 %	40 %	25 %

Table 3 Mixture concentration ratios used for flooding [19]

The results showed the mixture 3 gave the most promising result as it gave 20% additional incremental oil recovery due to the higher concentration of Iron Oxide which dominates the effect of granting higher viscosity to enhance the sweep efficiency. Mohamed Tarek concludes in the end that a mixture of nanoparticles may be a better option for recovery than a singular nanoparticle, and the importance of the ratio of the nanoparticle within the mixture.

On the other hand, Ehtesabi et al. (2013) studied the influence of Titanium Oxide to enhance heavy oil recovery on sandstone cores. The paper explains thoroughly all the aspect of the application of Titanium Oxide, from synthesis of nanofluid, its stability, testing the influence for oil recovery and as well the mechanisms behind it. [20]

A regular waterflooding was first conducted to set the baseline, and the performance of water itself was approximately 49% as recovery factor. By injecting with Titanium Oxide 0.01% gave a significant jump of recovery factor up to 80%, while injecting 1% nanoparticles had the opposite effect as the value was even lower than without TiO_2.

The higher recovery factor by injecting TiO_2 can be explained by altering the wettability due to increasing the contact angle of oil droplets after the injection. During the characterization, the SEM image of the core revealed higher accumulation of nanoparticles in the entrance rather throughout the core itself shows the importance to study the deposition and concentration of these nanoparticles.

The possibility of applying hydrophilic Silica to an enhanced oil recovery method was investigated by Torsæter et al. (2013), as well as to find the major mechanisms behind these nanoparticles by conducting experiments as transparent glass micromodel for two – phase flooding experiment and core flooding with Berea sandstones. [21]

The interfacial tension has been mentioned to be a key factor as a mechanism for Silica nanoparticles for EOR purposes, while the contact angle is another measurement that can describe the wettability. Measurements were conducted in this paper by utilizing a SVT20 spinning drop and Goniometry KSV Cam instrument, respectively. The conclusions are such as:

- Hydrophilic Silica nanoparticles dispensed with synthetic brine have the ability to reduce the interfacial tension between water – and oil phase.
- Higher concentrations of nanoparticles result with lower interfacial tension
- 0.05 wt % of Silica nanoparticle was found to be the optimum concentration in regard of oil recovery as the value increased by 12%
- Silica nanoparticles can reduce the contact angle

Half of the known petroleum reserves in the whole world is in fact in carbonate rocks, and among these, 90% of them can be labelled as neutral to oil – wet. The wettability is an

important property to be able to understand how the fluid flows in the reservoirs, and since there are difficulties to recovery sufficient oil of carbonate reservoirs by conducting the standard waterflooding, Roustei et al. (2014) introduces Silica nanoparticles as a candidate to improve the oil recovery.

In this investigation, the experimental work has been divided into core flooding, and test of contact angles and interfacial tension. [22].The authors of this paper concluded following points:

- Silica nanoparticles can be considered as a good candidate to alter the wettability for carbonates from oil – wet to water – wet.
- Overall oil recovery hits 67%

Kharrat et al. (2012) performed core flooding test of silica nanoparticles displacing heavy oil. A five – spot glass micromodel was utilized as the porous media, while both dispersed nanoparticles of silica in water and distilled water were chosen to be injected. During the core flooding, an optimum concentration of nanoparticle was found to be at 3 wt.% among the chosen range of concentration. The solution with 3 wt.% gave an additional 26% ultimate oil recovery compared to waterflooding. The investigation also presents the mechanism behind the success of enhancing the oil recovery by revealing the great sweep efficiency as the whole reason and labelled by having higher percentage of Nano silica in the water. Lastly, a suggestion by the authors is to utilize Nano silica as an additive to the solution during waterflooding before applying any other EOR techniques. [23]

Another investigation of Nano silica is reviewed by Wang et al. (2015) as their objective is mainly focusing on the study of contact angle and wettability.

Nanofluids containing silica proves to alter the wettability of calcite surfaces from oil – wet to strongly water – wet which is a superior condition in terms of oil recovery. The lowest amount of nanoparticle concentration to be sufficient to be able to make a difference for the contact angle was found to be 1 – 2 wt.%. Additionally, the exposure time of nanofluids on the calcite surfaces is also to be considered.

Overall, Nano silica can be a great additive to the solution to enhance the alteration of wettability as the EOR mechanism to produce more oil. [24]

3. THEORY

The third chapter of the thesis will present the relevant theories for the further work in the experimental study, as well as the simulation part for the performance of the drilling fluids.

3.1 RHEOLOGY

In order to be able to describe any fluids, numerous diverse mathematical models have been occurred. These models offer correction for the unique type of fluid. Fluids in general can be described as either Newtonian, Plastic, Pseudo plastic or dilatant fluids. The correct rheological model has to be applied to the right fluid category as these models will determine parameters such as gel strength and the viscosity of the fluid. These properties express the behaviour of the fluid, as well the ability to suspend and transport the cuttings from the wellbore to the surface. The figure 4 shows the relation between the shear stress and shear rate for the various types of fluids. [12] [25]

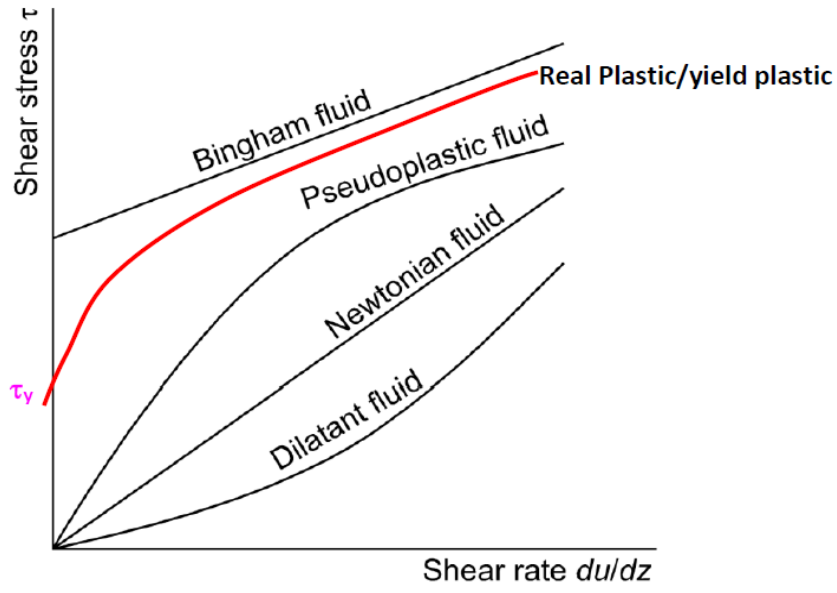

Figure 4 An illustration of shear stress – shear rate trends for different fluid types [26]

Plastic Viscosity: (PV)

The plastic viscosity term describes the resistance to flow caused by the mechanical friction found either between the particles suspended in the fluid, between the particle and the fluid, or among the fluid elements. Parameters such as the viscosity of the fluid, the size and shape of the additives in the fluid and the concentration of the additives influences the plastic viscosity. The determination of the plastic viscosity can readily be calculated by the following equation:

$$PV = \theta_{600} - \theta_{300} \quad (1)$$

Where the θ_{600} and θ_{300} are the reading of a viscometer at 600 RPM and 300 RPM shear rate, respectively. [12]

Yield Stress (YS):

While PV describes the resistance to flow caused by mechanical friction, the yield stress occurs because of attractive forces caused by the electrostatic forces among the particles in the fluid. The yield stress value will be heavily dependent of the shear rate, and reduces as the shear rate increases. In that case, the fluid is a shear – thinning fluid if it fulfils the mentioned character. [12]

$$YS = 2\theta_{300} - \theta_{600} \quad (2)$$

Gel Strength:

If a fluid is thick or even viscous under a static condition, but alters to a thinner fluid after shear strain is applied, the fluid will be categorized to have thixotropic behaviour. In other means, the shear stress is not constant for a certain rate, but rather alters as a function of shear rate. The gel strength describes the attractive forces between the suspended particles in a static fluid, and measures as a function of time. [12]

3.2 RHEOLOGICAL MODELS

In general, all fluids can either be classified in Newtonian – and Non – Newtonian fluids. These terms will be briefly described in the following subsections, and some rheological models will moreover be presented.

3.2.1 NEWTONIAN FLUIDS

The characterization of a Newtonian fluid is the independence of shear rate for the viscosity. For instance, the behaviour of a Newtonian fluid can be found in either water, oil or glycol due to containing no greater particles than molecules.

Due to that shear stress is directly proportional to shear rate, the relation between them graphically forms a straight line from the origin in the diagram. [12]

The following equation describes all Newtonian fluids:

$$\tau = \mu \cdot \gamma \qquad 3$$

Where τ is the shear stress, μ is the viscosity of the fluid and γ is the shear rate.

3.2.2 NON – NEWTONIAN FLUIDS

While most fluids do not tend to be classified to be a Newtonian fluid, the viscosity of non – Newtonian fluids relies on the shear rate. By its nature, drilling fluids can be described as non – Newtonian fluids and several models have been developed and presented in the following subsections: [12]

BINGHAM PLASTIC MODEL

The Bingham plastic model is characterized by three parameters, while the shear stress and strain are linearly related [12]. The rheological model presumes that the drilling fluid has a constant viscosity for all shear rates, as well as having a higher yield stress at very low shear

rates. However, these two properties are not observed in drilling fluid. The definition of Bingham plastic model is expressed as follows [25]:

$$\tau = \mu_p \gamma + \tau_y \quad (4)$$

Where, μp and τy are the plastic and yield strength of the drilling fluid, respectively.

POWER LAW MODEL

Regarding of the shear thinning beavhiour of drilling fluids, the Power Law model is more fitted to describe the fluid than the Bingham plastic model. Although, the Power Law model does not characterize the fluids at very low shear rate. The model is a two-parameter model, while the definition is given by the expression [12]:

$$\tau = \mathrm{K}\gamma^{\mathrm{n}} \quad (5)$$

where the consistence index and the flow behaviour index are symbolized with K and n, respectively, and can be calculated from the data obtained by the viscometer as:

$$n = 3.32\log(\frac{R_{600}}{R_{300}}) \quad (6)$$

$$K = \frac{R_{300}}{511^n} = \frac{R_{600}}{1022^n} \quad (7)$$

HERSCHEL – BULKLEY MODEL

The Herschel-Bulkley model is a yielded power law model and is better fitted to characterize the rheological properties of drilling fluid than both the Power Law – and Bingham Plastic model. The equation for the Herschel – Bulkley model is given as [12]:

$$\tau = \tau_0 + K\gamma^n \quad (8)$$

Where the τ and τ_0 is shear – and yield stress, and γ is the shear rate, and the latter symbols have been described in the Power Law model.

$$\tau_0 = \frac{\tau^{*2} - \tau_{\min}\tau_{\max}}{2\tau^* - \tau_{\min} - \tau_{\max}} \quad (9)$$

While the parameter τ^* is obtained by interpolation of the equivalent shear rate, γ^* value, which is given as:

$$\gamma^* = \sqrt{\gamma_{min} - \gamma_{max}} \quad (10)$$

UNIFIED MODEL

This model is a customized form of the Herschel-Bulkley model including to simplify it. The difference is the reduced shear yield point, and the equation is given as [12]:

$$\tau = \tau_y + K\gamma^n \qquad \text{where the } \tau_y = 1.066\ (2Q_3 - Q_6) \quad (11)$$

ROBERTSON AND STIFF MODEL

This rheological model has proven to be better in comparison to both Bingham – and Power Law model, but is far from the most popular due to the complexity as the equation shows [12]:

$$\tau = A(\gamma + C)^B \quad (12)$$

Where both A and B is the equivalent parameters such as K and n for the other rheological models, while C is the correction factor to the shear rate.

$$C = \frac{\gamma_{\max}\gamma_{\min} - \gamma^{*2}}{2\gamma^* - \gamma_{\max} - \gamma_{\min}} \quad (13)$$

Where γ^* is the shear rate value which is determined by interpolation from the shear stress, τ^*:

$$\tau * = \sqrt{\tau_{\min} * \tau_{\max}} \quad (14)$$

3.3 VISCOELASTICITY

The behaviour of viscoelasticity can be presented by the materials composed of both solids and fluids. For instance, a drilling fluid exhibit the nature of a viscoelastic substance. This means a drilling fluid can be both characterized in regards of elasticity and of viscosity under deformation due to having suspended particles in an aqueous solution.

The properties of a viscoelastic material rely upon time. The alteration of either shear stress or shear rate can influence the viscosity, either increasing it or decreasing it. In a combination of applying higher shear stress to the subject, and time, the viscosity increases. Although, like most, an ideal amount of applied shear stress can be found, since higher shear stress causes heating as well. Higher temperatures will in fact reduce the value of viscosity. [27]

During applying deformation to the drilling fluid, the property of elasticity can store energy which influences the pressure drop and how the fluid flows. Hence, the vital knowledge of viscoelasticity as describes properties such as solid suspension, gel structure and gel strength, and hydraulic sagging. In order to define the viscoelasticity to a drilling fluid mixture, a rheometer can conduct test such as oscillatory test to evaluate and describe the importance of viscoelasticity. [28]

The rheometer has the ability to define the viscoelasticity by using a simple basis rule of the Two – Plates model of an oscillatory test. The sample of the chosen subject is firstly carefully placed upon the cleaned lower plate which is stationary, while the upper plate will press the sample between the two plates. Additionally, the upper plate will also perform shear stress upon the sample as the upper plate moves in oscillatory way throughout the test. By the time the rheometer is running the test, the selected sample between the plates will experience different sinusoidal deformation, strain. As the deformations takes place, the stress will be measured and plotted into the program. The following figure 5 shows how the behaviour of both strain and stress is during the test as a function of amplitude, time and phase angle.

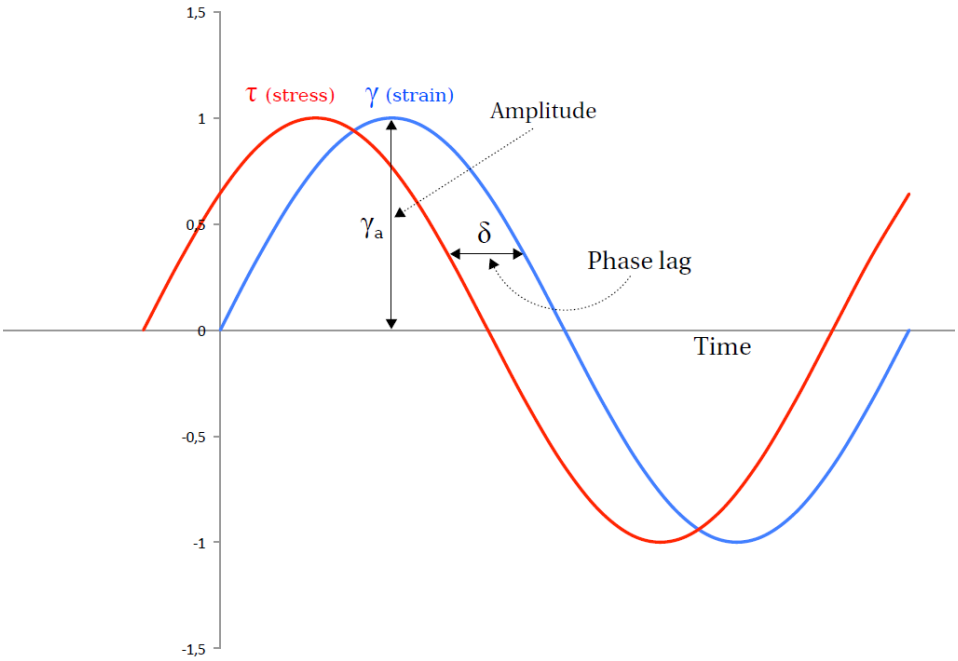

Figure 5 Stress – strain reaction for an oscillatory computation of a viscoelastic material [29]

The following definitions are the computational shear stress, and the shear strain applied to the selected sample [28]:

$$\tau(t) = \tau_o \sin(\omega t + \delta) \quad (15)$$

$$\gamma(t) = \gamma_o \sin(\omega t) \quad (16)$$

$$\tau(t) = \tau_o[\sin(\omega t)\, cos\delta + \cos(\omega t)\, sin\delta] \quad (17)$$

$$\tau(t) = \gamma_0\left[\left(\frac{\tau_o}{\gamma_0} cos\delta\right)\sin(\omega t) + \left(\frac{\tau_o}{\gamma_0} sin\delta\right)\cos(\omega t)\right] \quad (18)$$

$$\tau(t) = \gamma_0[G'\sin(\omega t) + G''\cos(\omega t)] \quad (19)$$

These equations are defined for the Storage – and the Loss Modulus, respectively [28]:

$$G' = \left(\frac{\tau_o}{\gamma_0} cos\delta\right) \quad (20)$$

$$G'' = \left(\frac{\tau_o}{\gamma_0} sin\delta\right) \quad (21)$$

While, the damping factor is defined as the ratio of the Loss - and the Storage Modulus:

$$tan\delta = \left(\frac{G''}{G'}\right) \quad 22$$

$$\delta = tan^{-1}\left(\frac{G''}{G'}\right) \quad 23$$

As described for the damping factor equation, the symbol, δ, defines the parameter which alters regarding to the fluid and is known as the phase angle.

The table 4, represents the different scenarios schematically for the relation between the viscoelasticity behaviour and damping factor.

Phase angle	$0 < \delta < 45$	$\delta = 45$	$45 < \delta < 90$
Behaviour	Elastic dominated	Transitional	Viscous dominated
G' and G''	G' > G''	G' = G''	G' < G''

Table 4 The given categories of viscoelastic material obtained by an oscillatory measurement [27]

For any ideally viscous fluid, the phase angle would be equal to 90 degrees and the Loss modulus would be in charge over the Storage modulus for this particular fluid.

On the other hand, an ideally elastic fluid would result in having the Storage modulus be greater than the Loss modulus for the fluid, as well as the phase angle would be equal to zero.

In the middle ground between the mentioned cases, the phase angle would be 45 degrees and the Loss modulus, and the Storage modulus will be equal as the fluid has a transitional behaviour as the table 4 states. [28] [27]

3.3.1. OSCILLATORY AMPLITUDE SWEEP TEST

The basic principle of an oscillatory amplitude sweep test is to keep the frequency constant throughout the test, while the amplitude of the oscillations is varying. Additionally, the temperature of the selected fluid is also kept constant.

The subjected fluid sample will undergo a deformation in form of the applying strain to it. Although, the internal structure of the fluid does not alter during the deformation.

Parameters such as the Loss modulus and the Storage modulus will be generated with nearly constant values in unique levels as a linear horizontal range will be produced on graph of the test. The range is better known as Linear Viscoelastic Range, LVER, and is presented in the following figure 6. This horizontal range on the graph is solely achieved under the lower amplitudes of oscillations. However, if the applying oscillations have higher amplitudes, the strain will be higher which leads into a critical point where the internal structure will undergo an irreversible deformation. The deformation of the internal structure is represented as the Linear Viscoelastic Range changes from the constant horizontal graph into a nonlinear viscoelastic range. In the end, the Oscillatory Amplitude Sweep test can offer determination of parameters such as flow point and yield point of the sample fluid due to the resulting data and graph.

The flow point of the fluid can be described as the point where the fluid has the ability to start to flow, and the parameter can be determined where Storage modulus and Loss modulus is equal. Graphically, the determination of the flow point can be found as these curves of the modulus crosses each other. As mentioned earlier, the behaviour of the fluid at this point is transitional which means that the phase angle is 45 degrees as well as the 50/50 behaviour regarding viscosity and elastic.

While the flow point can be found where the curves crosses each other, the yield point can be determined graphically where the curves of the Loss – and Storage modulus begins to alter from the horizontal plateau.

As the behaviour of the sample fluid is more elastic pre the yield point and fulfils the character as a gel, the behaviour is the opposite after the flow point. Viscosity as a behaviour dominates after the point where the curves meet as the illustration shows.

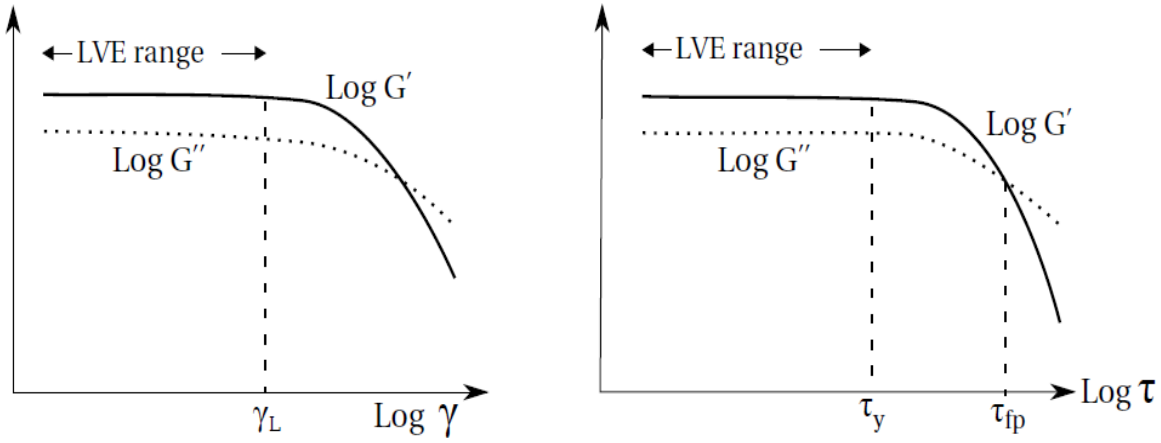

Figure 6 Graphically showing parameters such as gel – character on the left-hand side, while yield point and flow point is presented on the right-hand side [27]

3.4 TORQUE & DRAG

During the drilling operation, torque and drag on the drilling string is among the key issue for both drilling and intervention of the well. Because of the interaction between the drill string and casing/wellbore, the drag force on the drilling string is decisive for the limit of drilling.

Different loads on the drill string is shown in figure 7. By utilizing force balance, the differential force per differential length on a modest segment is given as:

$$\frac{dF}{ds} = \pm\mu\left(\sqrt{\left(\beta w_s sin\theta + F\frac{d\theta}{dS}\right)^2 + \left(Fsin\theta\frac{d\varphi}{ds}\right)^2}\right) + \beta w_s cos\theta \qquad 24$$

where φ is the azimuth, θ is the inclination, + and – symbolize running out - and running into the hole, respectively.

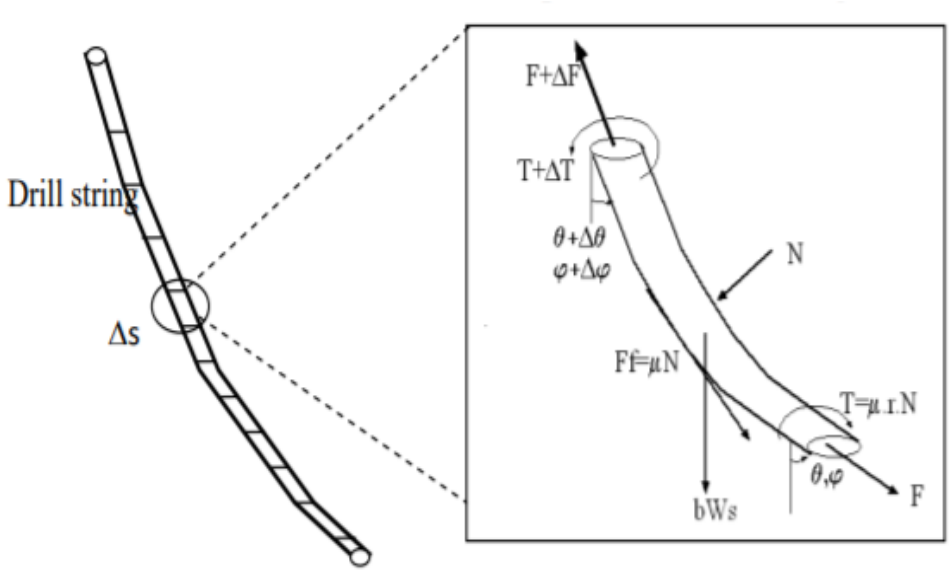

Figure 7 A segmented string and the associated loads [26]

The definition of toque at the top of the drill string is given as the torque on bit and the sum of the torques to overcome the rotational frictional force [26]:

$$T_{i+1} = T_i + \sum_{i=1}^{n} \mu_t r_i N_i (S_{i+1} - S_i) \qquad 25$$

Where T_i is the torque on bit, while μ_t is the tangential coefficient of friction.

As observed, both of torque and the drag equations are a function of the coefficient of friction. To be able to reduce the force in the drill string, the increasement of the lubricity of the drilling fluid is urgent. Therefore, this thesis work will later highlight an experimentally study of the effect of nanoparticle on the tribology of the drilling fluid. [26]

3.5 HYDRAULICS

As the fluid flows through circulation system of drilling equipment, the pressure loses. The pump pressure can be defined as the sum of all pressure losses and given as [26]:

$$\text{Pump pressure} = P_{surf} + \Delta P_{\text{pipe}} + \Delta P_{\text{bit-nozzles}} + \Delta P_{\text{annulus}} \quad (26)$$

The effective circulation density (ECD) is can be calculated by the following expression: [13]

$$\text{ECD(sg)} = \text{ESD(sg)} + \frac{\Delta P_{\text{annulus}}(\text{bar})}{0.0981 * \text{TVD(m)}} \quad (27)$$

Where ESD is the static mud density, and $\Delta P_{annulus}$ is pressure loss in the annulus

Both the hydraulics and ECD of the drilling fluids will later be evaluated with assistance of using the Unified model summarized in the following table 5. [25]

Unified model	
Pipe Flow	**Annular flow**
$\mu_p = R_{600} - R_{300}, [cP] \quad \tau_y = R_{300} - \mu_p, [lbf/100ft^2] \quad \tau_0 = 1.066 \cdot (2 \cdot R_3 - R_6)$	
$n_p = 3.32 \cdot log\left(\frac{2 \cdot \mu_p + \tau_y}{\mu_p + \tau_y}\right)$ $k_p = 1.066\left(\frac{\mu_p + \tau_y}{511^{n_p}}\right)$	$n_a = 3.32 \cdot log\left(\frac{2 \cdot \mu_p + \tau_{y-\tau_y}}{\mu_p + \tau_{y-\tau_y}}\right)$ $k_a = 1.066\left(\frac{\mu_p + \tau_y - \tau_0}{511^{n_a}}\right)$ $k = [lbf \cdot sec^n/100ft^2]$
$G = \left(\frac{(3-\alpha)n+1}{(4-\alpha)n}\right) \cdot \left(1 + \frac{\alpha}{2}\right)$ $\alpha = 1$ *for pipe* $\quad$ $\alpha = 1$ *for annuli*	
$v_p = \frac{24.51 \cdot q}{D_P^2}$	$v_a = \frac{24.51 \cdot q}{D_2^2 - D_1^2}$ $v = [ft/min]$
$\gamma_w = \frac{1.6 \cdot G \cdot v}{D_R} = [sec^{-1}]$	
$\tau_w = \left[\left(\frac{4-\alpha}{3-\alpha}\right)^n \tau_0 + (k \cdot \gamma_w^n)\right] = [lbf/100ft^2]$	
$N_{Re} = \frac{\rho \cdot v_p^2}{19.36 \cdot \tau_w}$	$N_{Re} = \frac{\rho \cdot v_a^2}{19.36 \cdot \tau_w}$
$f_{laminar} = \frac{16}{N_{Re}}$ $f_{transient} = \frac{16 \cdot N_{Re}}{(3470 - 1370 \cdot n_p)^2}$ **Turbulent:** $f_{turbulent} = \frac{a}{N_{Re}^b}$ $a = \frac{\log(n) + 3.93}{50} \quad b = \frac{1.75 - \log(n)}{7}$	$f_{laminar} = \frac{24}{N_{Re}}$ $f_{transient} = \frac{16 \cdot N_{Re}}{(3470 - 1370 \cdot n_a)^2}$ **Turbulent:** $f_{turbulent} = \frac{a}{N_{Re}^b}$ $a = \frac{\log(n) + 3.93}{50} \quad b = \frac{1.75 - \log(n)}{7}$
$f_{partial} = (f_{transient}^{-8} + f_{turbulent}^{-8})^{-1/8}$	
$f_p = (f_{partial}^{12} + f_{laminar}^{12})^{1/12}$	$f_a = (f_{partial}^{12} + f_{laminar}^{12})^{1/12}$
$\left(\frac{dp}{dL}\right) = 1.076 \cdot \frac{f_p \cdot v_p^2 \cdot \rho}{10^5 \cdot D_p} = [psi/ft]$ $\Delta p = \left(\frac{dp}{dL}\right) \cdot \Delta L = [\text{psi}]$	$\left(\frac{dp}{dL}\right) = 1.076 \cdot \frac{f_a \cdot v_a^2 \cdot \rho}{10^5 \cdot (D_2 - D_1)} = [psi/ft]$ $\Delta p = \left(\frac{dp}{dL}\right) \cdot \Delta L = [\text{psi}]$
$\Delta p_{Nozzles} = \frac{156 \cdot \rho \cdot q^2}{\left(D_{N1}^2 - D_{N2}^2 - D_{N3}^2\right)^2} = [psi]$	

Table 5 A summary of equations associated with the Unified rheological model [25]

3.6 ROCK FLUID PROPERTIES

The following subsections will review the properties for the rock media and the fluid that will either be stored or flowing through it. Parameters such as the porosity, permeability and wettability are among important properties to characterize the condition for the rock media.

3.6.1 POROSITY

Porosity can essentially be described as the quantity of storing fluids in empty voids within a rock media. The porosity measurement is defined as the ratio of the pore volume to the bulk volume and is commonly be expressed in percentage or in fraction.

$$\emptyset = \frac{V_p}{V_b} = \frac{Bulk\ volume - \ Grain\ volume}{Bulk\ volume} \qquad 28$$

Porosity may be the most vital property of a reservoir due to the ability to indicate the quantity of oil and gas in the particular reservoir. Although, the porosity is quite varying, and depends on factors such as size and shape of the particles, the degree of cementation and packing of the particles. [30]

Throughout the depositional process, porosity has been firstly developed and may be distinguished as the primary porosity of the rock media. While the secondary porosity occurs after the deposition of the sediment and alters the rock properties due to geological processes as fracturing, dolomitization and dissolution.

In additional to the classification of the porosity, the measurement of the important rock property may also be differentiated. Effective porosity includes only the ratio of interconnected pores in the media to the bulk volume, on the contrary the total porosity is the ratio of all pores in the rock media to the bulk volume. [30]

3.6.2 PERMEABILITY

In context with reservoir rock, permeability can easily be described as the ability to transfer a fluid through its system. Permeability may also be defined as the communication between the pores/voids within the rock. Hence, systems with more well – interconnected pores have higher value of permeability such as sandstones. While shales tend to be the opposite, due to the lack of sufficient communication between the pores and may often be defined as impermeable systems.

Henry Darcy conducted an experiment in 1856 which confirmed the following relationship for the permeability measurement:

$$q = \frac{A\,k}{\mu\,\Delta l}\,\Delta p \qquad 29$$

Where q is the flowrate

A is the cross – sectional area of fluid flow

k is the permeability

μ is the viscosity of the flowing fluid

Δl is the length of the system

Δp is the pressure drop

Hence, the relationship is called the Darcy's Law, and the unit for permeability is named after him as well. Although, the unit is often in 1/1000 fraction which implies to millidarcy, mD. [31] [32]

3.6.3 RELATIVELY PERMEABILITY

The literature differs the term of permeability as the absolute permeability often refers to a singular phase fluid, while the relatively permeability describes the ability to transport the fluids, oil, gas or water through the porous rock. The relatively permeability is among the most important reservoir properties as it influences the communication between the interconnected pores.

Additionally, the literature defines two separate permeabilities: The effective permeability is defined as the capacity to conduct any fluid while being not fully saturated. While the relatively permeability is defined as the proportion of any fluid coexisting with other fluids to the absolute permeability of the rock media.

$$k_{ro} = \frac{k_o}{k} \qquad 30$$

Where k_{ro} is the relatively permeability, k_o is the effective permeability of oil and k is the absolute permeability.

An illustration with curves for the relatively permeabilities as a function of the saturation have been graphically plotted below. The curves in the figure 8 describe the processes such as drainage, a process where the wetting phase content reduces (often water) and imbibition, a process with a rising content of the wetting phase, respectively. [30]

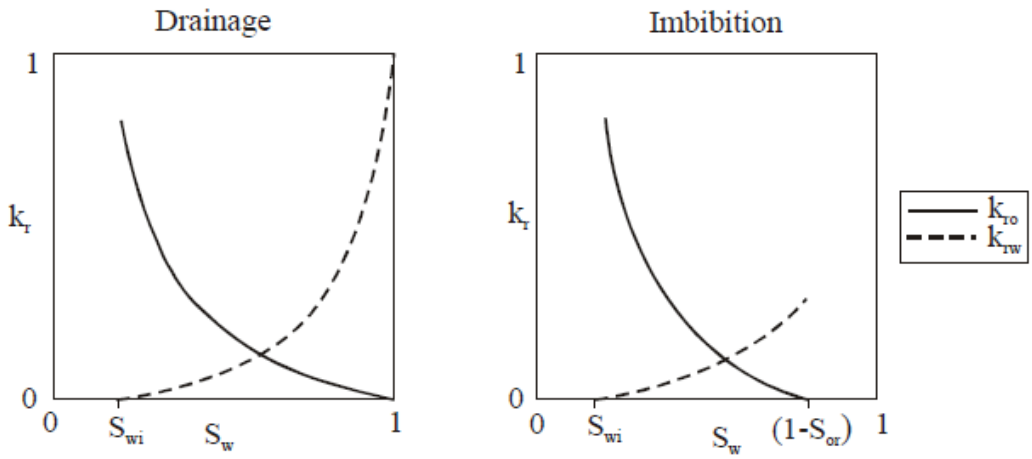

Figure 8 Common curves for relatively permeability for drainage – and imbibition process at water wet systems [30]

3.6.4 CONTACT ANGLE & WETTABILITY

Whenever a liquid is in direct contact with the surface of a solid, the liquid itself can be observed to either compose into minor droplets on the solid – surface, or fully expand itself over the surface. As in the first scenario, the droplets of the liquid will have contact angles between the surface and the droplets. While the latter scenario, the liquid will wholly wet the

surface. An illustration as seen below presents how an oil droplet appears on the surface of a solid while surrounded by water. The typical so-called oil – water – solid system can be expressed by the Young's equation in terms of including contact angle and the tension between the fluids. [30]

$$\cos\theta = \frac{\sigma_{SO} - \sigma_{SW}}{\sigma_{WO}} \qquad 31$$

Where σ is the interfacial tension for either so (solid – oil), sw (solid – water) and wo (water – oil) and θ is the contact angle measured through the phase of water as seen in figure 9.

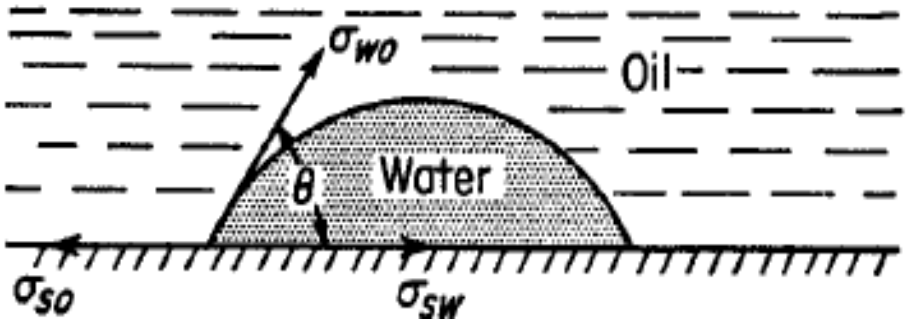

Figure 9 Interfacial tensions for oil – water – solid system at equilibrium [30].

The wettability of a rock – fluid system can be defined as "the tendency of one fluid to spread or to adhere to a solid surface in the presence of other immiscible fluids". This term has been proved to be an important factor to the production of hydrocarbons as it decides the original distributions of the fluids in the reservoir, as well as the flow. [33]

The evaluation of the wettability is often made by measuring either the contact angle which two immiscible liquids develop with the surface, or by measuring the interfacial tension. The table 6 presents the correlation between the contact angle and the preference of the wettability.

Contact Angle [degree]	Wettability preference
0 – 30	Strongly oil wet
30 – 90	Preferentially oil wet
90	Neutral wettability
90 – 150	Preferentially water wet
150 – 180	Strongly water wet

Table 6 Wettability preferences given by the contact angle [32]

3.6.5 CAPILLARY PRESSURE

On any occasion where two immiscible fluids such as water and oil co-exist in the voids of a porous media, a discontinuity of pressure will be generated beyond the interface between them. The divergence between the pressures is often called as capillary pressure and consists of the pressure from the non – wetting phase subtracting the pressure of the wetting phase.

$$P_c = P_{non-wetting} - P_{wetting} \quad (32)$$

Where P_c is the capillary pressure, while the rest is the pressure for either the wetting phase or non – wetting phase.

The capillary pressure can in additional also be described by the equation of Laplace. The following equation by Laplace states implies that the curvature between fluid interfaces cause the capillary pressure.

$$P_c = \sigma \left(\frac{1}{r_1} + \frac{1}{r_2}\right) \quad (33)$$

Where P_c is the capillary pressure, r_1 and r_2 are the principle radii of the curvature and σ is the tension between the fluids.

In the reality, the capillary pressure is heavily connected and influenced by the surrounding fluids, especially the saturation of the given fluids. The figure 10 illustrates the relation between the saturation of the fluid and the coexisting capillary pressure, as well as the various processes during an oil – water system. [30]

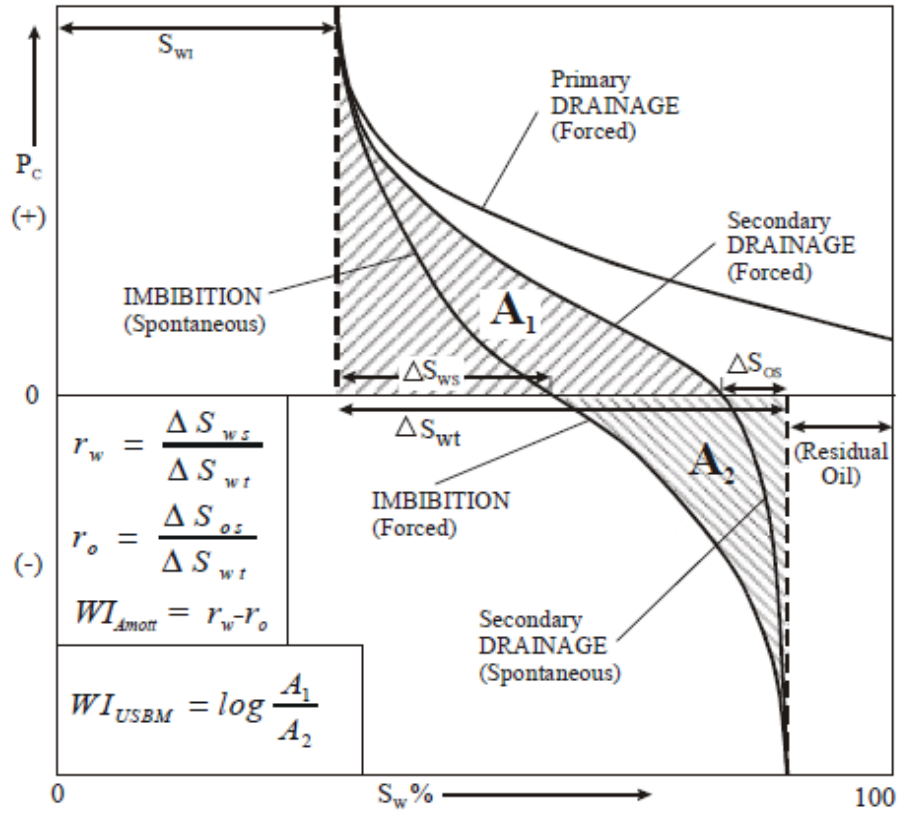

Figure 10 Typical capillary pressure versus saturation relationship [30].

For the oil – water system, the processes of displacing the fluids in the two – phase flow rock media can be differentiated into either imbibition or drainage process. As shown in the figure 10, the drainage process refers to displacement of the wetting phase from completely saturation to the point called irreducible water saturation where the saturation of the wetting phase no longer reduces due to the applied capillary pressure. Unlike the drainage process, the curve of imbibition on the illustration presents the displacement of the non – wetting phase starting from the irreducible water saturation point, while ending at the point of residual oil saturation which is the ratio of unremovable oil apart of the effective porosity. [30]

4. ADDITIVES USED IN THIS THESIS WORK

Several unique additives with their respectively abilities and functions will be presented and described in this chapter.

4.1 BENTONITE

A fine – grained natural rock such as clay which composes mostly minerals of clay and hints of metal oxides, organic matter and quartz. In the course of drilling processes in the oil and gas industry, clay is most commonly utilized as an additive for drilling fluids.

As a member of the category of clay, bentonite is often added in drilling fluids to serve purposes as a viscosity agent and to minimize the filter loss during drilling.

Since the drilling fluids prepared in this thesis work is WBM, the Bentonite plays a vital part among the additives of the drilling fluid systems. Bentonite as a clay was originally found in Wyoming, and Wilbur C. Knight gave the name of the clay due to the exploration of Cretaceous Benton Shale. This particular clay composes the majority of its chemical composition of a clay mineral group called smectite, may also be better known as montmorillonite clay group. Montmorillonite introduces the ability of swelling and has qualities of thixotropic.

Even though the mineral group smectite is the majority of bentonite composition, other clay mineral groups such as kaolinites and illites are also represented in Bentonite. As the chemical composition of bentonite in the table 7 shows, bentonite composes additionally 10 – 30 % non – clay minerals. [34] [35]

Bentonite can be categorized into two different classes depend upon how the swelling process conducts in contact with water. In fact, the swelling process is differentiated by either composed of Calcium – ions or Sodium – ions, where the process of swelling the clay is surface hydration and osmotic swelling, respectively.

Component	Percentage of chemical composition
Silica, SiO_2	64.32
Aluminium Oxide, Al_2O_3	20.74
Cumulative water	5.14
Ferric oxide, Fe_2O_3	3.03
Sodium Oxide, Na_2O	2.59
Magnesium Oxide, MgO	2.30
Calcium Oxide, CaO	0.50
Ferrous Oxide, FeO	0.46
Potasium Oxide, K_2O	0.39
Sulfuric Anhydride	0.35
Titanium Oxide, TiO_2	0.14
Phosphoric Anhydride	0.01
Other minor constituents	0.01

Table 7 The components of Bentonite [35]

The swelling ability of surface hydration as the swelling process is lower whenever Calcium – ions dominates in Bentonite. Surface hydration takes place whenever molecules of water are adsorbed to crystal surfaces of the clay, and as well as the water molecules seized the oxygen atom.

On the other hand, the osmotic swelling occurs when there is lower concentration of cations in the surroundings than in the between the unit layers of the clay structure which will allow water to slip through and an interruption between layers in the clay structure exists. Additionally, sodium – saturated Bentonites tend to have a higher swelling ability compared to surface hydration. The higher swelling ability leads to larger expansion which has to be a part of the evaluation in terms of stability of the Bentonite.

As the description of the composition of Bentonite has been mentioned above, the group of clay minerals named smectite rules the majority of clay minerals in bentonite.

The smectite mineral groups can either have the Octahedral layer or the Tetrahedral layer as the figure 11 explains. [13] [34]

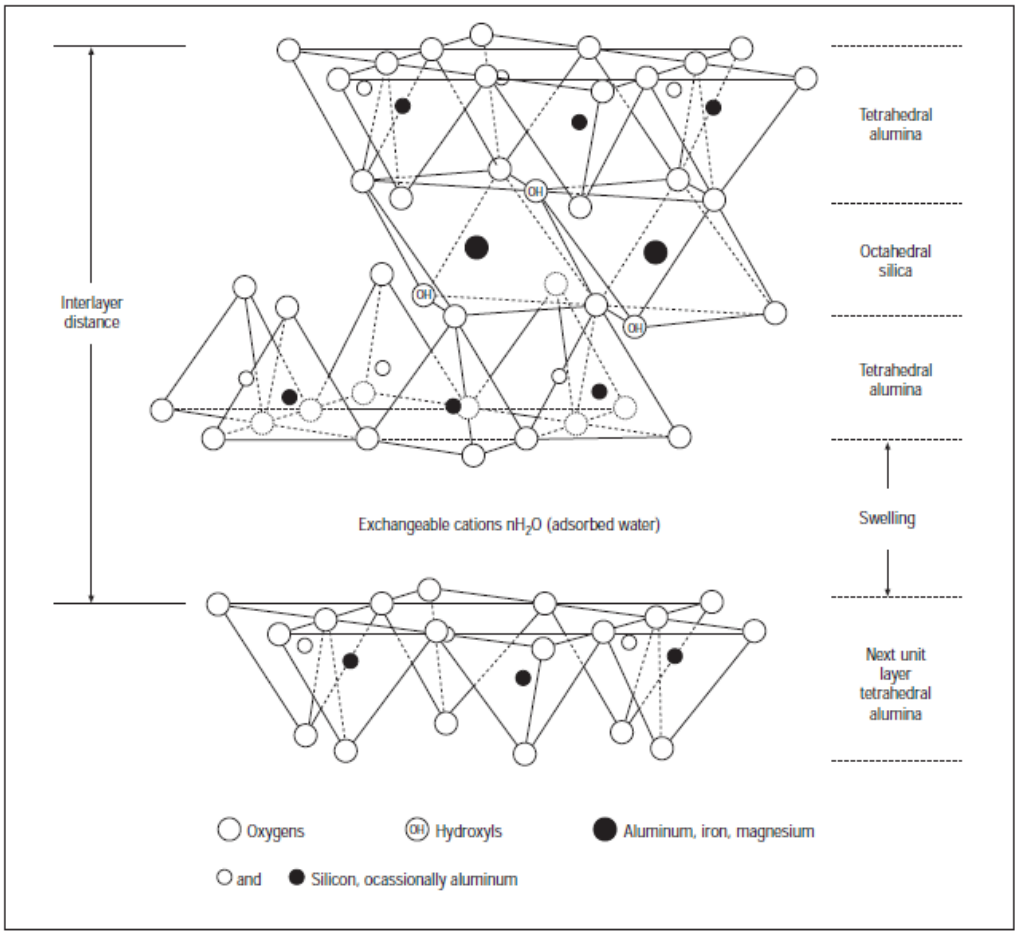

Figure 11 Typical clay structure [13]

Figure 11 shows the possibility to have assorted different combinations of chemicals in the two structures. For instance, the tetrahedral layer is composed of either oxygen – or a group of hydrogen oxygen distributed among the four corners of the clay structure. A silicon atom is placed in the centre of the tetrahedral structure and surrounded by the Oxygen – or Alcohol group in the corners of the structure. Another possibility which the figure shows, is the tendency of connection between the tetrahedral structures which allows them to keep together and have their bottom – bases on the same plan – level.

As mentioned and described previously, the properties of the clay minerals play an important part of how successful the drilling process may be. Due to the importance, knowledge about the properties such as shear stress, viscosity and yield point of the utilized fluid and their

behaviour under conditions below surface should be investigated more thoroughly. However, to understand more about the properties, the following various conditions of clay particles suspended in solutions have to be characterized, as well as differentiated. [13]

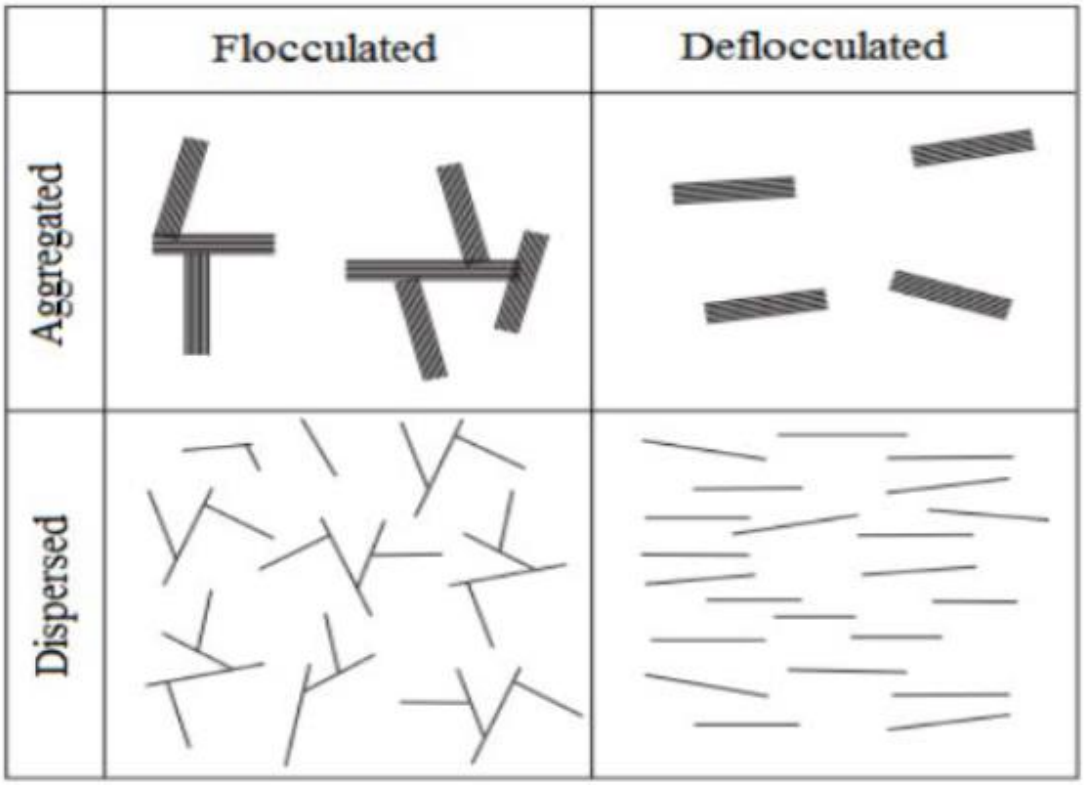

Figure 12 The different clay conditions [12].

4.1.1. FLOCCULATED SYSTEM

A solution of suspended particles of clay can be described as flocculated when the net attraction – forces between the clay particles is zero. The neutralized charge permits the particles to attach themselves to each other which assembles unrestricted structures. In terms of the clay system, the attachments between particles are either edge – to – surface or edge – to – edge This occurs only whenever the particles possess available positive charged ions on the edges.

At any time, if the system of clay minerals flocculates, the viscosity verges on to increase, especially will a huge leap of the value of yield point be observed, as well as an increment of filter loss. [13]

4.1.2 DEFLOCCULATED SYSTEM

On the other side, this system can be described as the opposite as flocculated system. Deflocculated system for the clay particles develops whenever there exist solely repulsive forces between the individual clay particles. This condition for deflocculated system is regular achieved by adjusting the pH to be more an alkaline– solution which leads the particles to possess negative charged ions. However, a completely deflocculated system is rare to exist naturally without the aid of chemicals. These chemicals are called as deflocculators and serves the purpose to neutralize the presented positive charged ions in the system. Both the values of viscosity and yield point will be low, a result of non-electrical attraction forces between the clay particles. [13]

4.1.3 AGGREGATED SYSTEM

The description of an aggregated system of a solution of suspended clay particles is when the singular particles connect together as aggregates showed in the figure 12. The basic structure of any clay systems contains sheets, while the crystal structure contains stacks of them. In terms of using Bentonite, the individual sheets may be separated by hydration and mechanical forces in the system. Generally, a strong flocculated system of clay will after a while always turn into an aggregated system. In an aggregated system, the filter loss will be high, while the plastic viscosity will be low. [13]

4.1.4 DISPERSED SYSTEM

This system is the opposite of what an aggregated system would be. The description of the dispersed system can be where all the aggregates is split into several individual crystals or groups of crystals.

Relying upon the pH value of the clay system, the negative and positives charged ions may coexists on the edges of particles. Similarly, to the aggregated system, dispersed system can also be either flocculated or deflocculated systems. In general, a good drilling fluid with Bentonite is under the conditions of a dispersed system and deflocculated system. [13]

4.2 CMC – Carboxymethyl Cellulose

This chemical goes under several names such as cellulose gum or tylose powder, but is most common as carboxymethyl cellulose (CMC) which is derived from cellulose with the carboxymethyl groups which the name comes from. The carboxymethyl group (- CH_2 – COOH) is bounded to a hydroxyl group, and the structure of CMC is shown below. As a polymer, the CMC is applied in drilling fluid to adjust the viscosity of the liquid. Additionally, CMC may also manage the fluid loss in terms of drilling fluids. [37] [38]

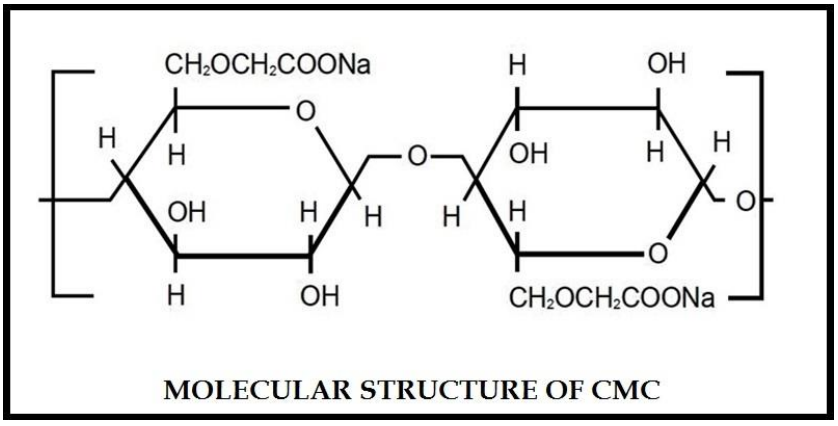

Figure 13 The molecular structure of Carboxymethyl Cellulose [39]

4.3 DUOVIS

For the diversity of the experimental work, another polymer was also introduced regarding to design the drilling fluid systems. The biopolymer, Duovis was included in the other batch of drilling fluid system to examine the influence of nanoparticles in drilling fluids. Duovis appears as a cream – to – tan powder and has the rare ability to transform the fluid into having a thixotropic and greatly shear thinning behaviour. Minimal amount of the biopolymer is required to reach the benefits of Duovis as it serve the purpose to increase the viscosity of the fluid system regarding the suspension of cuttings and transportation. [36]

4.3 KCl – Potassium Chloride

A metal halide salt with the chemical formula as KCl, may be better known as potassium chloride among scientists. This particular metal halide salt consists of a chloride and a potassium atom. This chemical has a density of 1.984 g/cm^3, and its appear as a white in colour, and may taste and look like as salt such as NaCl.

In terms of the oil and gas industry, potassium chloride is broadly approved as an additive to drilling fluids due to its solubility in water and as well to be acknowledged to be among the better additives regarding shale – swelling. Drilling in shales will almost certainly encounter challenges, and due to the instability in drilling in shales, including potassium chloride might play a vital part to succeeding in drilling.

In fact, since the KCl is easily soluble in water, the ions of the potassium, K^+, can freely be attracted to against the opposite charged surface of clay – surface plates to provide stability in shales. [40] [41]

4.4 SEAWATER

Figure 14 shows the ionic composition of the pure seawater which has been utilized in this thesis work. The seawater was in fact fetched from Stavanger harbour called Vågen in the centre of Stavanger city which is a part of the North Sea.

As shown in the figure, the fluid composes majority of both Chlorine and Sodium, 55.74% and 30.98%, respectively. The total of ions content is therefore 33.39 g/L.

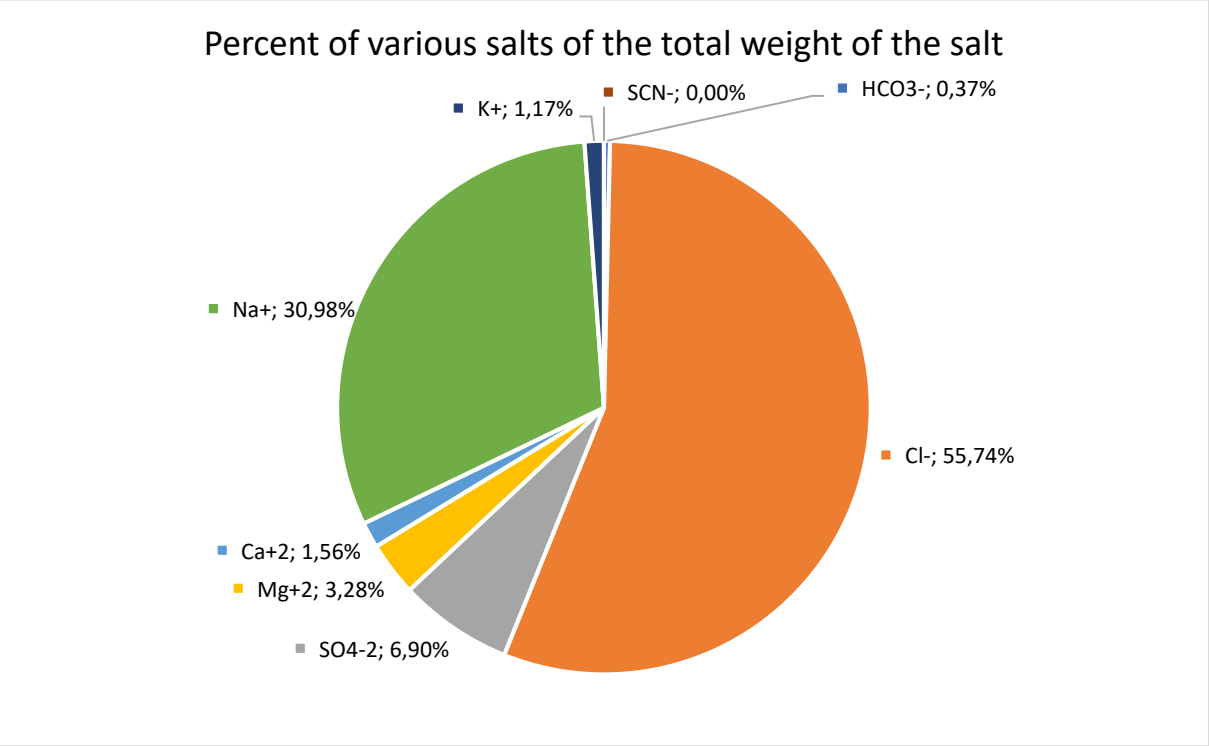

Figure 14 The salt components of seawater [42]

4.5 OIL

The selected oil for the majority of the experimental work was Decane, a hydrocarbon which is more specific categorized as an alkane. The common attribute among alkanes is the tree – structure of atoms where there are only single bonds between carbon – carbon atoms. Even though there exist 75 unique isomers of this alkane, Decane is most common with the chemical formula $CH_3(CH_2)_8CH_3$ also known as "n – Decane".

Quite like other alkanes or paraffins, the characteristics of these hydrocarbons are such as

easily combustible, non – polar solvent and as well impossible to dissolve in water.
Under normal conditions, will n – Decane have density as 730 kg/m^3, while the viscosity of the solvent is 0.838 mPa s. [43]

4.6 NANOPARTICLES

SiO_2 is the chemical formula for the chosen nanoparticle substance in this particular thesis, and Silicon Dioxide may often also be named as easily as Silica. These particles can be found worldwide, and is quite abundant in sand, existing i.e. in quartz. [44]

The exact silica nanoparticles used in this thesis work has been purchased from EPRUI Nanoparticles and Microspheres Co. Ltd. According to the research of literature study, Silicon Dioxide has been extensively applied in structural materials, pharmaceutical and electronic industries.
Additionally, due to the abundance and low cost, SiO_2 has also been investigated in the oil and gas industry. The potential of enhancing the oil recover has been proved, and can be found summarized in the literature study, section 2.2.

The purchased Nano – silica from EPRUI Nanoparticles and Microspheres Co. Ltd was in this thesis, experimentally tested in terms of enhancing oil recovery and as well the drilling fluid. In order to understand more about the nanoparticles and how these particles may alter the EOR and DF, characterization of the Silica nanoparticles had to be conducted.

Scanning Electron Microscopy (SEM) imaging was used to determine the size of the particles, while Energy Dispersive Spectrograph (EDS) was used to determine which elements was present in the particles. The sample of Nano – powder had to be coated with Palladium before preparing the sample for imaging in SEM – apparatus. The coating of Palladium will ensure the bombardments of electrons will travel easily on the surface of Silica nanoparticles, resulting a more accurate image and better contrast. The SEM images revealed the Nano-sized of the particles was averaging 15 nm.

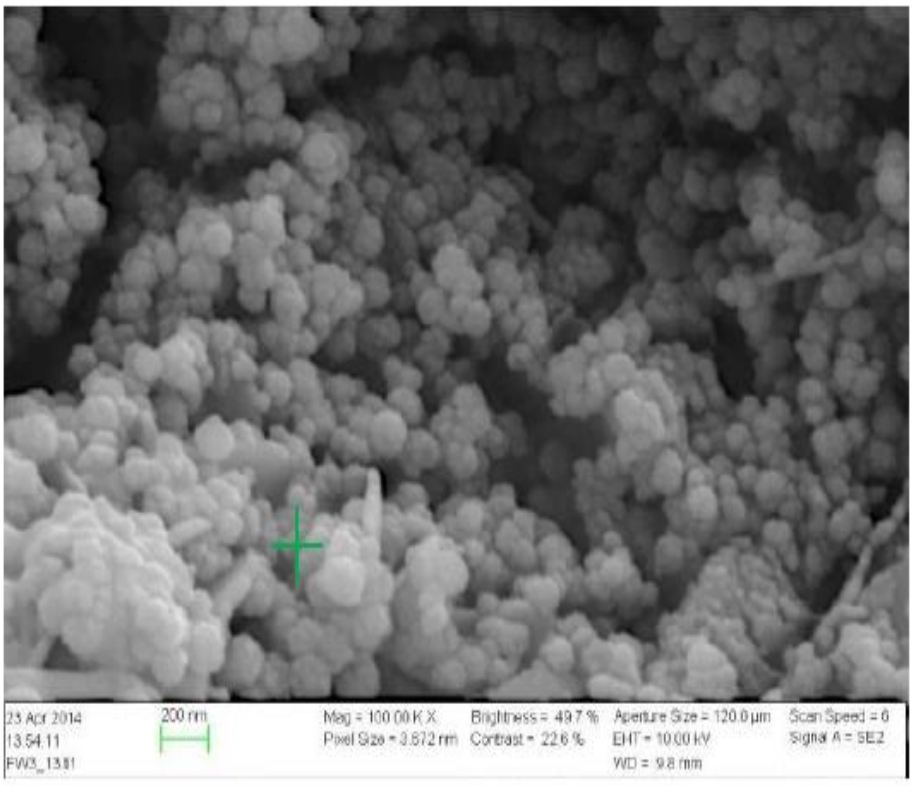

Figure 15 Scanning Electron Microscopy (SEM) image of commercial SiO_2

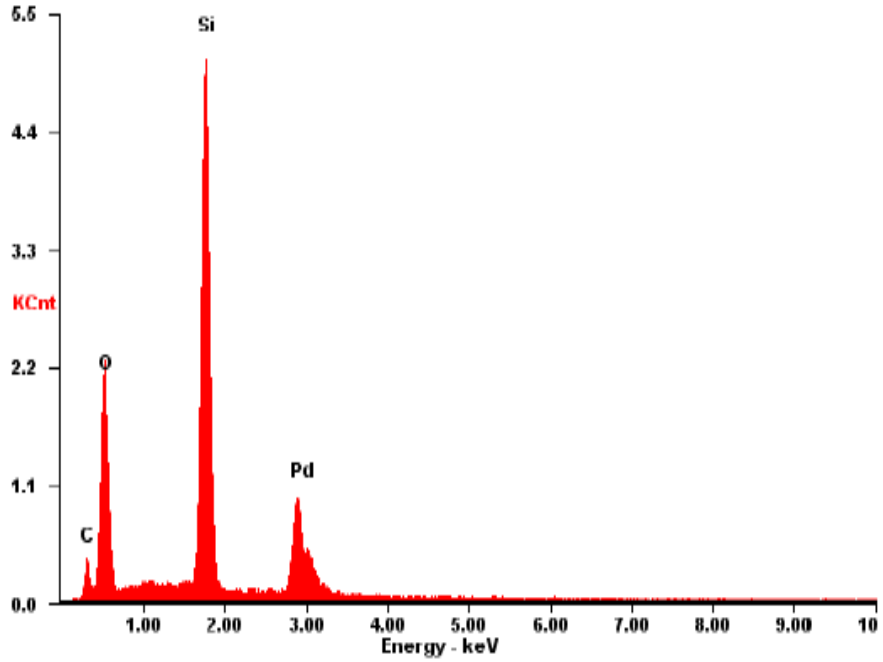

Figure 16 The element analysis of SiO_2 obtained by Energy Dispersive Spectrograph.

4.7 EOR MECHANISMS

In this section of the thesis, the importance of understanding the nanoparticle's role for enhanced oil recovery mechanisms is highlighted. For in the recent investigations of the relation between the nanoparticle, rock media and the hydrocarbon has showed promising results. In order to develop and utilize the nanotechnology in the production of oil and gas, the mechanisms of the enhanced oil recovery have to be revealed and studied thoroughly.

Currently, the application of nanotechnology in the production part of the industry can be categorized into three parts: Nano catalysts, Nano emulsion and nanofluids (NF). The following text will highlight only the latter part as it is what the thesis is about.

4.7.1 IFT REDUCTION

The interfacial tension plays a central part to find out how the distribution of the fluid is in the rock media, as well as the flow in it. Due to those reasons, the interfacial tension value is important to achieve to understand the enhanced oil recovery technique.

Usually, the most common method to measure the interfacial tension between an aqueous solution and crude oil is to conduct a pendant drop method. In the pendant drop method, a capillary needle is filled with the crude oil and generates an oil droplet surrounded by the chosen aqueous solution. Additionally, the conditions under the experiment is important to take account for as well, such as pressure and temperature which may alter the fluids properties. To be able to calculate the value of interfacial tension, the generated oil drop has to be analysed by a proper video system and the associated software. The lower the IFT is, the easier it is to allow the oil to flow. [45]

4.7.2 WETTABILITY ALTERATION

As mentioned earlier in the text, the description of the wettability of a rock is the tendency to either spread or adhere wholly over the surface of the rock while an immiscible fluid coexists. To be able to control completely over the extraction of hydrocarbons, to understand how to affect the fluid saturation, capillary pressure and relatively permeability is crucial.

Nanofluids have previously shown to be able to change the wettability of the rock, although the lack of further investigation has not seen these being utilized yet.

At the moment, there is three main methods to measure the wettability of the rock surface: Amott test, core displacement test and contact angle method. The latter method is the most common to be utilized as it is easier to conduct and is also conducted later in the thesis. [46]

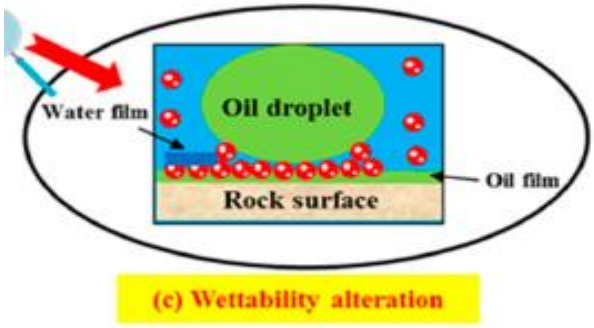

Figure 17 The mechanism behind alteration of wettability [44]

4.7.3 REDUCED MOBILITY RATIO

Another crucial parameter in terms of enhancing the oil recovery is the mobility ratio of the injected fluids to the oil in the porous media. The following equation shows how the mobility ratio can be calculated [48]:

$$M = \frac{\lambda_{\mathrm{i}}}{\lambda_{\mathrm{o}}} = \frac{k_{ri}\,\mu_o}{k_{ro}\,\mu_i} \qquad 34$$

In the equation, the term i and o states for the fluid injected and the oil. λ, k_r and μ_o stands for the mobility, relative permeability and viscosity, respectively.

The usual issues for enhancing oil recovery in terms of the mobility ratio are the poor sweep efficiency, poor conformance and the risk of viscous fingering of the fluid injected.

Nanoparticle has the ability to reduce the high mobility ratio caused by the conventional injected fluids such as CO_2 or water which both have lower viscosity than the oil. The ability to enhance the viscosity of the injection fluid and lower the ratio of mobility. [48]

4.7.4 DISJOINING PRESSURE

When the suspended nanoparticles in a nanofluid is in direct contact with the oil phase in a porous media, these nanoparticles tend to form a wedged film. The film serves the purpose to separate the droplets of oil from the surface of the porous media which leads to greater recovery compared to the conventional way. The reason why the nanoparticles forms this wedged film is due to a structural disjoining pressure. The injected nanofluid will make use of the pressure, as this forces the nanoparticles into the cramped area ahead. The nanoparticles form the arrangements as the figure 18 illustrates and leading to increasing the entropy of the fluid since the they have better space in the nanofluid itself. The development ends with the arrangement of nanoparticles take the advantage of the additional disjoining pressure at the region rather than in the liquid. [49] [50]

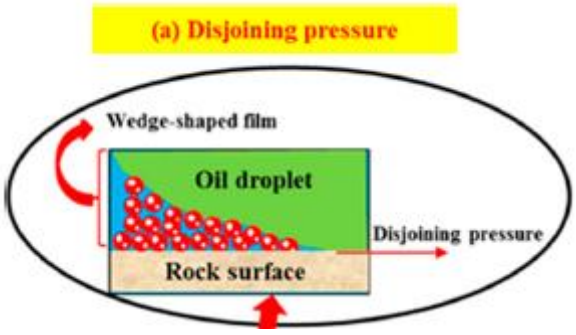

Figure 18 The mechanism behind disjoining pressure [44]

5. EXPERIMENTAL WORK

The main objective of this thesis is to examine the significance by applying nanotechnology in terms of oil and gas industry. The fourth chapter of the thesis will present the experimental work as it is divided into investigation of nanoparticles in both the performance of drilling fluids and enhanced oil recovery. While based on the extensive literature study, Nano Silica will be designed and studied in the mentioned application areas.

5.1 IMPACT OF NANO - SiO_2 in EOR

Subsequent will the preparation of the nanofluid be presented, and will besides be characterized, and investigated in terms of affecting the enhanced oil recovery.

5.1.1 PREPARATION OF SILICA NANOFLUIDS

The procedure of formulating the systems of nanofluid:

1. Pour 250 mL deionized water into a mixing cup.
2. Weight both the amount of salt (7,5 g) and nanoparticles for the respectively fluid system listed in the table 8
3. Use a mechanical mixer to blend the fluid with the salt first and add the nanoparticles after that. The time of the mechanical stirring should be around 15 min to obtain a homogenous solution.
4. Pour the fluid system into a beaker and place the beaker to the ultrasonicator.
5. Adjust the amplitude and the timer for X and 1 hour, respectively.
6. Finally, the beaker with the solution of nanoparticles should be left for 12-hour magnetic stirring.

Fluid system	**SiO_2 concentration [wt %]**	**Deionized water [g]**	**NaCl [g]**
A	0,025	250	7,5
B	0,050	250	7,5
C	0,075	250	7,5
D	0,100	250	7,5
E	0,150	250	7,5

Table 8 The formula for the designed nanofluid system with vary concentrations of SiO_2

Figure 19 Left: Magnetic stirrer Right: Ultrasonicator

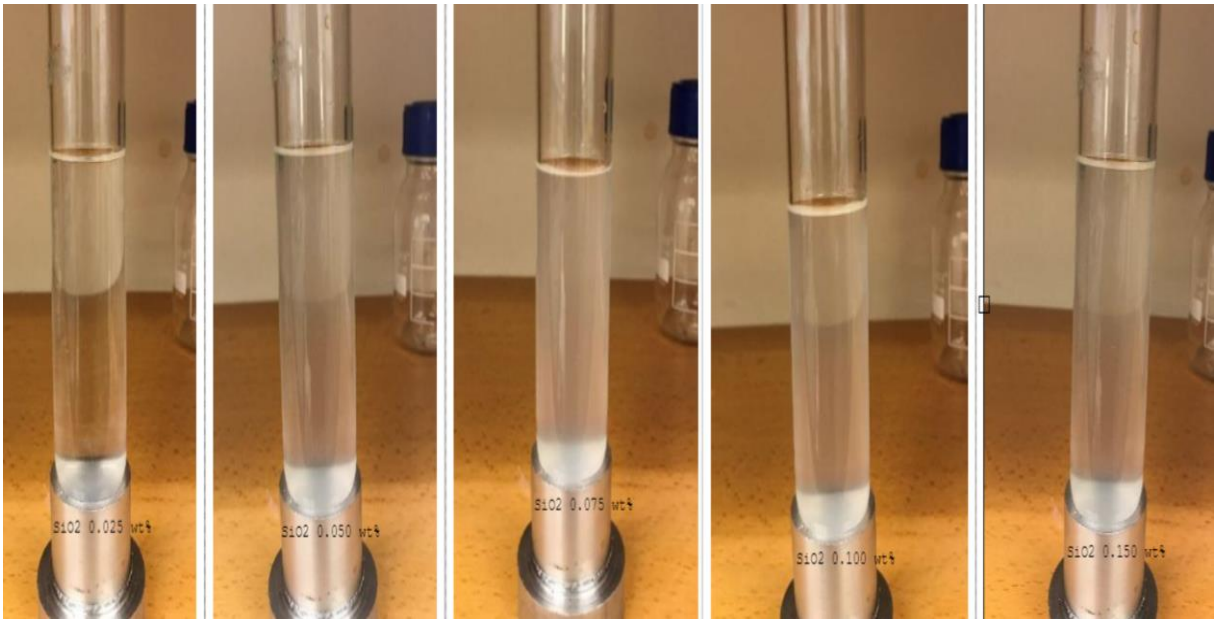

Figure 20 Visual appearance of the formulated nanofluids with diverse concentrations

The stability of the nanofluids was visually examined as the figure 20 presents, and the stability was approved after 24 hours with no evidence of accumulations of particles in the bottom.

5.1.2 DENSITY & VISCOSITY OF SiO_2 NANOFLUIDS

The formulated nanofluid had to be characterized, and both the density meter and the rheometer were provided by Anton Paar, modelling DMA 4100M and MCR 302, respectively, were conducted to measure the density and viscosity. The temperature was kept constant at 20 C throughout both tests, and the final results are presented in the table 9.

Fluid system	Concentration of SiO_2 [%]	Average Viscosity [mPa s]	Density [g/cm3]
A	0.025	1.09	1.0244
B	0.050	1.09	1.0253
C	0.075	1.16	1.0257
D	0.100	1.18	1.0260
E	0.150	1.07	1.0263

Table 9 The measured viscosity and density values for the associated nanofluid systems.

5.1.3 EFFECT OF SiO_2 NANOFLUIDS ON INTERFACIAL TENSION

Interfacial tension is among the most crucial part to describe the condition in the reservoirs, as well as being one of the major enhanced oil recovery mechanisms described in Section 4.7. In this subsection, the preparation of the tensiometer and conducting the Du Noüy ring method will be demonstrated.

5.1.3.1 PREPARATION OF DU NOÜY RING METHOD

1. A platinum ring should hang as the figure 21 shows.
2. The ring has to be cleaned before use of the tensiometer.
   The platinum ring should first be soaked with White Spirit, and then with Acetone.
   Let it dry off by air.
3. The measuring cup should be cleaned thoroughly with soap, before rinsed with distilled water. Lastly, wipe off with a paper towel.
4. Pour the chosen fluid into the measuring cup.
5. The instrument has to be placed upon a vibration – free substratum.
   Adjust the instrument to be fully horizontal.
6. Regulate the lever to make it within the black areas on the cursor.
7. At last, centre the ring above the surface of the fluid in the measuring cup.

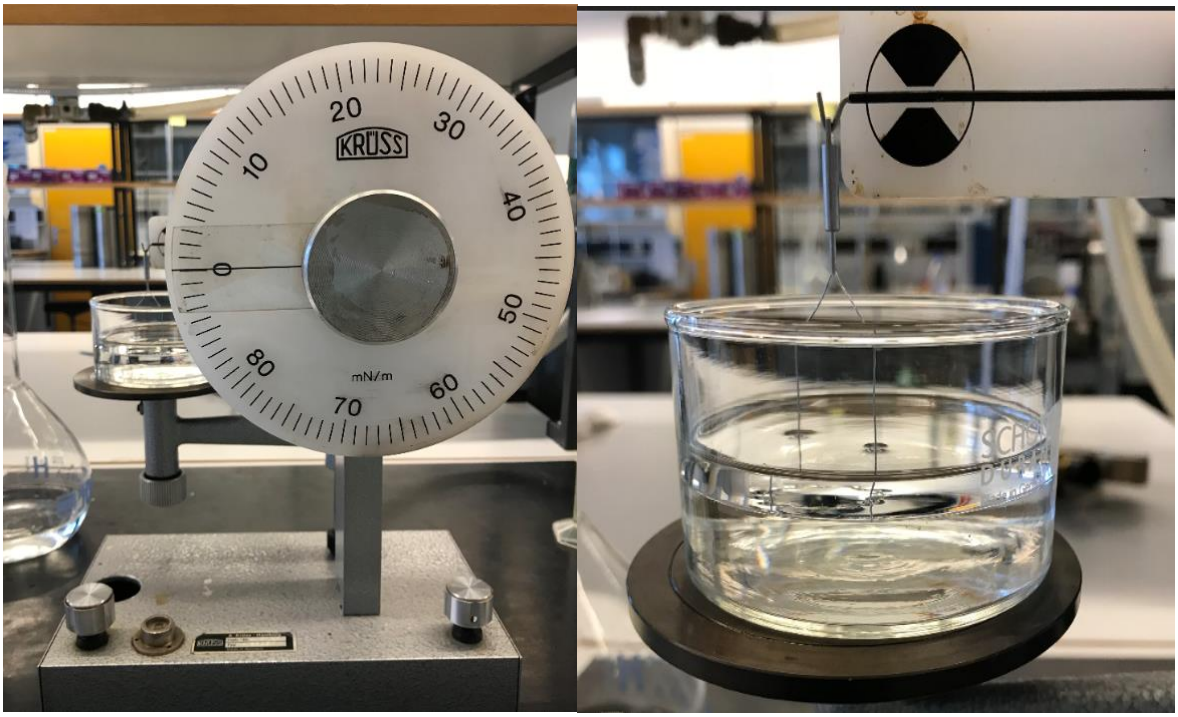

Figure 21 Tensiometer for Du Noüy Ring method

5.1.3.2 CALIBRATION

The tensiometer from Krüss is basically linear compensated from the factory, which means the measured surface tension between air and distilled water should result with a correct value as 72,75 mN/m at 20 C.

Although, over a longer period of time of using the instrument, the result might differ from the correct value as stated above. Another factor as replacing the original platinum ring will also affect the result. Only a calibration of the tensiometer is sufficient to be able to correct the divergence, and in order to calibrate the instrument, a measurement of a double – distilled water has to take place.

The surface tension of the double – distilled water should be within the values provided by the figure 22. For instance, the measured value for the surface tension is 71,00 at room temperature, the factor of calibration should be:

$$k = \frac{72{,}75}{71{,}00} = 1{,}02 \qquad 35$$

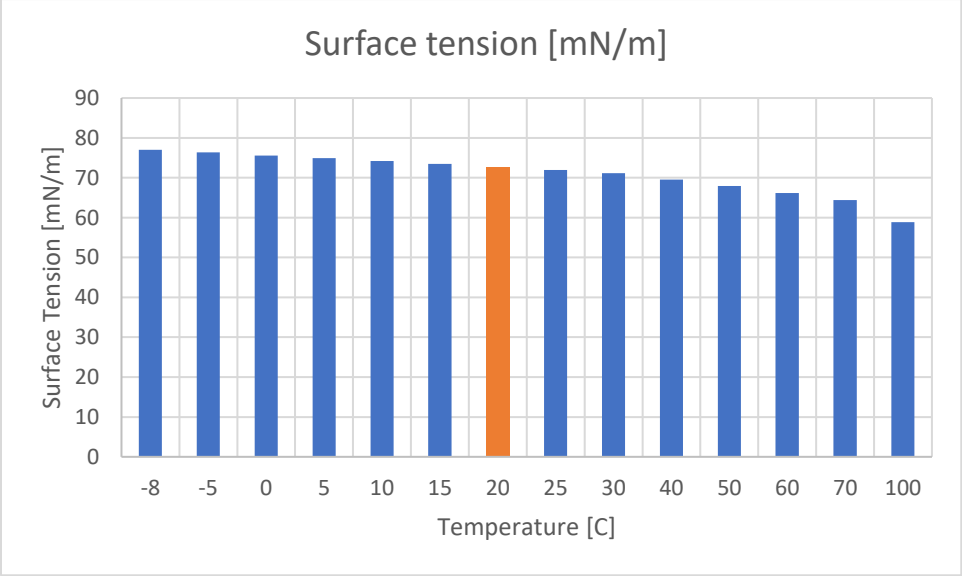

Figure 22 The surface tension for water in different temperatures

5.1.3.3 CORRECTION FACTOR

The following equation can be applied whenever the tensiometer has been calibrated, and the tension of either surface or interfacial can be calculated by:

$$\sigma = \sigma^* \cdot k \cdot F \qquad 36$$

Where σ = surface/interfacial tension

σ^* = uncalibrated surface/interfacial tension

k = calibration factor for the tensiometer

F = correction factor for the platinum ring and fluid

To fully measure the surface tension and the interfacial tension, the value read of the measuring disc has to be corrected with a correction factor, F, which depends both on the size and shape of the platinum ring, as well as the volume of the fluid that is lifted during the measurement. The fully calculation can be found in the Appendix D.

$$F = \left[0{,}725 + sqrt\left(\frac{0{,}01452 \cdot \sigma^*}{\frac{U^2}{4} \cdot (\rho_2 - \rho_1)} + 0{,}04534 - \frac{1{,}679}{\frac{R}{r}}\right)\right] \cdot 1{,}07 \qquad 37$$

$$U = 2 \cdot \pi \cdot (R_i + R_o) = 2 \cdot \pi \cdot (R + R) = 4 \cdot \pi \cdot R \qquad 38$$

Where U = wetting length of the ring, [cm]

σ^*= uncalibrated surface/interfacial tension, [dynes/cm]

r = radius of the cross section of thread of ring, [cm]

R = radius of platinum ring, [cm]

ρ_1 = density of oil, [g/ml]

ρ_2 = density of NF, [g/ml]

5.1.3.4 MEASURED IFT RESULT

Whenever a measurement of the interfacial tension shall be conducted between two immiscible fluids, the fluid with the highest density shall be poured in the measuring cup before the ring shall be lowered into it.

Add another 1 cm of the other fluid into the measuring cup. In order to avoid the latter fluid to be in contact with the platinum ring, use i.e. a pipette and carefully add the fluid against the wall of the measuring cup.

Lower the platform by adjusting the screw (12) and raise the lever with the screw attached to the measuring disc (3). Never let the lever get away from the centre of the cursor (6). Adjust the platform and the lever alternatively in order to observe whenever the ring loses the grip at the interfacial between the fluids. The following figure 23 presents the obtained corrected IFT measurements for the different fluid systems, as well as the change of IFT in %.

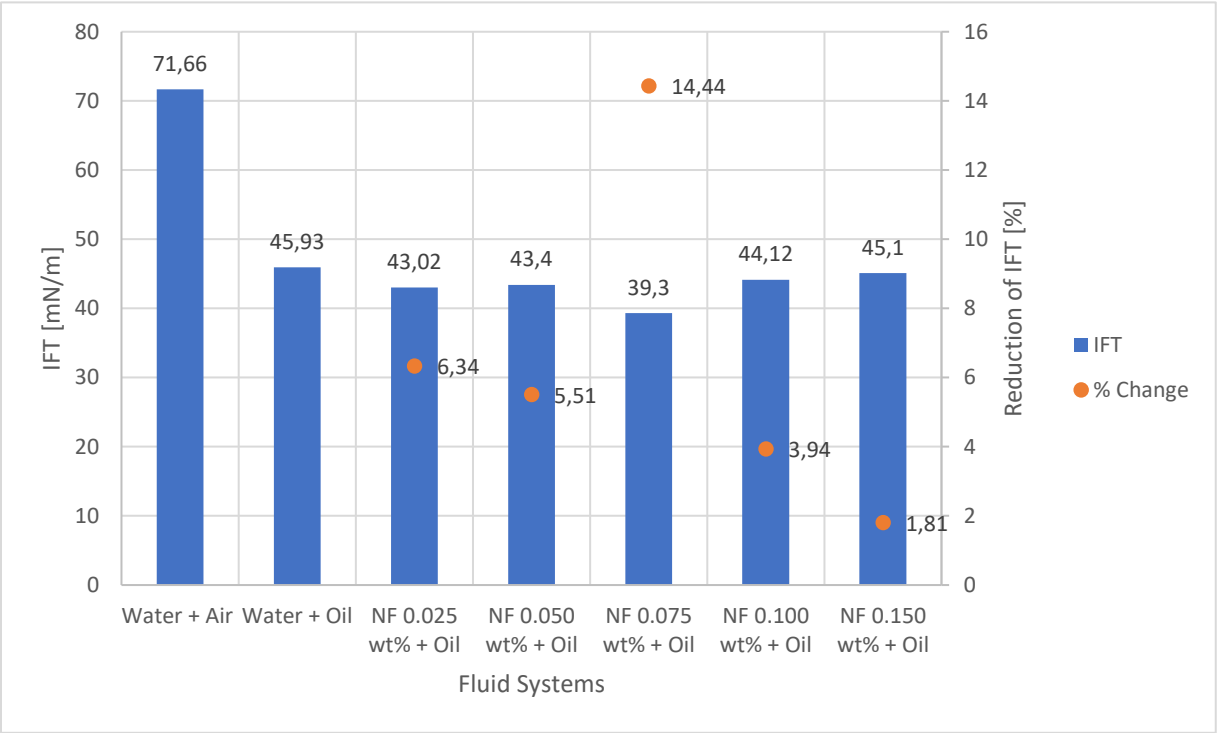

Figure 23 : A graphically presentation of the IFT values obtained for the different fluid systems

5.1.3 EFFECT OF SILICA NANOFLUIDS ON CONTACT ANGLE

The drop shape analyser has the ability to measure the contact angle in numerous ways. Due to our arrangement where the objective is to measure the contact angle between the glass plate (solid) and the oil drop (low density liquid) surrounded by brine or nanofluid (high density liquid), the measuring method such as captive bubble fits the bill.

The following procedure describes how to measure the contact angle by conducting the Krüss drop shape analyser:

1. Clean and dry the fluid container of glass, and the glass plate with Ethanol before placing the arrangement as the following figure 26 shows.
2. Use a pipette to extract the chosen surrounding phase and fill up the container. Remember to avoid bubbles or air trapped beneath the glass plate.
3. Adjust the position of the system table in front of camera.
4. Extract some of the chosen oil type with a syringe, and place an oil drop beneath the glass plate by utilizing a hooked needle tip.
5. Adjust system settings such as contrast, brightness and illuminance to aid the software to be able to get the right calculations to measure the contact angle.
6. Start measuring and repeat the previous steps for any other samples.

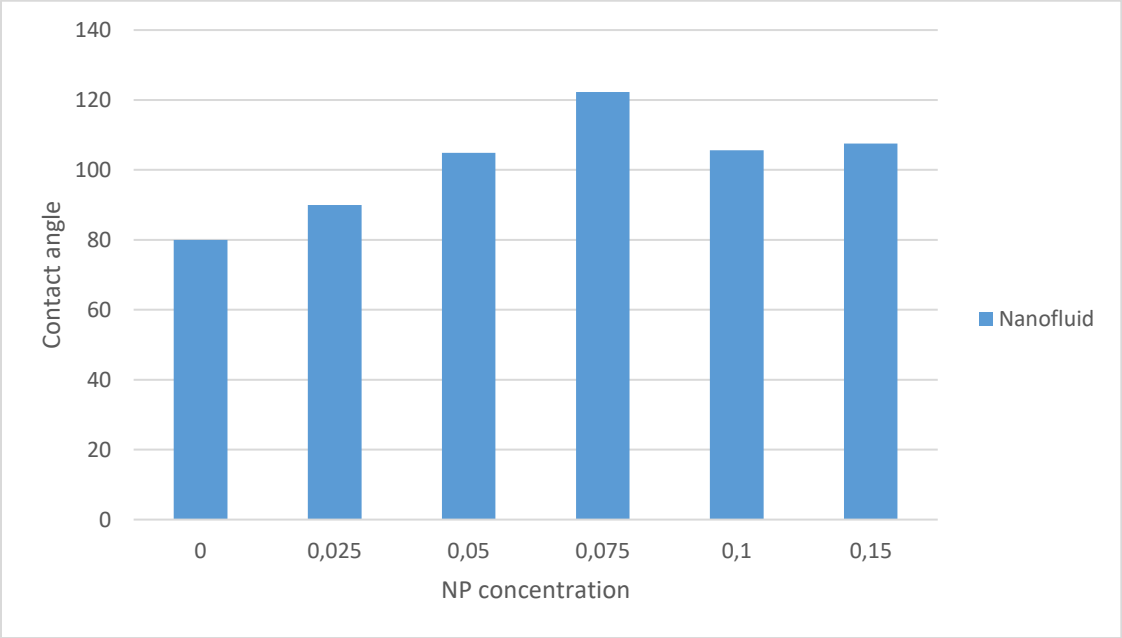

Figure 24 A graphically presentation of the contact angles for varied fluid systems.

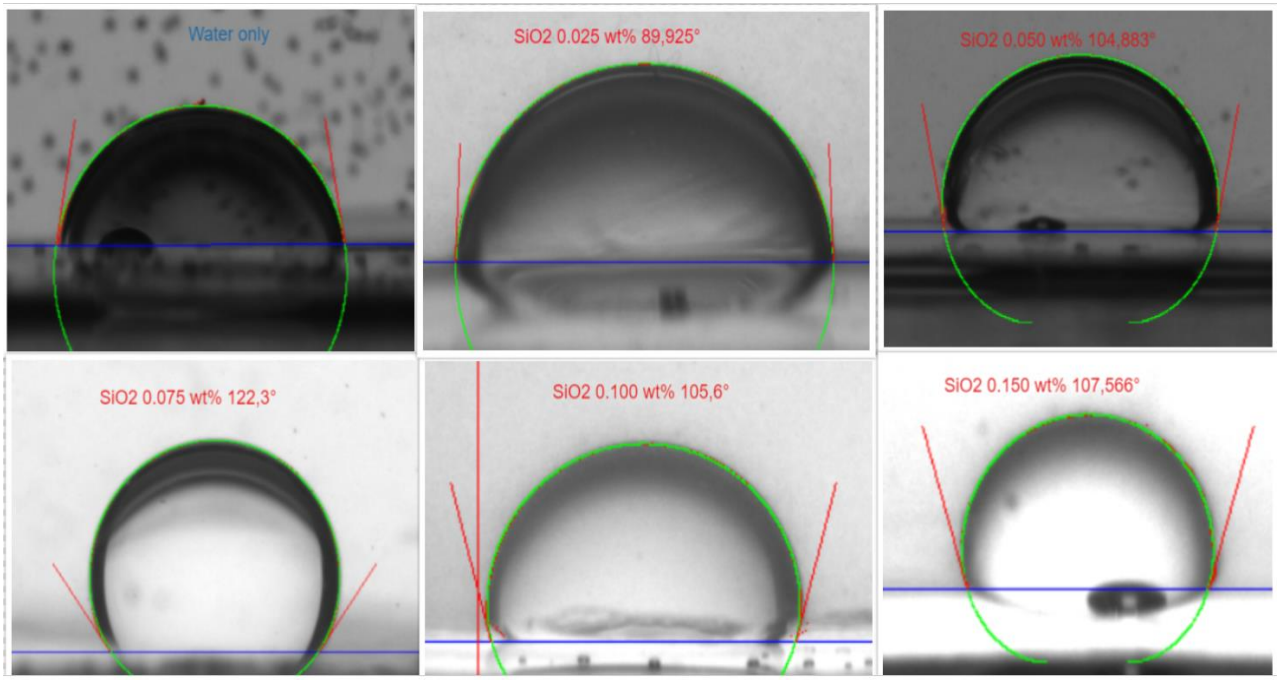

Figure 25 The contact angle measured by Krüss drop shape analysis system.

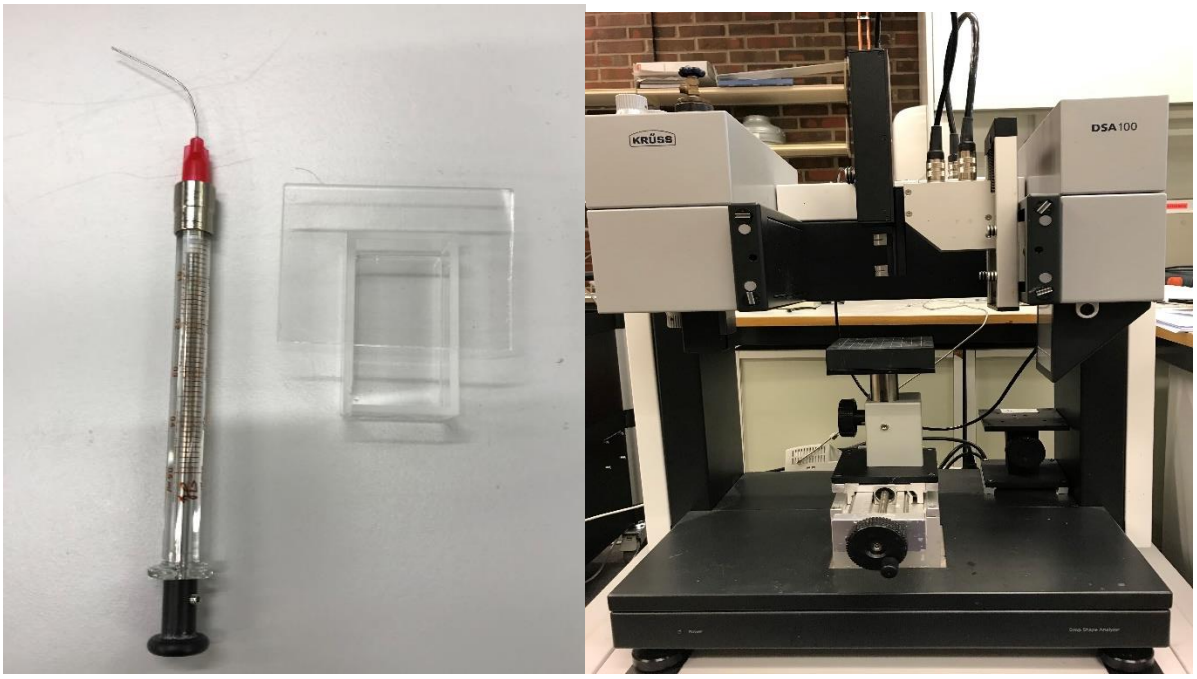

Figure 26 A hooked needle of the syringe, and the glass container setup for the CA measurements with the drop shape analyser

5.1.4 CORE FLOODING

In this following section of the experimental work, flooding test will be presented as a part of the investigation of the performance of nanoparticles regarding EOR. Different concentrations of nanoparticles in fluid systems will be utilized as a part of a tertiary recovery method. Additionally, the core plugs will be heated up to 70 C during the flooding tests. A schematic illustration of the setup for the experimental work is presented below with the major components.

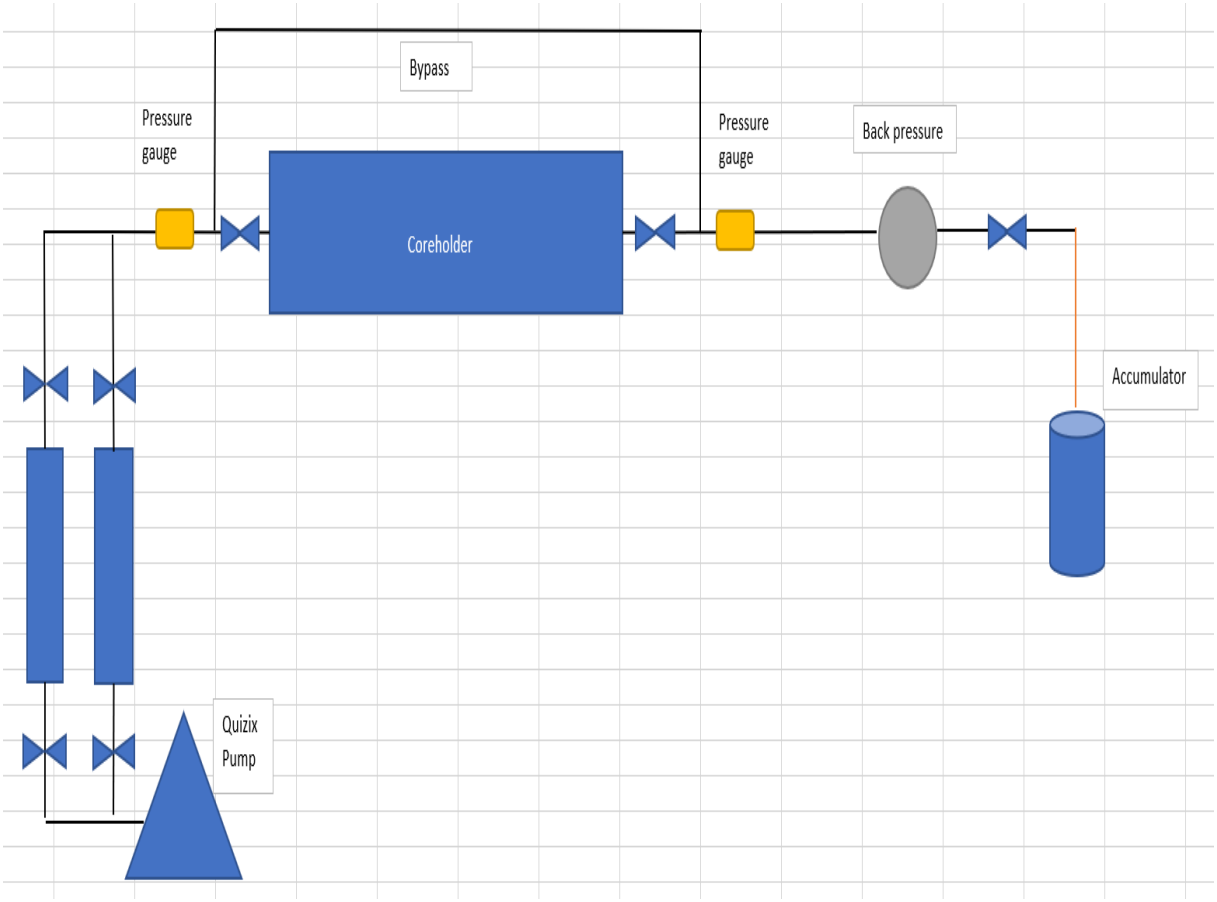

Figure 27 A schematic figure of the core flooding setup at IRIS

5.1.4.1 Saturation of seawater

Just after the bulk measurements of the Berea sandstone cores had been recorded and calculated, the selected core plug will have to be saturated completely with seawater. A vacuum pump was firstly connected to core holder as the core is rigged up as the illustration shows the setup for this part of laboratory work. The purpose of vacuuming the core plug is to ensure there is no fluids left in the pores of the Berea sandstone. The period of the extraction of any eventually existing fluids in the pores was approximately 30 minutes.

After the extraction, a container of seawater was connected back as the figure 27 shows, and the saturation of the core has begun. Additionally, the pore volume of the core was recorded as the parameter is able to determine the porosity.

5.1.4.2 IRREDUCIBLE WATER SATURATION

In the next step of the laboratory work for flooding the cores, the wholly saturated cores with seawater will undergo a drainage process. The forcing fluid is decane and will be injected at a constant rate of 3 mL/min under ambient conditions, and the process will take place until no more water is being produced. The amount of water produced under the drainage process will be recorded, and after 20 pore volumes, the irreducible water saturation was established for the core. The following equation will determine the value of irreducible water saturation.

$$S_{wi} = 1 - \frac{V_w}{V_{pore}} \qquad 39$$

Where S_{wi} is the irreducible water saturation, V_w is the produced water volume and V_{pore} is the pore volume of the core plug.

5.1.4.3 MEASURE PERMEABILITY

As the pore volume of the cores was found in Section 5.1.4.1 to determine the porosity, the other important parameter of the porous media will be measured in the section. The absolute permeability of the sandstone cores will be determined by using either oil or water in various scenarios. Especially, the permeability before and after injecting Nano silica will be highlighted as the parameter may explain the influence of silica.

The schematic figure 27 shows the setup of the flooding experiment where the cores are placed in their respectively core holders which initially is pressurized to 10 bars as a sleeve pressure.
In order to keep the flow consistent and stable at all time, a Quizix dual piston pump was introduced with the containers filled up with either seawater, distilled water or silica nanofluid.

In terms of varying the injecting fluids for purposes as saturation and drainage process, the pressure will also differ at the inlet and outlet for the different fluids. The differential pressure is recorded during the flooding tests of core plugs, as the calculation of the permeability depends upon it. The following Darcy equation shows the relation for determining the permeability of the cores:

$$\frac{q}{A} = \frac{k}{\mu \, \Delta l} \, \Delta p \qquad 40$$

Where q is the flowrate, A is the cross – sectional area, k is the permeability, μ is the viscosity, Δl is the length of the core and Δp is the differential pressure.

Core	Vp mL	Nanofluid wt%	Rate water mL/min	dP (pre) mbar	K abs mD	Rate nano mL/min	Inj nano mL	Rate water mL/min	dP (post) mbar	K Abs mD	K ratio (%)
1	19,368	0.050	3	426	75,58	1	80	3	431	74,70	-1,16
						3	90				
3	19,596	0.075	3	358	89,64	1	100	3	348	92,21	+2,87
						3	60				

Table 10 Measuring the permeability before and after injection of nanofluid for the various cores.

5.1.4.4 FLOODING TESTS

In this section, the experimental flooding of the Berea sandstone cores will be reviewed as well present the procedure. After the irreducible water saturation was achieved in Section 5.1.4.2, the temperature of the oven was increased up to 70 C and left to age for 12 hours. The temperature of all the following experimental work for flooding remained at 70 C.

The residual oil saturation had to be obtained as well, and by flooding seawater until the oil production stopped in the process of imbibition. Water flooding was firstly conducted to core plugs as step one of a tertiary recovery technique. Seawater was injecting at a constant rate at 3 mL/min through the core, and the volume of produced oil will determine the recovery factor. The water flooding establishes a baseline for the experimental work and will be the reference level regarding the enhanced oil recovery by nanofluid.

The second step is to inject the chosen concentration of nanofluid by 1 mL/min and ramped up to 3 mL/min if the oil production stagnates. Lastly, a flooding by seawater once again will complete the tertiary recovery method as it will eventually reveal the impact of nanofluid in terms of enhancing oil recovery.

Figure 28 presents the recovery factor as the pore volumes of the injected fluid increases. A dashed line represents the original recovery factor if the enhanced oil recovery technique was not introduced.

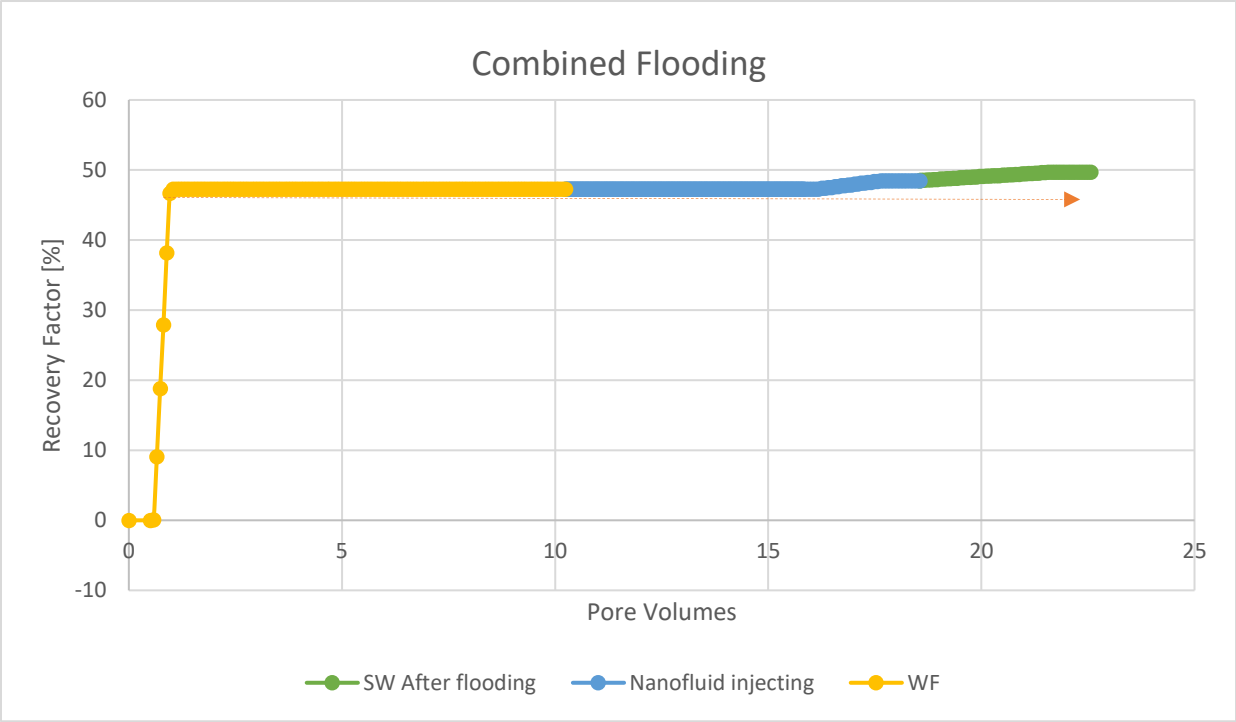

Figure 28 The ultimate recovery factor for core 3 with the function of cumulative injected PV

5.2 IMPACT OF NANO - SiO_2 in DRILLING FLUIDS

As mentioned, the experimental work will be divided into two parts. This section will firstly formulate drilling fluid systems with nanoparticles, review the influence of including nanoparticles of SiO_2 in drilling fluids, and evaluate the final attributes.

5.2.1 INFLUENCE OF SILICA IN CMC DF

In this section, the influence of silica nanoparticles in drilling fluid containing CMC as a polymer was studied thoroughly. The concentrations of the nanoparticles were relatively low and were the lower part of the selected range of them in the EOR investigation. Although, the lower concentrations of Nano silica have proved to be the better solutions for enhancing the ultimate oil recovery in the literature study, a higher concentrations of silica nanoparticles were also included in this investigation.

5.2.1.1 PREPARATION OF CMC DF

Additives	Base fluid (BF)	BF+0.025g SiO_2	BF+0.050g SiO_2	BF+0.075g SiO_2
Water, g	500	500	500	500
Bentonite, g	25	25	25	25
KCL, g	2.5	2.5	2.5	2.5
CMC, g	0.5	0.5	0.5	0.5
SiO_2, g		0.025	0.050	0.075

Table 11 Formulation of the designed CMC based drilling fluid systems

As the name of the subsection mentions, Silica nanoparticles along with CMC as the polymer was firstly prepared and latter investigated for the impact of nanoparticles in drilling fluids. The secondary intention behind the design of these drilling fluids mentioned in the table 11 above, is to namely to figure out how the salt, polymers and nanoparticles of Silica would affect each other in the mixture. Additionally, the objective also covers the determination of which system of drilling fluid has the superior results, as well as the best potential. In order to stabilize the designed drilling fluids, salt was included as the main stabilizer agent. While Bentonite was added into the recipe to be able to control the filtrate loss of the drilling fluid, and the function of polymer is to give the mixture a boost of viscosity as this plays as one of the key factors of the rheology.

The preparation of the drilling fluid – systems was made of the following additives, and in such procedure respectively as well:

- Water
- Salt
- Polymer
- Nanoparticles
- Bentonite

The correct amount of the additives can be found in the table 11, and in order to have a baseline for the investigation, a drilling fluid system with no nanoparticles was prepared additionally. While other systems had various containing Silica nanoparticles to investigate the difference effect of the concentrations to their rheology properties. On the other hand, the remaining additives such as salt, polymer, water and Bentonite were held at a constant amount throughout the investigation and for all drilling fluid systems.

The first step of the procedure of preparing the numerous drilling fluids, water from the tap was poured into a mixing cup for the Hamilton mixer. Due to the salt can easily be mixed in water, the potassium chloride was directly added into the mixing cup and solely mixed with a spoon.
The next step is rather trickier, as the polymer has a tendency to agglomerate into lumps which often is impossible to blend into the designed mixture. The vital part of adding CMC as the polymer in the system is to carefully add small particles of it into the system and mix it. Add only small amount at the time, and repeat these steps until all of the given amount of CMC is fully blended into the drilling fluid mixture. Lastly, add the correct amount of the Silica nanoparticles for the given system, as well as the Bentonite afterwards.

Thereafter, all of the finished systems of drilling fluids have to be allowed to age for 48 hours to obtain accurately swelling process of Bentonite.

5.2.1.2 RHEOLOGICAL RESULTS OF CMC DF

In this particular section, the characterization of the drilling fluids prepared in the previous section will be focused. The following fundamental properties of their rheology respectively will be interpreted.

In the following figure 29, the data of viscometer for CMC was obtained by conducting shear stress on the chosen drilling fluids. The figure shows an alteration of shear stress for the systems containing various concentration of Silica nanoparticles in comparison to reference system with no nanoparticles added to it. The values for shear stress for all the drilling fluid containing nanoparticles were found to be lower than the reference drilling fluid.

In fact, the drilling fluid containing the highest concentration of Silica nanoparticles had the highest reduction of shear stress. While the drilling fluid containing 0.050 g of Silica nanoparticles proved to have the lowest reduction among the nanoparticle – treated drilling fluid systems. From the obtained viscometer – values presented in the figure, the plastic viscosity (PV), yield stress (YS) and lower shear yield stress (LSYS) were calculated and presented according to the Bingham plastic model in figure 5.12.

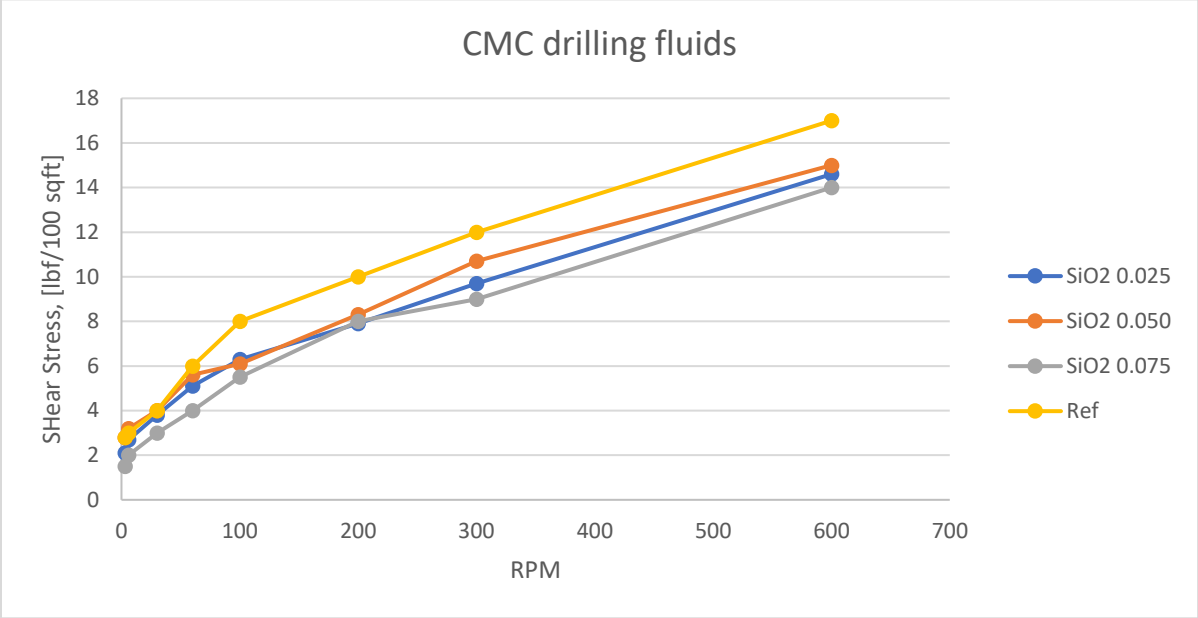

Figure 29 A plot of the measured values obtained by Fann Viscometer for CMC based systems

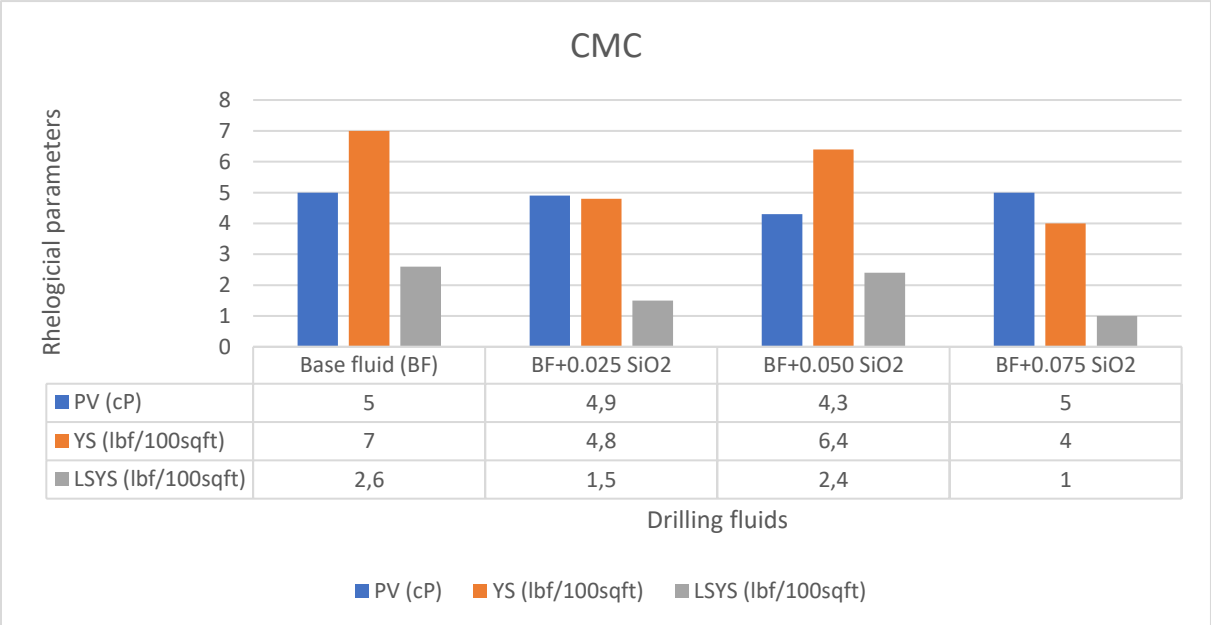

Figure 30 Calculated parameters such as PV, YS and LSYS in regard of Bingham model for CMC based drilling fluids.

According to the Bingham plastic model:

- The plastic viscosity value remained the same for the drilling fluid containing the highest concentration of Silica nanoparticles compared to the reference fluid with no nanoparticles.

  While the PV value decreased the most for SiO_2 0.050g, by 14 % reduction. The last fluid showed a small differ from the reference fluid system, and barely decreased by 2% of the plastic viscosity value.
- Similar to the plastic viscosity, the yield stress values decreased for the drilling fluids containing any nanoparticles.

  The highest difference for the yield stress alteration can in this scenario be found for the SiO_2 0.075g, by 42,8%. This differs from the PV results, where the same fluid system did not alter the PV value at all. Meanwhile, SiO_2 0.025 g and SiO_2 0.050 g decreased the yield stress by 31,4% and 8,6% respectively.

5.2.1.3 FRICTION MEASUREMENTS OF CMC DF

The figure 31 shows the obtained values of the CSM tribometer which measures the friction within the various drilling fluids. The idea behind this is to study the impact of lubrication of the drilling fluids containing any nanoparticles compared to the reference fluid system. As mentioned earlier in the section 5.2.1, in this particular investigation of friction measurements, one fluid system was included additionally to the original drilling fluid systems. The new one is namely a reference drilling fluid with 0.3 wt% as showed in figure.

The figure shows both the coefficient of friction (at the left-hand side of the diagram) as post diagram, and as well as the change of the coefficient of friction in terms of percentage (at the right-hand side of the diagram) as the orange curve.

Clearly, the drilling fluid containing only 0.025g of Silica nanoparticle as the most optimum in regards of reduction of coefficient of friction. The reduction in terms of percentage is actually 15%, and for the system containing 0.050g of Silica nanoparticle reduced by 13%, while the

rest of the nanoparticle treated drilling fluid actually gave higher values than the reference level was.

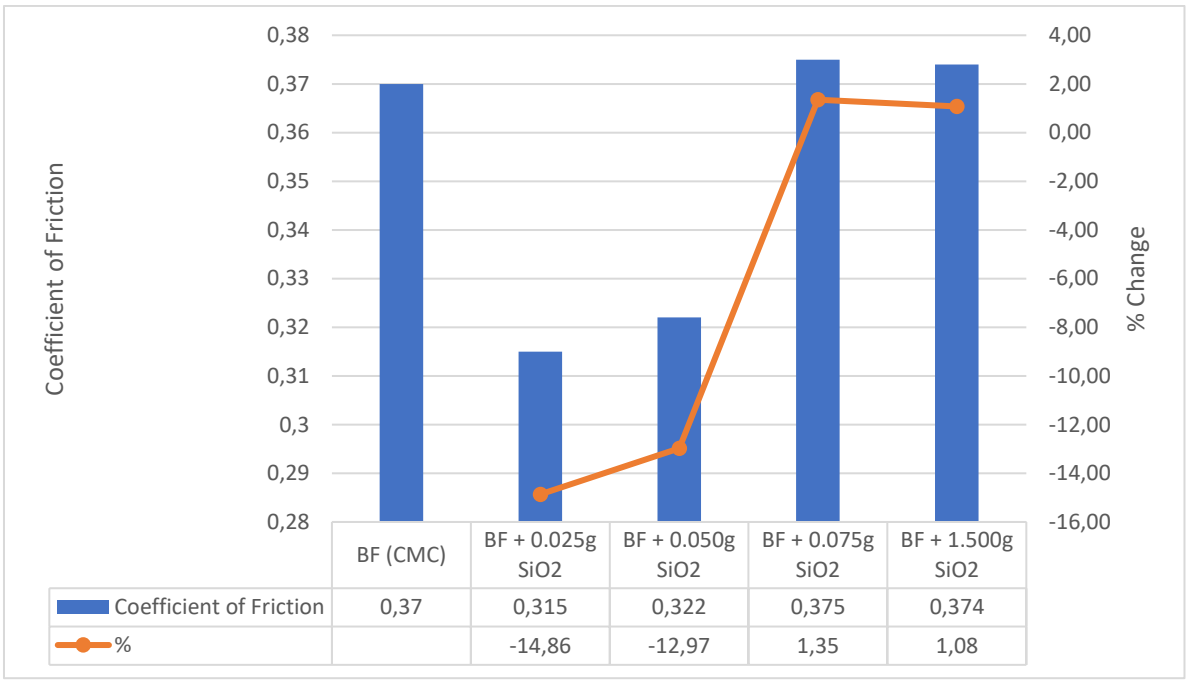

Figure 31 Coefficient of friction for the various CMC based drilling fluid systems obtained by tribometer.

5.2.2 INFLUENCE OF SILICA ON DUOVIS DF

In this segment of the experimental work, the influence of Silica nanoparticles was studied thoroughly in drilling fluids with Duovis as the polymer. The selected concentrations of nanoparticles were 0.025g, 0.050g and 0.075g. Even though these are low concentrations compared to the water in the system, the included range of concentration has been proved to be the optimum for Silica nanoparticles in literature studies.

5.2.2.1 PREPARATION OF DUOVIS DF

In this part of the investigation of the performance of Silica nanoparticles in drilling fluids, Duovis as a polymer has been chosen to be studied. The major objective of the study is to obtain the knowledge of how nanoparticles such as Silica can alter the rheology of the drilling fluids and give better results than the conventional drilling fluids applied today.

Additives	Base fluid (BF)	BF+0.025 SiO_2	BF+0.050 SiO_2	BF+0.075 SiO_2
Water, g	500	500	500	500
Bentonite	25	25	25	25
KCL	5	5	5	5
Duovis	0.5	0.5	0.5	0.5
SiO_2	0	0.025	0.05	0.075

Table 12 The formulation of the Duovis based drilling fluid systems

The procedure of preparation of the drilling fluids containing Duovis as polymer and Silica as nanoparticles can be found in the previous section 5.2.1.1. The additives and the right amount of each additives can be found in the table 12, and as the table presents, the only alteration from each system is the increment of nanoparticles included. Every other additive remains constant all over the drilling fluid systems.

5.2.2.2 RHEOLOGY RESULTS OF DUOVIS DF

Rheology as mentioned earlier in the thesis, is the study of the flow matter, and since drilling fluids fall into the category as a liquid, will rheology properties aid in the characterization of the designed drilling fluid systems.

A Fann viscometer was conducted in order to achieve shear stress values which have been plotted with the respectively rotational speed in RPM. The figure 32 below shows the data obtained by viscometer for the various drilling fluid systems containing Duovis as the polymer.

The figure shows minor alteration in terms of shear stress compared to the reference fluid system. There is slightly an increasing of shear stress for the drilling fluids with nanoparticles, although there are non– linear correlation between higher concentration of nanoparticles and higher shear stress value. In fact, the highest value of shear stress was achieved by using the medium concentration (0.050g SiO_2) of nanoparticles. This might be an optimum value.

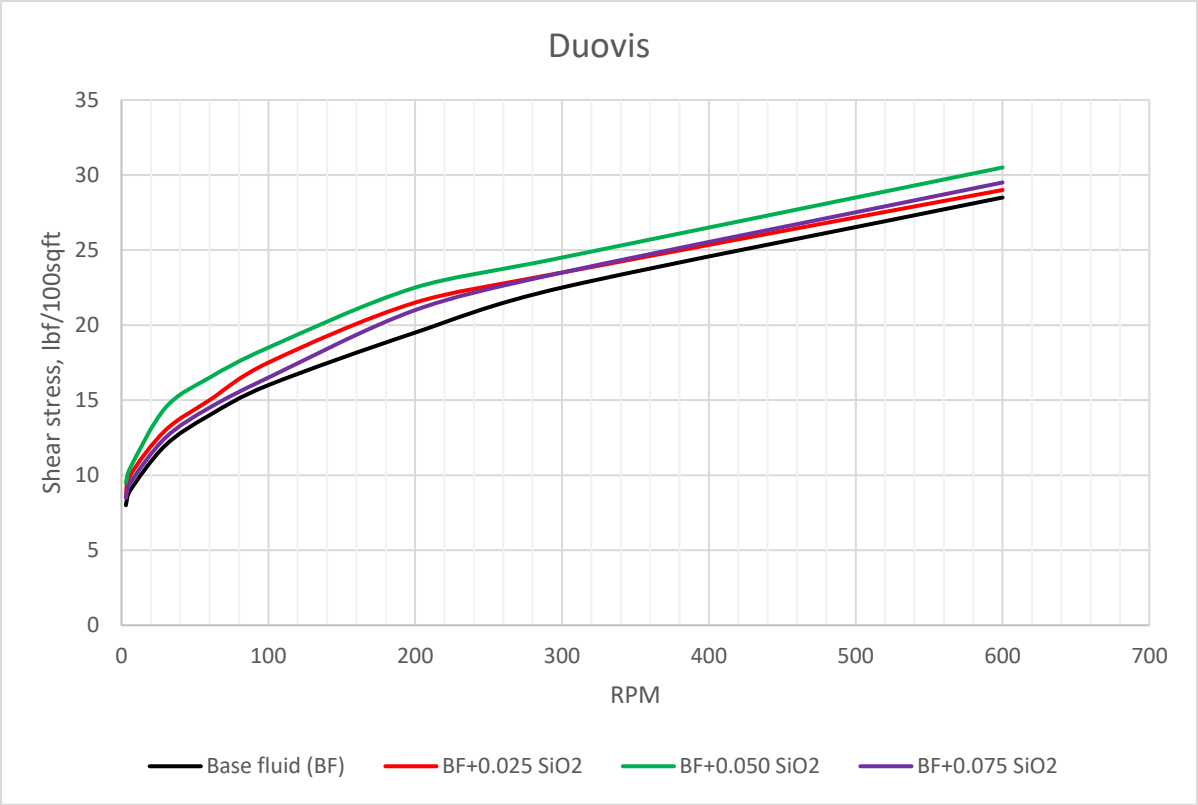

Figure 32 A plot of the measured values obtained by Fann Viscometer for Duovis based systems

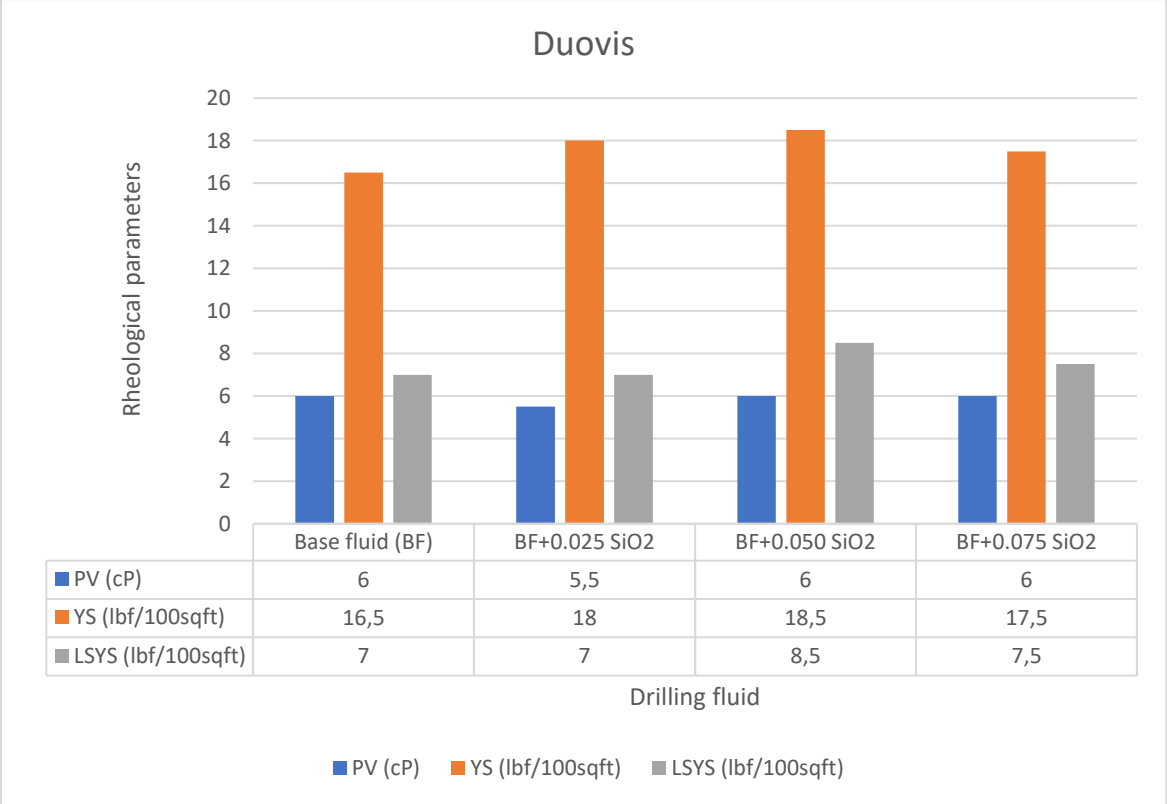

Figure 33 Calculated parameters such as PV, YS and LSYS in regard of Bingham model for Duovis based drilling fluids

According to the Bingham plastic model, the parameters of the figure 33 above presents:

- The values for plastic viscosity remains mostly consistent for the systems with Douvis as polymer in the drilling fluid system.
  Although, the fluid system containing 0.025g Silica as nanoparticles differs with 8,33% lower value for the plastic viscosity.
- The yields stress values for all drilling fluids with nanoparticles have risen compared to the reference level obtained by the base fluid.
  Even if there might be a trend which shows an optimum value for the fluid containing 0.050g Silica which increased the yield stress by 12,12%.
  The increase of the YS value for the fluid containing 0.025g and 0.075g Silica nanoparticles was 9% and 6%.
- The lower shear yield stress values vary only for the fluid containing higher concentrations than 0.025g Silica nanoparticles.
  Again, the best result was given by the drilling fluid which contained 0.050g Silica.

5.2.2.3 FRICTION MEASUREMENTS of DUOVIS DF

In this section, the coefficients of friction were all achieved by using a CSM tribometer. Several tests were conducted in order to avoid error of measurements and the average values are introduced in the figure 34 for both the drilling fluids containing Silica nanoparticles and the base fluid (BF) free for nanoparticles. As the figure shows, the coefficient of friction does not differ that much for the lower concentrations of nanoparticles, in fact the reduction is by an averaged 11% compared to the reference level.

Unlike the lower concentrations of nanoparticles, the higher concentration of Silica nanoparticles did not differ in terms of coefficient of friction, in fact, the reduction was only 3%.

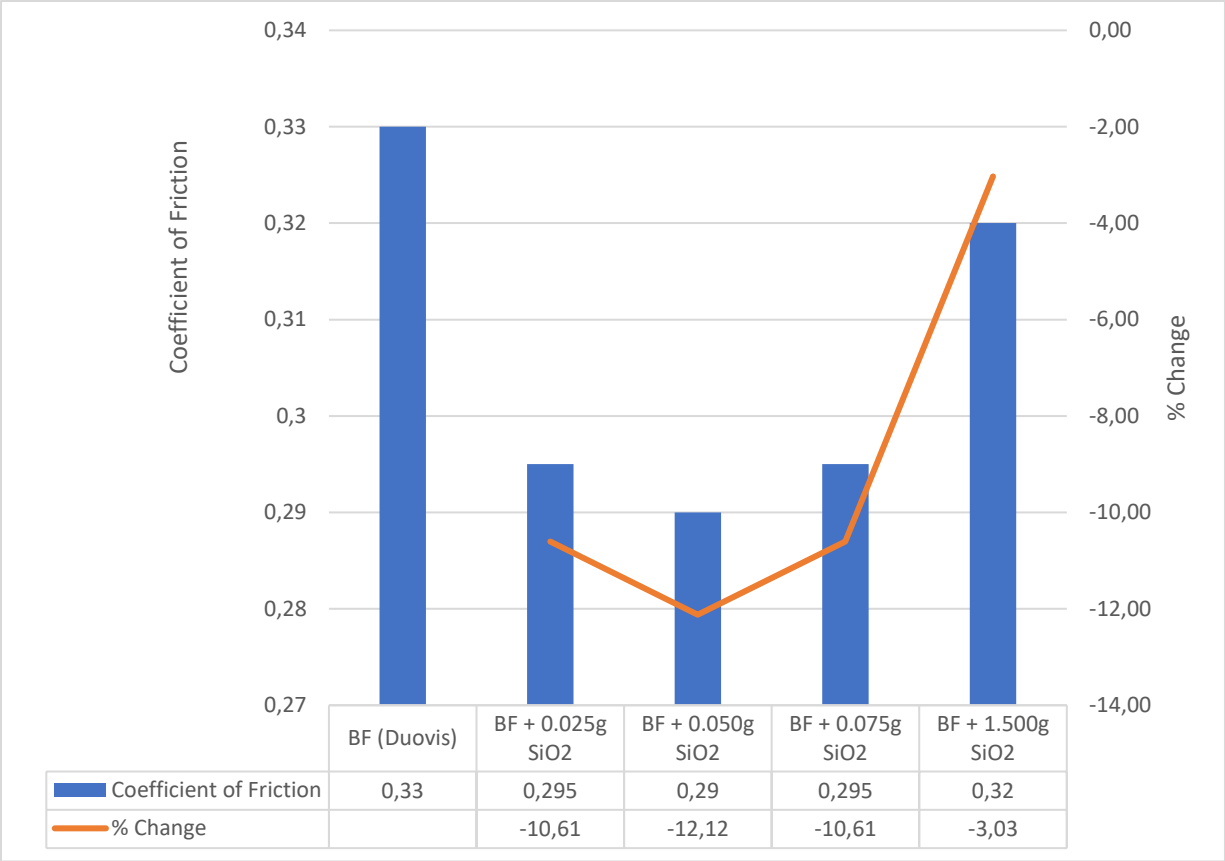

Figure 34 Coefficient of friction for the various Duovis based drilling fluid systems obtained by tribometer.

5.2.3 MEASUREMENTS OF VISCOELASTICITY

This subsection of the experimental work for the thesis will introduce the measurement of viscoelasticity. The viscoelasticity is a parameter which describes the behaviour of a fluid containing suspended particles, and will therefore have both an elastic and viscous behaviour depending on the applied stress for a given time.

5.2.3.1 AMPLITUDE SWEEP TEST

The performance of the oscillatory amplitude sweep tests is presented for the various drilling fluids. In regard to the simplicity, only Ref Duovis based DF performance will be shown graphically, while the remaining of drilling fluids amplitude sweep test will be placed under Appendix A.

Firstly, in order to have a homogenous solution, the selected fluid had to be mixed beforehand of the test. The amplitude sweep test was conducted under room temperature at 20 degrees. A syringe was utilized to place a sample of the fluid in the parallel plate, as the frequency was constantly kept at 10 rad/s although the strain ranged between 0,0005% and 100%. After the test was finished, the resulting values could be used to produce a plot containing parameters such as shear stress, both storage – and loss modulus, and damping factor for the sample of drilling fluid. The plot as shown below can be interpreted to determine flow the value of shear yield point, flow point and the linear viscoelastic range, LVER.

Accordingly, to the plot in figure 35 produced by the amplitude sweep test for drilling fluid, Ref Duovis, the values for Loss modulus are lower compared to the Storage Modulus values ahead of the cross point. Due to the fact of that, the plot indicates the drilling fluid to have a more elastic behaviour, as it has generated a gel structure.

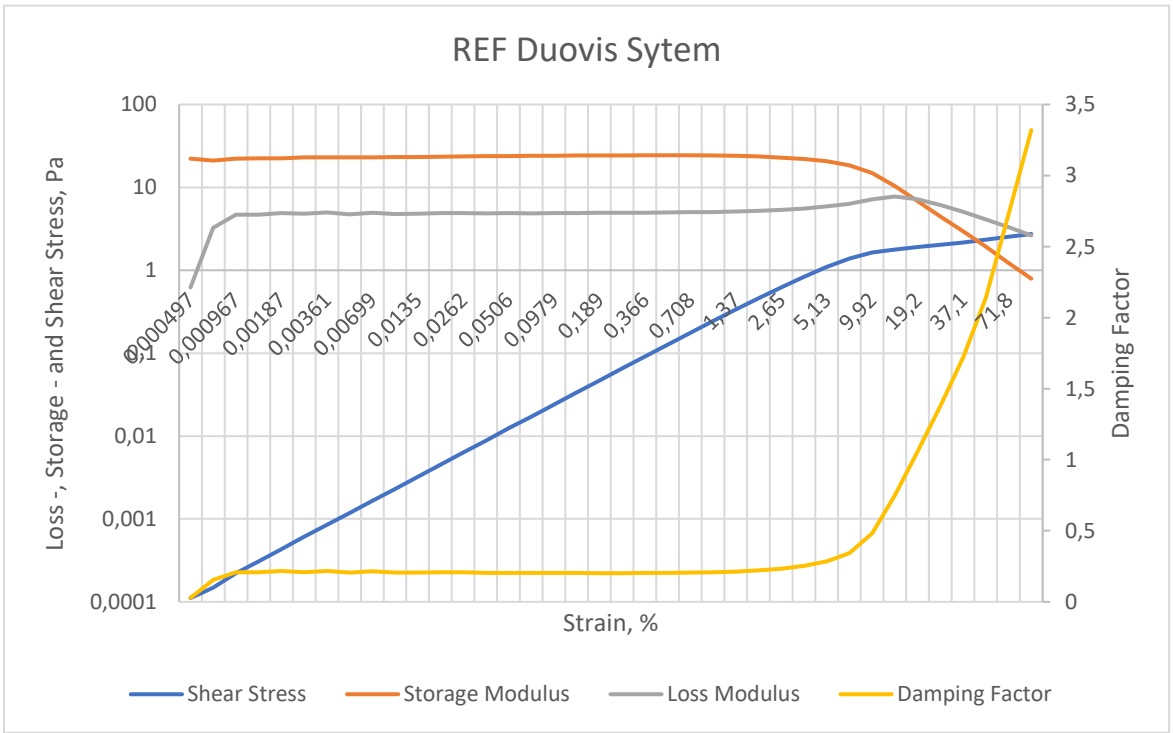

Figure 35 A diagram of amplitude sweep measurements for Ref Duovis

As mentioned previously, the plot can be informative and also determine the value of the flow point. The flow point may be found at the cross point between Loss modulus and Storage

modulus. The flow point as described in Section 3.3.1, is the transitional point where the fluid begins to flow, and indicates the transition of the viscous behaviour dominating over the elastic behaviour.

On the other hand, the last parameter of the plot is the damping factor which has for the most part of the test, relatively low values. But increases rapidly whenever the transition between the behaviours start to take place.

5.2.3.1.1 SHEAR STRESS VS. FLOW POINT

The flow point is the point where the values for Loss – and Storage modulus are equal, and also the point where sample transit the elastic performance to a viscous performance as it starts to flow.

The histogram in figure 36 presents all the drilling fluids performances regarding the shear stress value at the flow point.

As presented, the Ref CMC drilling fluid system scores the highest value for shear stress at the flow point among all the systems, while Ref Duovis containing 0.050g SiO_2 had the lowest value during the Amplitude Sweep Test. For the CMC based drilling fluid systems, the performances of Nano silica tend to reduce the value of shear stress with higher concentration of the nanoparticles. In fact, the drilling fluid containing CMC with 0.075g SiO_2 has decreased the shear stress by nearly 25% compared to the drilling fluid with non-nanoparticles. However, the tendency for the shear stress value at the flow point for Duovis based drilling fluid systems increases with higher concentration of nanoparticles. Except for Ref Duovis containing 0.050g SiO_2. This system does not increase the shear stress, but reduces the value by 6.5% compared to the reference system with only Duovis and no additional Nano Silica.

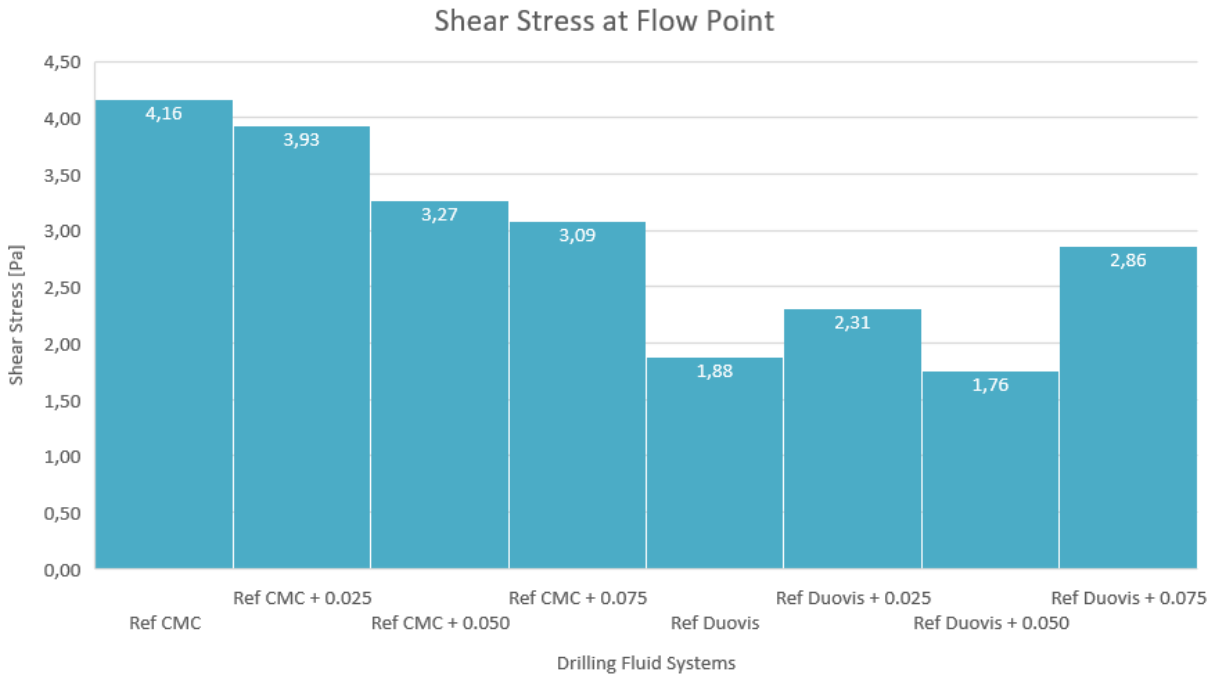

Figure 36 Shear stress value at the flow point for the CMC – and Duovis based different drilling fluid systems

6 PERFORMANCE OF SIMULATION

The nanoparticle designed drilling fluid systems, and their respective reference systems with non-additional nanoparticles were moreover studied by running several simulations. Only the most promising fluids in terms of the achieved frictional values, were included in the simulation.

This chapter presents the influence of SiO_2 nanoparticles in the hydraulics, rheological modelling and torque and drag.

6.1 RHEOLOGICAL MODELS

The obtained rheological values by utilizing the Fann Viscometer in Section 5.2, will be the fundamental work for the following simulations. There are several models which can describe any non – Newtonian fluids such as Power Law -, Robertson & Stiff -, Herschel Bulkley -, Unified and Bingham Model. The intention is to find the most correlated model to the selected fluids, as well to acquire the influence of SiO_2 nanoparticles.

6.1.1 REFERENCE CMC SYSTEM

As seen in the following figure 37, the graphs for the different rheological models have been obtained by the calculations of the RPM values for the fluid system. While the table 13 is the reciprocal parameters and equations for the models.

		Parameters					
Model	**Equation**	**τo,τy, A**	**k, C**	**n, B**	**μp, μ**	**% Error**	**cP**
HB	17,205 + 0,6912*γ^0.4695	2,496	0,161	0,67210		4,00	
Unified	2,7742+0,0625*γ^0.822	2,774	0,0625	0,822		7,26	
Power Law	1,565*γ^0.3393		1,565	0,3393		6,36	
Bingham	0,0146*γ+4,3697	4,370			0,0146	22,67	6,99048
RS	0,6912*(17,204861+γ)^0.46	0,6912	17,2049	0,4695		2,30	

Table 13 The equation and parameters for the different rheological models regarding Ref CMC

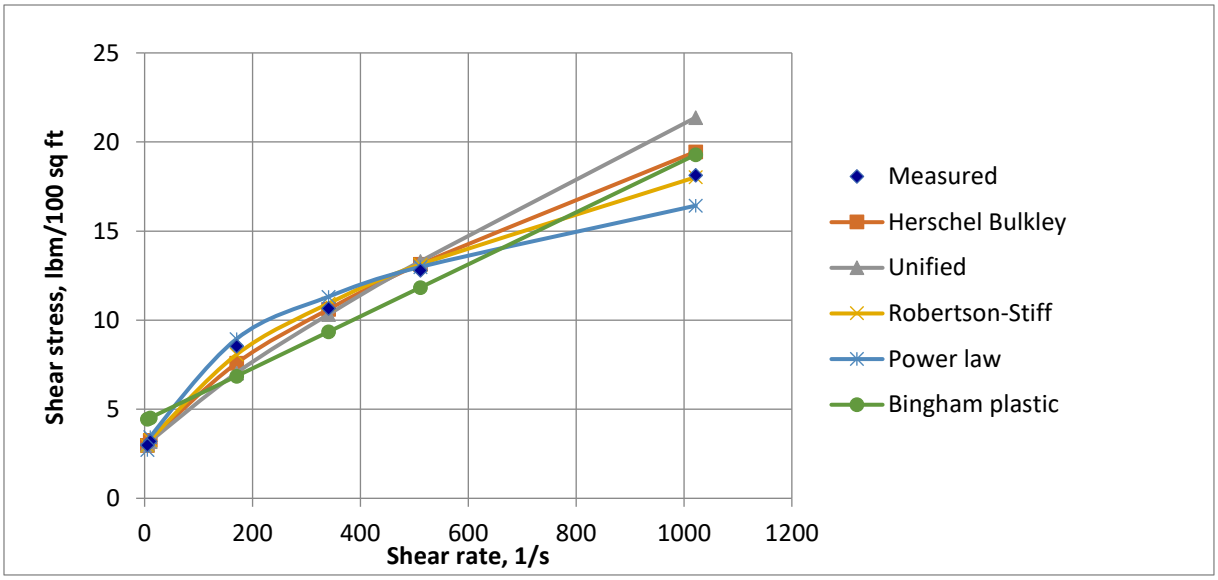

Figure 37 The different rheological models for Ref CMC drilling fluid system

6.1.2 CMC + 0.025 SiO_2 SYSTEM

The figure 38 below shows the acquired graphs for the CMC based drilling fluid including 0.025g Silica. In the same manner, the Bingham graph differs from the rest, and is the least correlated model for the drilling fluid system. The table 14 summarizes the different models with both parameters and deviations in percentage.

		Parameters					
Model	**Equation**	**τo,τy, A**	**k, C**	**n, B**	**μp, μ**	**% Error**	**cP**
HB	0,2331*γ^0,586 +1,74164	1,742	0,2331	0,58600		4,54	
Unified	1,6005+0,3023*γ^0,5461	1,601	0,3023	0,5461		4,44	
Power Law	1,2562*γ^0,3424		1,2562	0,3424		6,63	
Bingham	0,0127*γ+3,3592	3,359			0,0127	18,39	6,08076
RS	0,5417*(17,739+γ)^0,4762	0,5417	17,7399	0,4762		5,38	

Table 14 The equation and parameters for the different rheological models regarding CMC + 0.025g SiO_2

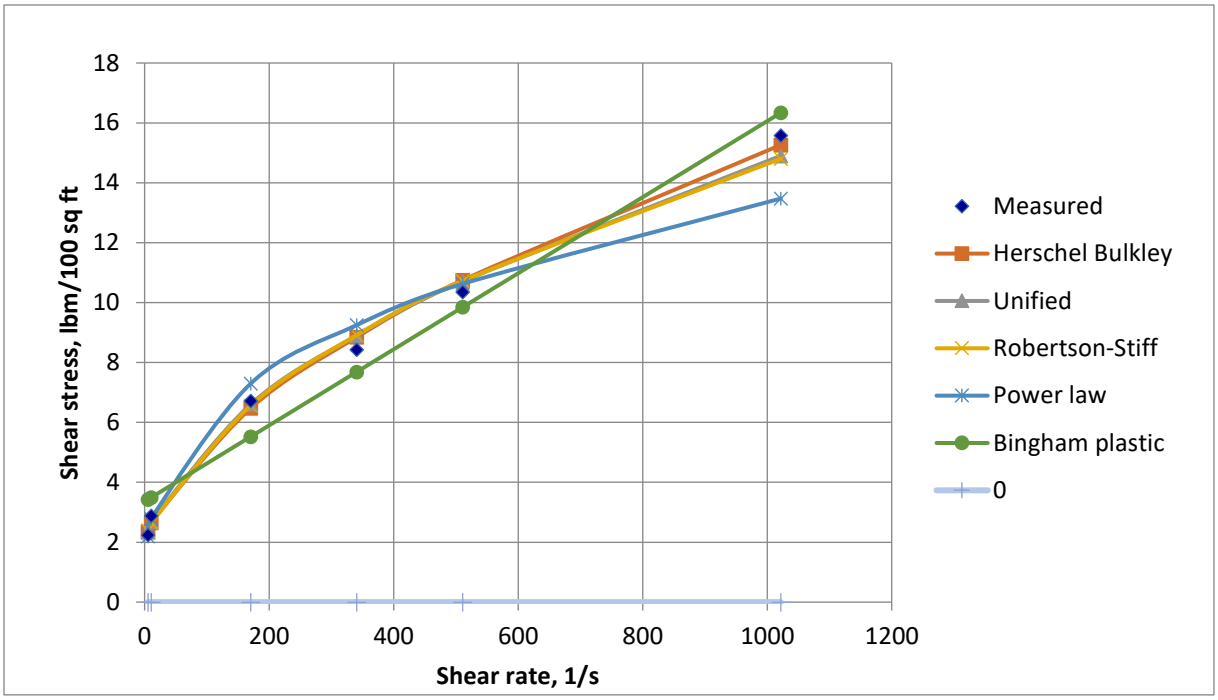

Figure 38 The different rheological models for CMC + 0.025 SiO_2 drilling fluid system

6.1.3 REFERENCE DUOVIS SYSTEM

On the other hand, the other polymer system had additionally been simulated as well. Equivalently, the Bingham model does not correlate well with any of the systems so far in comparison with the other rheological models as shown graphically in the figure 39 and numerically in the table 15.

		Parameters					
Model	Equation	τo,τy, A	k, C	n, B	μp, μ	% Error	cP
HB	7,411 + 0,5259*γ^0,5542	7,411	0,5259	0,55420		2,34	
Unified	7.469+0.4971*γ^0.5628	7,469	0,4971	0,5628		2,52	
Power Law	5.6287*γ^0.2316		5,6287	0,2316		4,24	
Bingham	0.0209*γ+11.218	11,218			0,0209	15,49	10,00692
RS	2.77*(23.6332+γ)^0.344	2,7698	23,6332	0,344		1,44	

Table 15 The equation and parameters for the different rheological models regarding Ref Duovis

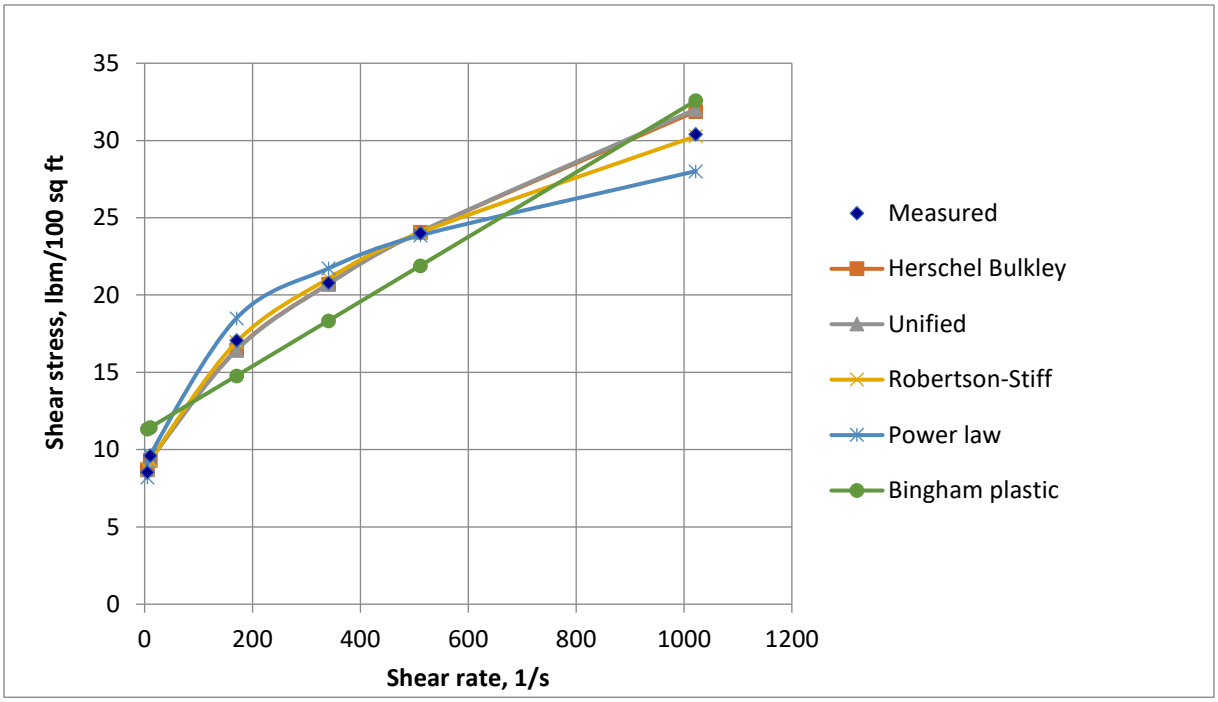

Figure 39 The different rheological models for Ref Duovis drilling fluid system

6.1.4 DUOVIS + 0.050g SiO_2 SYSTEM

Similarly, trend occurs for the mentioned fluid system as well in figure 40. The Bingham rheology model does not fit any of the drilling fluid systems, as it differs a lot. The other models seem to have minor deviation percentages. While, table 16 summarizes the rheological models with the respectively parameters.

		Parameters					
Model	Equation	τo,τy, A	k, C	n, B	μp, μ	% Error	cP
HB	0,6613*γ^0,5295 +8,73512	8,735	0,6613	0,52950		3,38	
Unified	9,0695+0,4925*γ^0,5745	9,070	0,4925	0,5745		4,28	
Power Law	6,8809*γ^0,216		6,8809	0,216		3,07	
Bingham	0,0213*γ+13,32	13,320			0,0213	16,16	10,19844
RS	3,8899*(19,562963+γ)^0,3066	3,8899	19,5630	0,3066		1,63	

Table 16 The equation and parameters for the different rheological models regarding Duovis + 0.050g SiO2

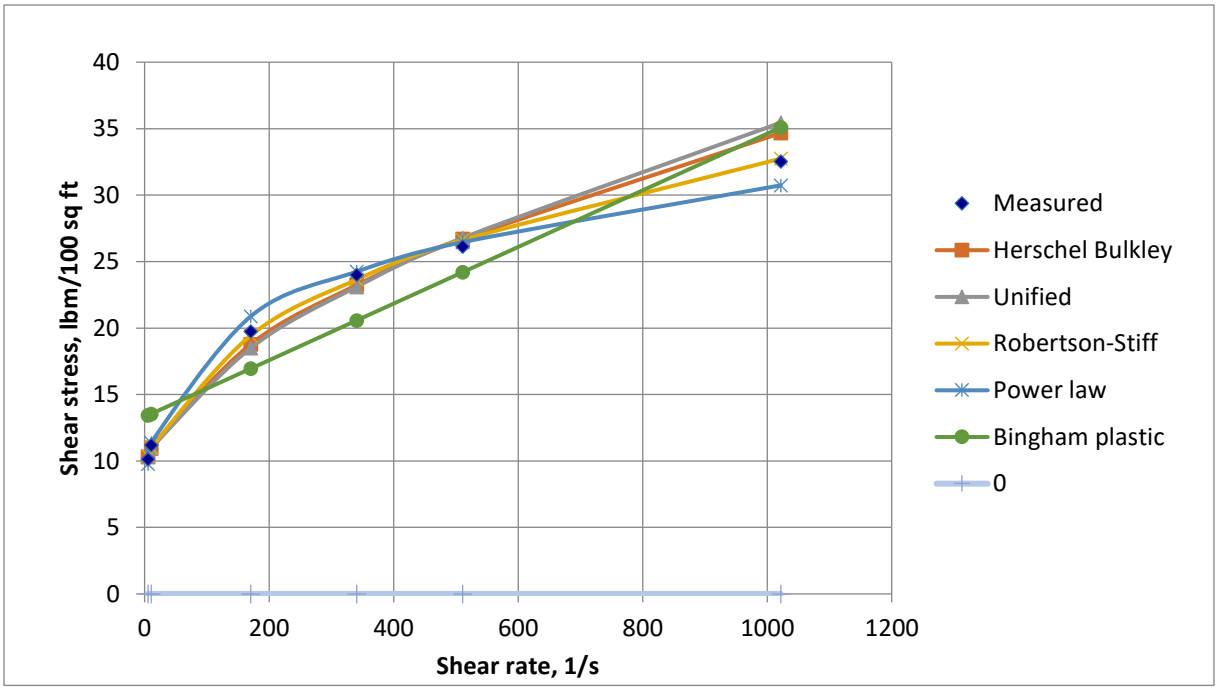

Figure 40 The different rheological models for Ref Duovis + 0.050g SiO2 drilling fluid system

6.1.5 COMPARISON of RHEOLOGICAL MODELS

The table 17 summarizes all the associated parameters for the different rheological models and the selected drilling fluid systems. Additionally, the table also shows the different deviation for each parameter to describe further the impact of including the SiO_2 nanoparticles.

As mentioned earlier, the Bingham model does not correlate with the description of the behaviour for the fluids. Although, the other models such as Power Law, Robertson and Stiff, and Unified seem to be all good models to represent the rheology of the fluid.

Model	Parameter	Ref CMC	CMC + 0.025g SiO2	Ref Duovis	Duovis + 0.050g SiO2
Bingham	YS	4,37	3,36	11,22	13,32
	% deviation		-23,13		18,74
	PV	0,01	0,01	0,02	0,02
	% deviation		-13,01		1,91
Power Law	k	1,57	1,26	5,63	6,88
	% deviation		-19,73		22,25
	n	0,34	0,34	0,23	0,22
	% deviation		0,91		-6,74
Herschel Bulkley	To	2,50	1,74	7,41	8,74
	% deviation		-30,23		17,85
	k	0,16	0,23	0,53	0,66
	% deviation		44,78		25,75
	n	0,67	0,59	0,55	0,53
	% deviation		-12,81		-4,55
Robertson & Stiff	A	0,69	0,54	2,77	3,89
	% deviation		-21,63		40,44
	B	0,47	0,48	0,34	0,31
	% deviation		1,49		-11,05
	C	17,20	17,74	23,63	19,56
	% deviation		3,11		-17,21
Unified	Ty	2,77	1,60	7,47	9,07
	% deviation		-42,27		21,44
	k	0,06	0,30	0,50	0,49
	% deviation		383,68		-0,93
	n	0,82	0,55	0,56	0,57
	% deviation		-33,56		2,08

Table 17 A summary of rheological models with the parameters and deviations in terms for the various drilling fluid systems.

6.2 SIMULATION OF HYDRAULICS

The associated theory for the hydraulic simulation has been previously presented in Section 3.5. While, in this part of the experimental work, the performance of the hydraulics will be evaluated in terms of ECD and Total Pressure Loss with the influence of nanoparticles included in the systems. The comparison of these hydraulic parameters will be valuable to further formulate and optimizing the drilling fluids. The Unified Model will be the selected rheology model to determine the necessity parameters, and the setup of the simulation is described in the next paragraph.

The simulation will be conducted by drilling a vertical well of 12 000 ft true vertical depth, and a casing of 8.5" has been placed. Furthermore, the well has been drilled with a drill bit with three nozzles, while the drill pipe's dimension is 5" and 4,5" as the outer diameter and inner diameter, respectively. For the simplicity for the simulation, the surface pressure was pre – set at zero, while the rate of pumping the drilling fluids with 8,539 ppm ranged from 0 – 600 gpm with an increment of 50 for each step.

The ECD values for Duovis – and CMC based drilling fluid systems have been plotted as a function of the flow rate as seen in the figures 42 and 44, respectively. The ECD value has raised at every flor rates under the simulation of Duovis based drilling fluid system containing 0.05g SiO_2 compared to the reference fluid. Even though the diagram shows an increasement, the alteration is only 0.7% in average. The Nano – treated DF should still be able to be used in narrow operational windows for drilling.

On the other hand, the CMC based drilling fluid system containing 0.025g SiO_2 reduced the ECD values for the most part of the flow rates. An observation can still be noted, as the fluid shows a transition of flow behaviour at 400 gpm, and further flow rates leads the ECD values nearly equivalent to each other.

Consequently, the relation between ECD and Total Pressure Loss can be found as the behaviour of the graphs is similarly for the respective systems. In fact, the ECD is a function of the friction loss, hence the higher-pressure losses for the Duovis DF with 0.05g SiO_2, while the

CMC system shows that nanoparticles manages to have lower pressure losses for the majority of the flow rates. This implies to the fact that CMC containing NPs can be suggested to be optimal DFs as the required pumping pressure of the fluid is overall lower.

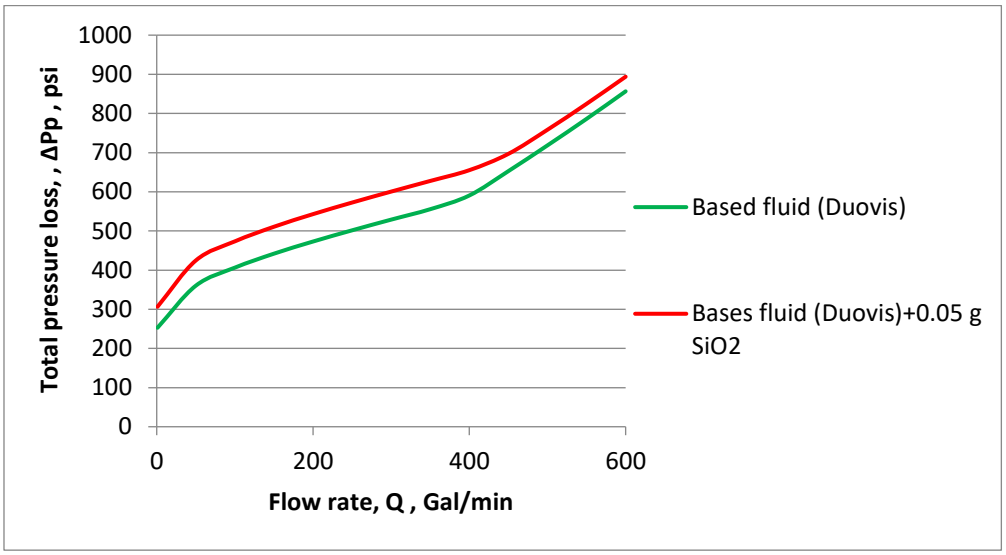

Figure 41 Comparing the performance of the Duovis DFs for total pressure loss

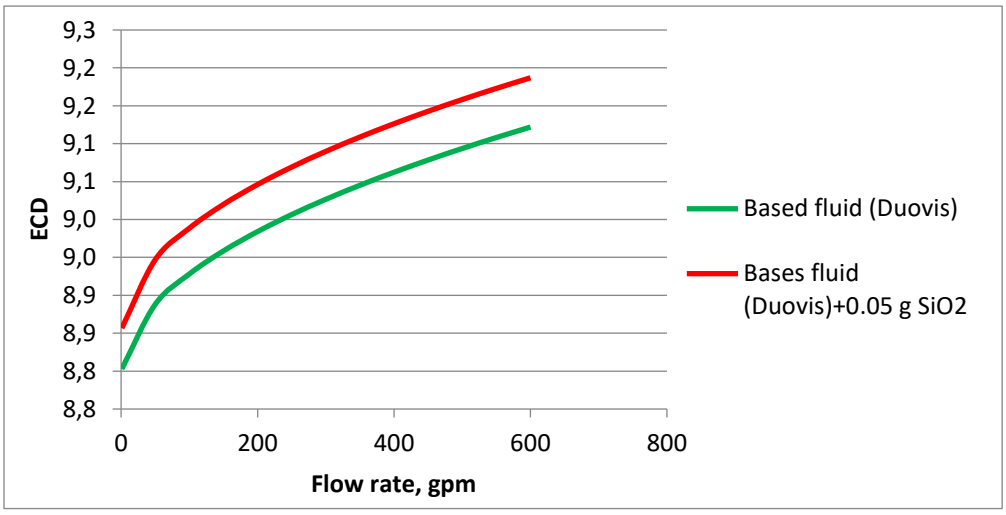

Figure 42 Comparing the performance of the Duovis DF for ECD

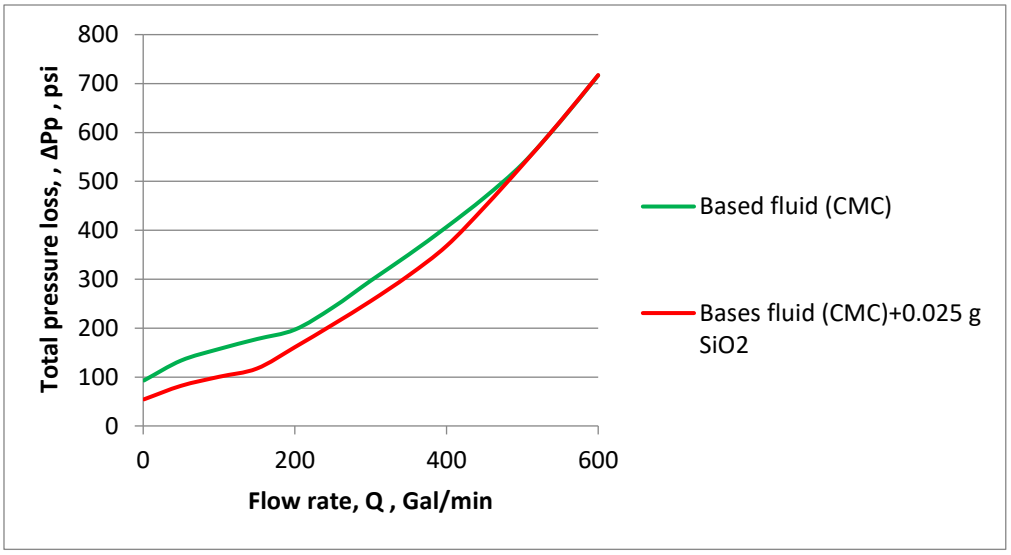

Figure 43 Comparing the performance of the CMC DFs for total pressure loss

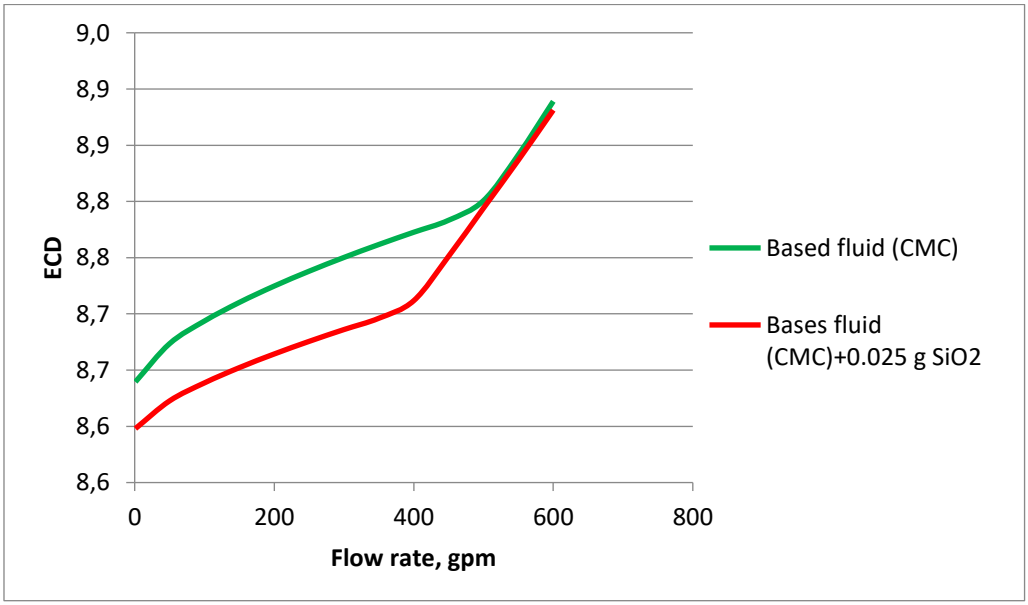

Figure 44 Comparing the performance of the CMC DFs for ECD

6.3 SIMULATION OF TORQUE AND DRAG

Both factors such as torque and drag can limit the drilling continuation, especially for wells with inclination. Oil based mud is often utilized under circumstances where the values for torque and drag become critical due to the lower coefficient of friction. In fact, the coefficient of friction can directly impact the torque value. However, the use of oil-based mud is expensive and not environmental friendly. The water-based mud with nanoparticles had proved to have lower coefficient of friction and may as well replace the oil-based mud due to the cost-efficient and better for the environment.

A software called Well Plan by Halliburton was utilized to perform the simulation of torque and drag. In order to check the influence of torque and drag for the various drilling fluid system, an inclined well with 11 000 ft measured depth had to be outlined as seen on figure 45.

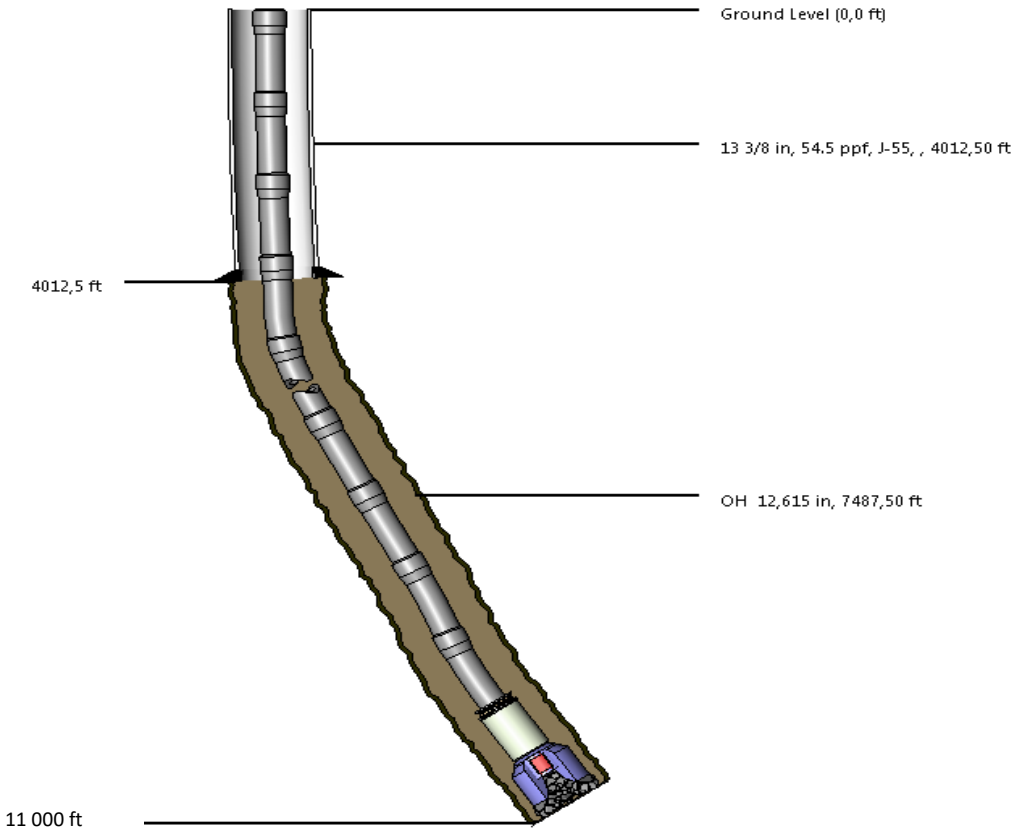

Figure 45 The setup for simulation of torque and drag on Well Plan

The speed for tripping in and tripping out was pre-set to 60 ft/min, while the flow rate was set to 500 gpm.

The following figures will present the drill string torque loads and drag forces for both the Reference CMC system and the CMC + 0.025g SiO_2 system, respectively. Accordingly, the figures show the trendlines for both the drilling fluid systems within the limit of either torque and tension which is within the safe operational window. The table 18 summarizes the performance of all the drilling fluid systems that was simulated by Well Plan software, and the influence of SiO_2 gave additional 5.10 – 6.20 % drilling extension for both systems.

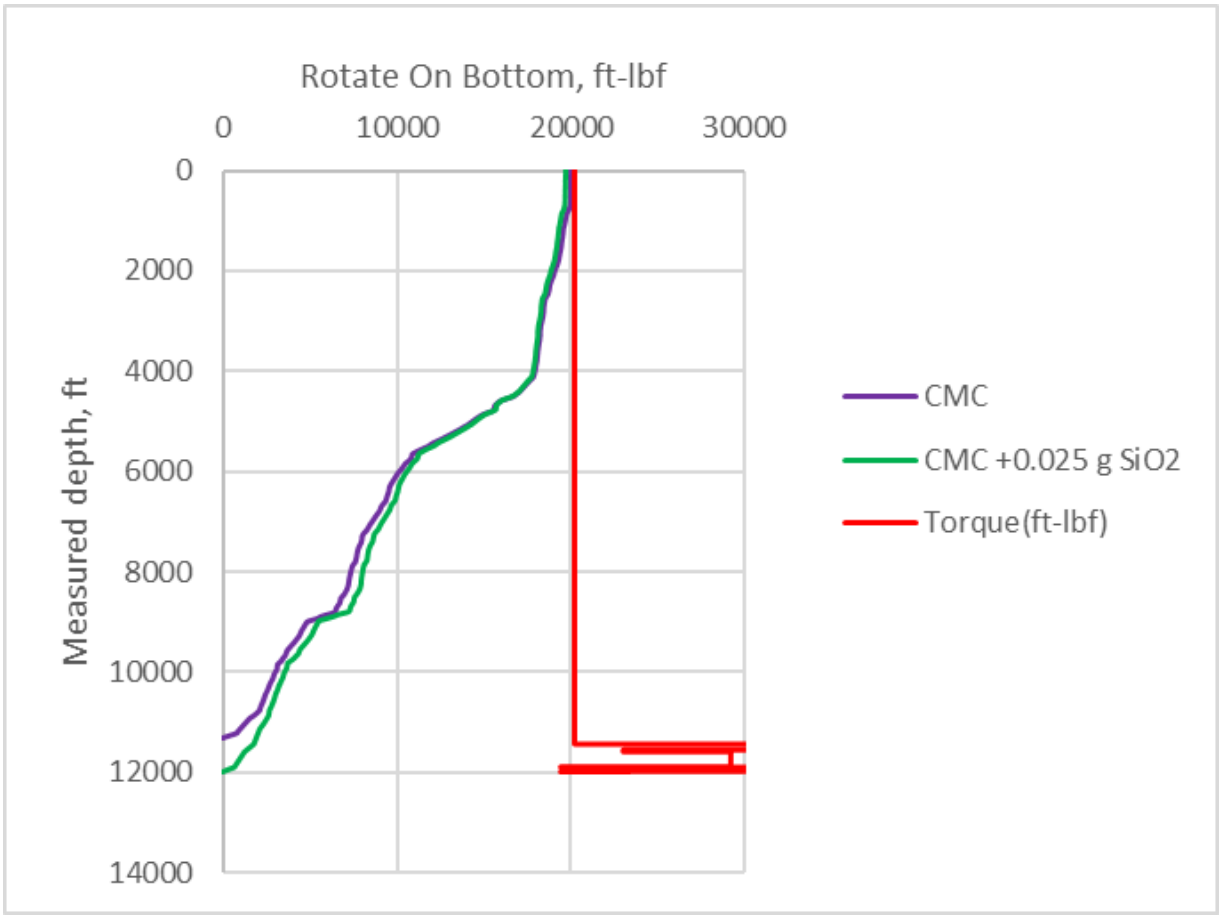

Figure 46 Comparing the performance of CMC DFs in terms of torque limit

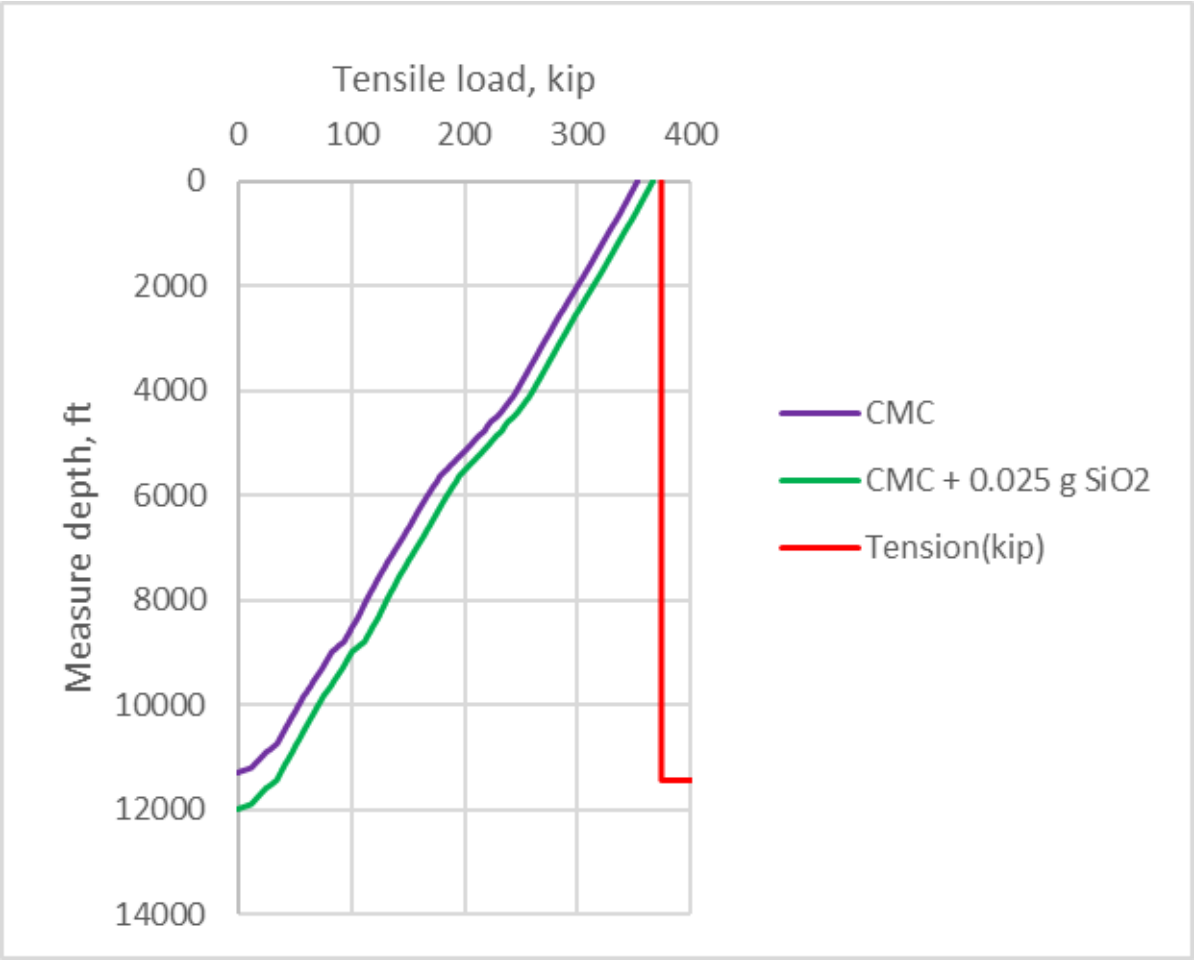

Figure 47 Comparing the performance of CMC DFs in terms of tensile limit

Fluid System	Coefficient of Friction	Measured Depth [ft]	% Alteration
CMC	0.37	11 300	
CMC + 0.025g SiO_2	0.31	12 000	+ 6.20
Duovis	0.33	11 800	
Duovis + 0.050g SiO_2	0.29	12 400	+ 5.10

Table 18 A summary table of prolonged measured depth of drilling for the selected drilling fluid systems.

7 SUMMARY & DISCUSSIONS

During this particular chapter, a reflection of the questions formulated in Section 1.2 will be presented, as well as a summary of the results achieved in the course of the experimental research.

7.1 DISCUSSION OF LITERATURE STUDY

The intention behind all the analysis conducted throughout the thesis is to reveal the performance of SiO_2 nanoparticles and learn all the benefits and disadvantages of including them in regard of oil and gas applications. The extensive literature inspection supplies important insight of nanoparticles in numerous scenarios, especially in terms of drilling fluids and enhanced oil recovery. The greatest advantage of using nanoparticles lies within the size of them which provides better ability for interaction due to higher surface to volume ratio compared to i.e. micro – and macro particles. The applications of nanoparticles have already been seen within other fields such as pharmaceutical and electronics.

In the interim for the following sections, the review of the applications of nanotechnology within enhanced oil recovery and drilling fluids will firstly be introduced, as well as the experimental work for the formulated nanofluid systems containing Silica.

The extensive literature study is presented in Chapter 2 proves the gifted potential of applying nanotechnology in the petroleum industry. Among the questions issued in Section 1.2, the comprehensive study of applications of nanoparticles can be suggested to be the solution in terms of providing improvement in drilling fluid and EOR.

As a part of the drilling process, the drilling fluid is among the most important part as the fluid serves the purpose to transport the cuttings and cool the drill bit. However, fluid loss is overall primarily the greatest concern due to the consequences such as lacking the necessitate rheological properties, damage to the formation and instability of the well.

Likewise, the enhanced oil recovery has as well limitations in terms of the conventional methods utilized in the current time. As at the stage of tertiary oil recovery, the recovery factor is after all not pleasing as the remaining original oil in place is ranging between 30 – 60%. The huge range of possible recoverable oil confirms the room for improvement in the enhanced oil recovery.

The summary of the broad investigation of nanotechnology applications has been presented in the table 1. As revealed in the table, promising benefits will be included by applying nanotechnology within EOR and drilling fluids and can be suggested to be a solution for issues of the current methods.

7.2 THE EFFECT OF NANO SiO_2 in CMC – and DUOVIS DFs

The preparation of the drilling fluid system with CMC has been mentioned earlier in the Section 5.2.1.1, and while the purpose is to show the influence of including SiO_2 nanoparticles, a reference system with no nanoparticles had to be made as well to become the baseline for the further study.

The results obtained by the Fann Viscometer presents reduced values compared to the reference system with no Nano SiO_2. However, the system with 0.050 g added nanoparticles performed the best among them. Almost like there was an optimum between the Nano treated drilling fluids with respect to the obtained shear stress values. The plastic viscosity remained nearly equal for all of the CMC based drilling fluid systems, except for the SiO_2 0.050g CMC system, as the PV value was reduced by 14%. Additionally, these drilling fluid systems can be classified as plastic fluids have the shear thinning behaviour which means that the apparent viscosity decreases as the RPM increases. Unlike the PV values, the yield stress results did not remain the same with nanoparticles involved, and the most significant differentiate was obtained by SiO_2 0.075g CMC system as the YS was reduced by 42,8%. The least reduced value was obtained when examined the SiO_2 0.050g CMC system, only by 8,6%.

The performance of the same nanoparticles in Duovis, a biopolymer, based – drilling fluid systems was the opposite in respect of the shear stress values given by the viscometer. All the

systems containing any nanoparticles had greater shear stress values, although the SiO_2 0.050g Duovis had the highest, while the latter two systems had nearly the same as shown in the diagram in Section 5.2.2.2. The PV values remained equally as in CMC based drilling fluid systems, with an exception for the SiO_2 0.025g which differs by - 8,3%. Lastly, the yield stress increases with containing nanoparticles, and yet again, the SiO_2 0.050g had the highest result.

The influence of including the nanoparticles such as SiO_2 relies heavily on the concentration, as there tend to be an optimum concentration in terms of getting the desired rheological properties. Moreover, the selected polymer to the system can be crucial for the rheology of the fluids as seen in the impact of shear stress and yield stress.

FRICTIONAL EFFECTS

The idea behind conducting frictional coefficient test by utilizing a tribometer is to study the effect of including nanoparticles to alter the lubrication of the drilling fluids. The coefficient of friction ranged between 0.33 (Ref Duovis) to 0.37 (Ref CMC), although the most promising result by including SiO_2 in form of nanoparticles gave approximately a minor gap of range (0.29 – 0.31). Clearly, the influence of SiO_2 nanoparticles was better in the CMC based drilling fluid systems as it reduced the coefficient by 15%. Another observation was found in the achieved values for nanoparticles in Duovis systems as the reduction by percentage was nearly the same for them all. On the other hand, the lower concentration of SiO_2 in the system meant greater reduction in terms of lubricity.

Furthermore, an addition of SiO_2 0.3g sample was included in each of the drilling fluid batches for the purpose to show a greater difference between the applying concentrations of nanoparticles.

In the end, both systems with nanoparticles did reduce the coefficient of friction, despite the CMC based drilling fluid systems had greater effect. The selection of the polymer for drilling fluids containing SiO_2 nanoparticles has to be evaluated in terms of the required rheological abilities, as well as the cost and availability of the polymer.

NFs INFLUENCE OVER THE VISCOELASTIC BEHAVIOUR

All along the experimental work of the drilling fluid systems, an oscillatory sweep test was conducted to study the viscoelasticity of the systems. As presented in Appendix A, the Storage modulus values was found greater than the Loss modulus pre the cross point for all the drilling fluid systems. The observations indicate that the fluid in the systems have a superior elastic behaviour, as well as the fluid is initially in a structure of gel – like. The flow point has simply been described as the point when the fluid initiates the motion of flowing. The values of the numerous flow point could be graphically calculated, and in comparison, the CMC – based drilling fluid systems gave higher shear stress values at these points. The shear stress was found to be decreasing as the concentration of nanoparticles increased for the CMC systems.

Adverse for any form of trend, the Duovis based drilling fluid systems had no correlation for the shear stress values, as it increased for 0.25g SiO_2 and 0.75g SiO_2, while the concentration in between reduced. The shear stress value was found to be highest for the CMC reference system, while the 0.50g SiO_2 Duovis based system had the lowest.

7.3 THE EFFECT OF NANO SiO_2 in EOR

Throughout the thesis, nanotechnology has been presented as a promising and fresh input to deal with the shortcomings of the conventional technology within enhanced oil recovery. The doubt of applying nanotechnology in the oil and gas industry has with the higher amount of research been steadily reduced with time. Several scientists report the beneficial by using these almost invisible particles to improve the recovery factor, and the mechanism behind EOR has been briefly described as well in the thesis.

SiO_2 nanoparticles has been designated to be highly inspected to be applied in EOR due to the availability, the abundance of the material on Earth, as well as the encouraging results that had been reported. In order to have the knowledge of how these nanoparticles would affect the oil recovery, the EOR mechanisms had to be discovered and evaluated. According to the literature study, the SiO_2 nanoparticles can strongly alter the wettability of the solid surface and even have an impact of the interfacial tension.

During the experimental work, the 0.075 wt.% SiO_2 NF had the most convincing results as the IFT was proved to be reduced by 14,44% as shown in the table 19 which additionally includes the other fluid systems as well. While the nanofluid adjusted the wettability of the rock media from preferentially oil wet to water wet. Theoretically, these factors meant that the Nano Silica could have the potential to improve the recovery of oil. Although, the recovery factor did not reflect the EOR mechanisms the NF brought into the core flooding experiments. A tertiary recovery technique was utilized with NF containing 0.050 wt.% SiO_2 to increase the recovery factor additionally by 2,42%, while the promising NF of 0.075 wt.% SiO_2 did not show any impact.

A contradiction in terms of what the results from EOR mechanism showed as the 0.075 wt.% SiO_2 should have been the victorious NF when the core flooding was conducted. An impairment of the permeability may be the reason behind the bad performance, as Elgibaly et al. (2017) concluded that higher concentration of nanoparticles increases permeability impairment. Additionally, the same authors highlighted the importance of the injection rate as higher rates may increase the possibility to create a blockage of pores in the core plugs. As seen in the core flooding part of the experimental study, only two cores were presented. Originally, three cores of sandstone were prepared, but one of the core got damaged during the setup of the drainage process and was useless to study the influence of the NF. Several factors such as the right temperature, concentration of the nanoparticles and various injection rate should have been studied thoroughly with a higher volume of measurements. The lack of measurements of many core flooding tests were due to the minimal resources as the cost of Berea sandstone cores and the rent of the rig for core flooding was steeply high.

Concentration of SiO2	**Interfacial Tension Alteration [%]**	**Contact Angle Alteration [%]**
0.025	**- 6,34**	**+ 12**
0.050	**- 5,51**	**+ 30,6**
0.075	**- 14,44**	**+ 52,3**
0.100	**- 3,94**	**+ 31,5**
0.150	**- 1,81**	**+ 34,0**

Table 19 Summary of the influence of Nano SiO_2 in regards of IFT and CA.

7.4 DISCUSSION OF THE SIMULATION RESULTS

Influence of Nano Silica in Torque & Drag

The obtained results by utilizing the tribometry on the different drilling fluid systems confirm the fact that including nanotechnology will improve the lubricity compared to the conventional drilling fluid with non-nanoparticles. In other words, the coefficient of friction was reduced, and as this factor is crucial for the torque value, the simulation showed the additional extension of drilling by 5.10 – 6.20 %.

Rheological Modelling for Drilling Fluids containing nanoparticles

The simulation of the drilling fluid systems with nanoparticles shows clearly that Bingham model does not suit the description of neither of the systems. The average of deviation by utilizing the Bingham model was found to be approximately 18%. In the contrary, the Robertson and Stiff model was found to be the most perfect rheological model as the deviation was around 2,7%.

Influence of Nano Silica on performance of the Hydraulics

The value of equivalent circulating density, ECD, is being controlled by factors such as flow rate, density and the rheology of the fluid itself. Controlling the ECD might be challenging for deviated wells, as well as longer drilled wells.

In the simulation of the hydraulics, the CMC based drilling fluid system with nanoparticles gave lower ECD for the most part of the flowrates, while the Duovis based drilling fluid system gave an incremental jump for the same flowrates. However, the alteration of the ECD is minor in terms of whole value, and will not be any significant effected.

8 CONCLUSION

In the recent years, the introduction of nanotechnology to the petroleum industry has gained recognition for the unique abilities it might bring, and the relevant available literature reflects the popularity among scientists. As for the literature study presented in the thesis, the nanotechnology seems to give the extra edge compared to the conventional technology.

The major intention behind the thesis was to investigate and evaluate the influence of Nano SiO_2 in enhanced oil recovery and in drilling fluids. The experimental work has been shown through both EOR and drilling fluid systems, and additionally, the performance of the drilling fluid has been simulated as well.

Berea sandstone cores were flooded with nanofluids containing different concentrations of SiO_2. Although, the NF + 0.050 wt.% SiO_2 aided additional 2.42% oil recovery, the incremental was not sufficient, as the waterflooding solely was equally good as for the NF + 0.075 wt.% SiO_2. Nonetheless, the experimental work shows the promising potential lying within the nanoparticles to reduce the IFT by 14.44% and alter the preference of wettability from neutral – to water wet.

On the other hand, the investigation of the impact the nanoparticles had upon drilling fluids were by studying mainly the rheology, while the performance was simulated in terms of hydraulics, rheological modelling and torque and drag with WellPlan. The following points will summarize the foremost outcomes of the drilling fluids with nanoparticles:

- Both CMC – and Duovis DF systems with nanoparticles improved the extended reach of drilling ranging between 5.10 – 6.20 %.
- Including nanoparticles had minor effect for the ECD
- Robertson and Stiff model was the best fitted rheology model to describe the behaviour of both systems.

As a result of the major observations and obtained knowledge during the thesis, nanotechnology can indeed be an agent to improve both the drilling fluid to be more competitive in the match with OBM, as well as improving the overall oil recovery. However, a suggestion is to further study the nanotechnology to be able to optimize the applications in the petroleum industry. The performance in the thesis proves the potential of applying nanotechnology to the ordinary methods, but the end products are not ideal and sufficient to be used in the fields yet.

APPENDIX

APPNEDIX A: AMPLITUDE SWEEP TEST RESULTS

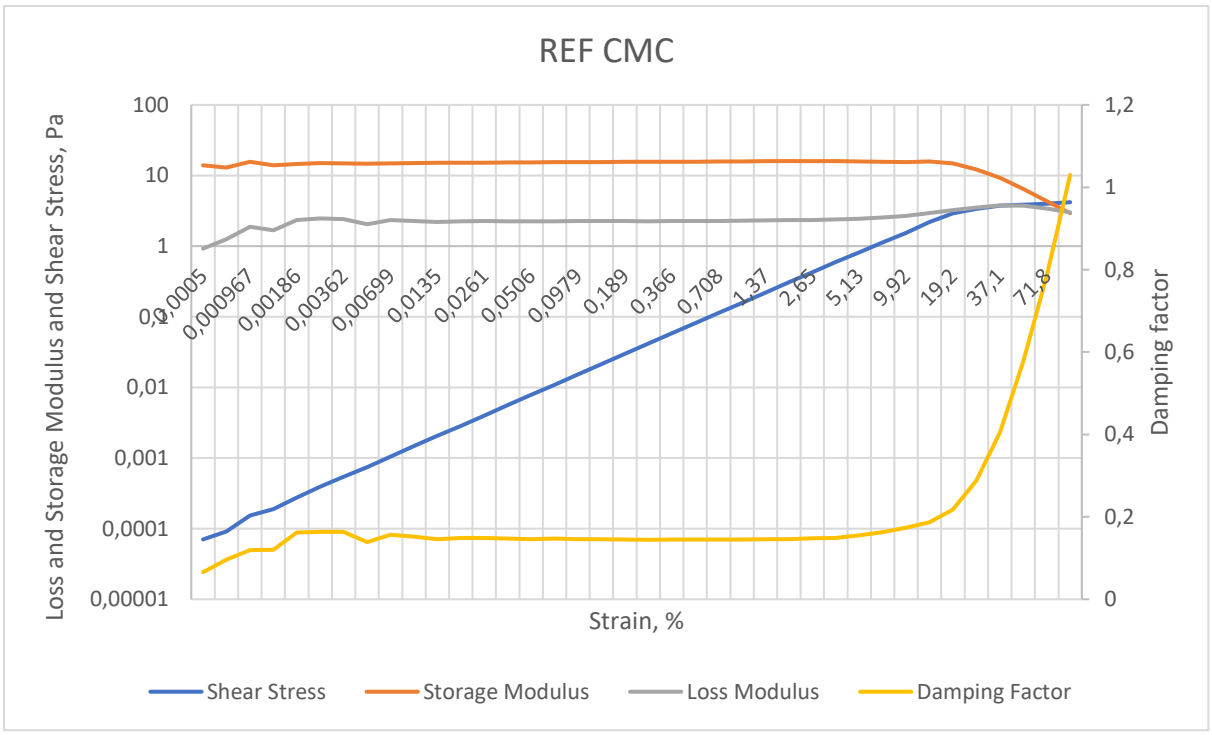

Figure 48 A diagram of amplitude sweep measurements for Ref CMC

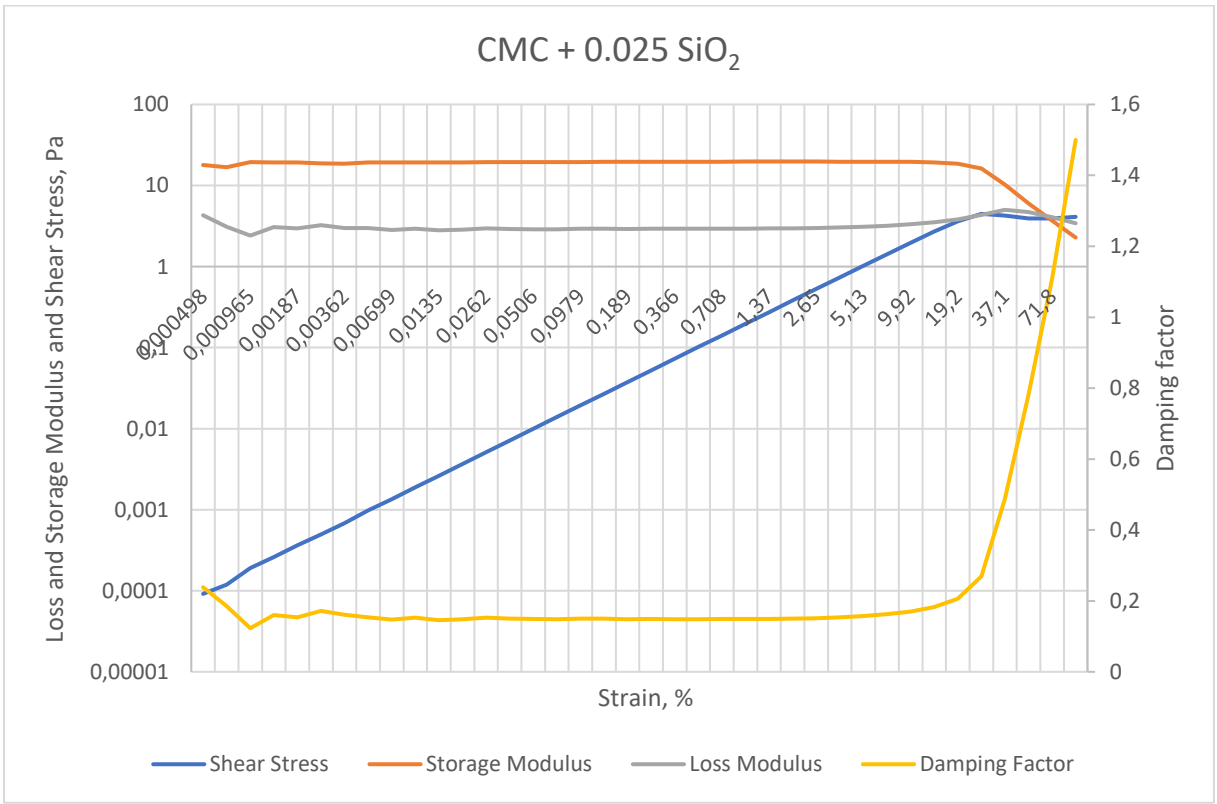

Figure 49 A diagram of amplitude sweep measurements for Ref CMC + 0.025 SiO_2

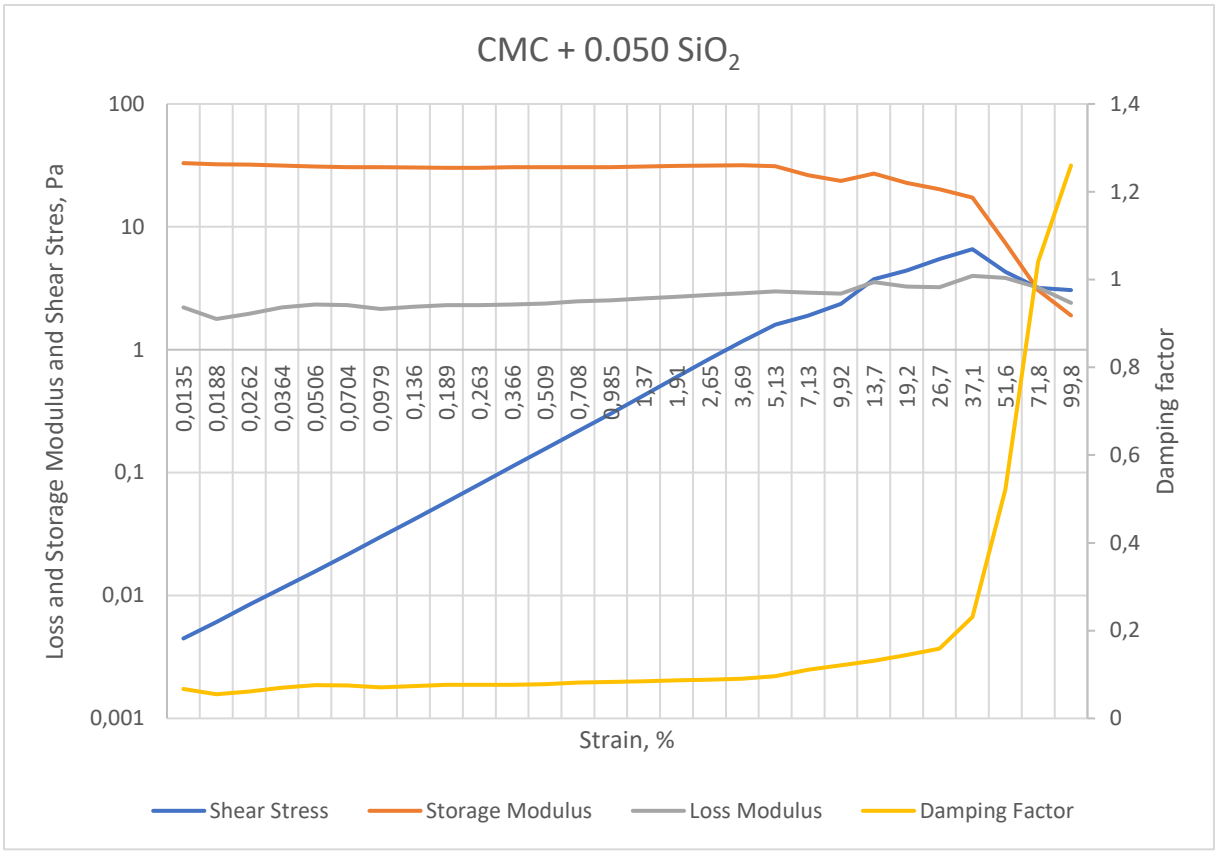

Figure 50 A diagram of amplitude sweep measurements for Ref CMC + 0.050 SiO_2

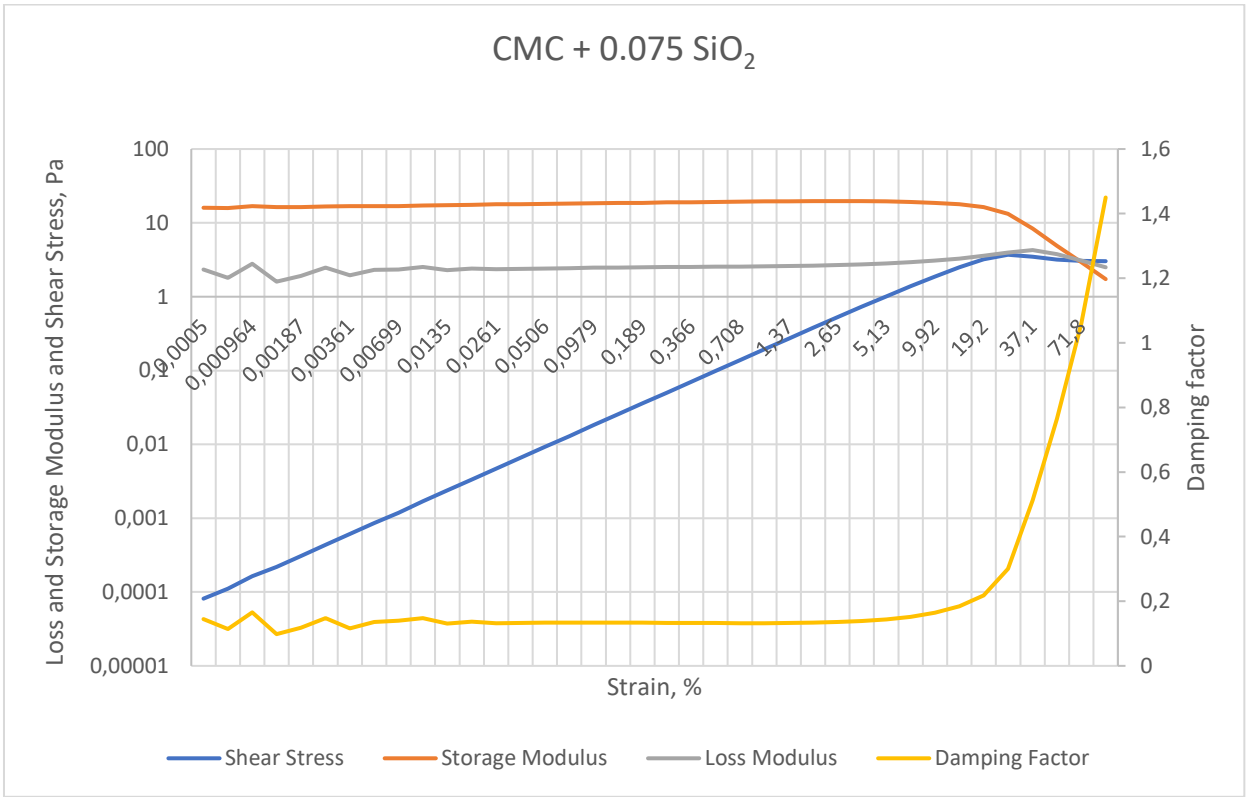

Figure 51 A diagram of amplitude sweep measurements for Ref CMC + 0.075 SiO_2

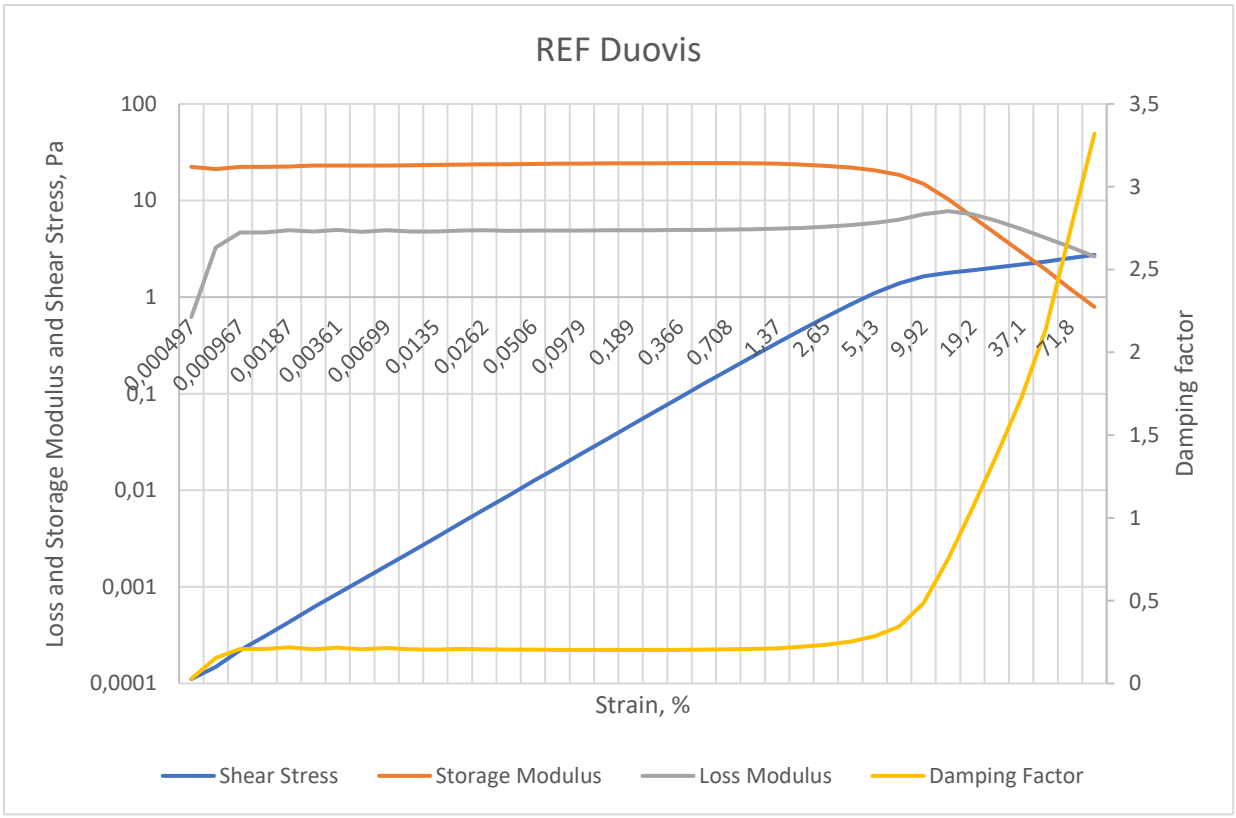

Figure 52 A diagram of amplitude sweep measurements for Ref Duovis

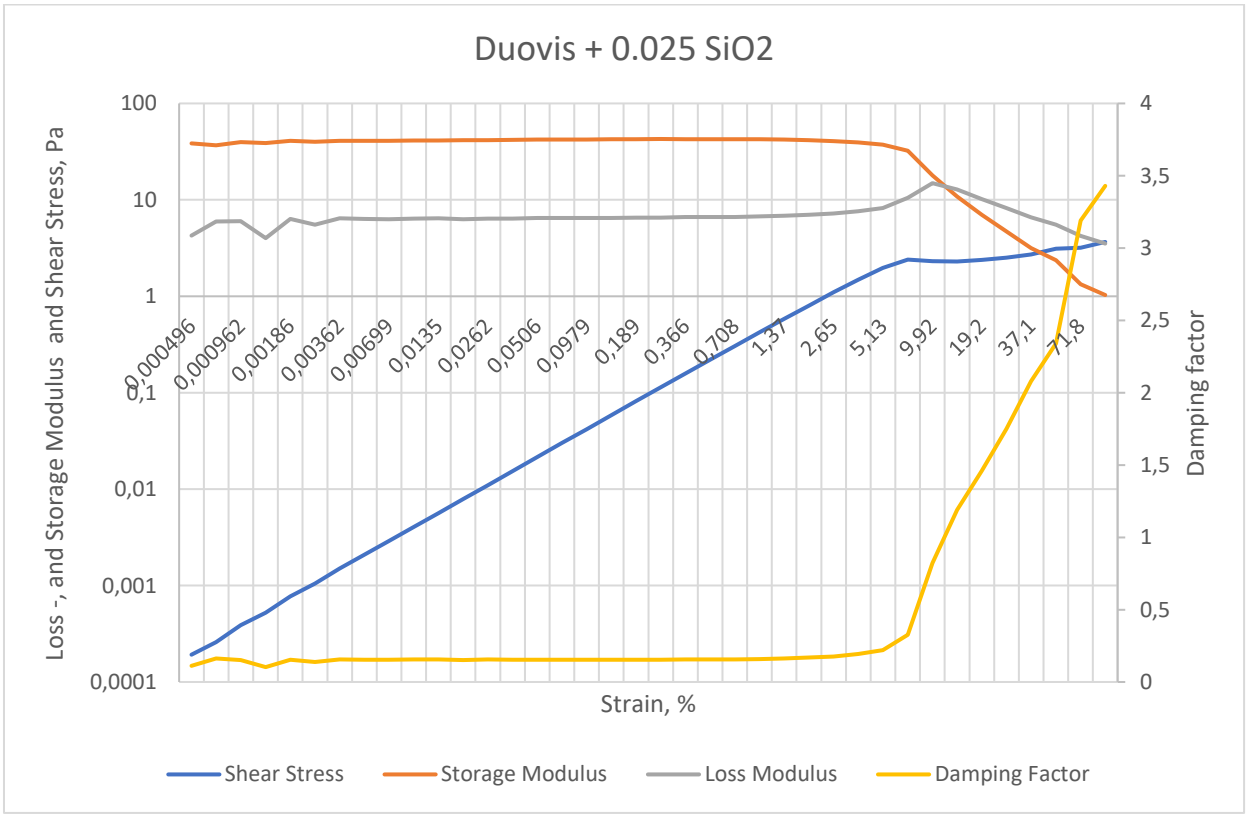

Figure 53 A diagram of amplitude sweep measurements for Ref Duovis + 0.025 SiO_2

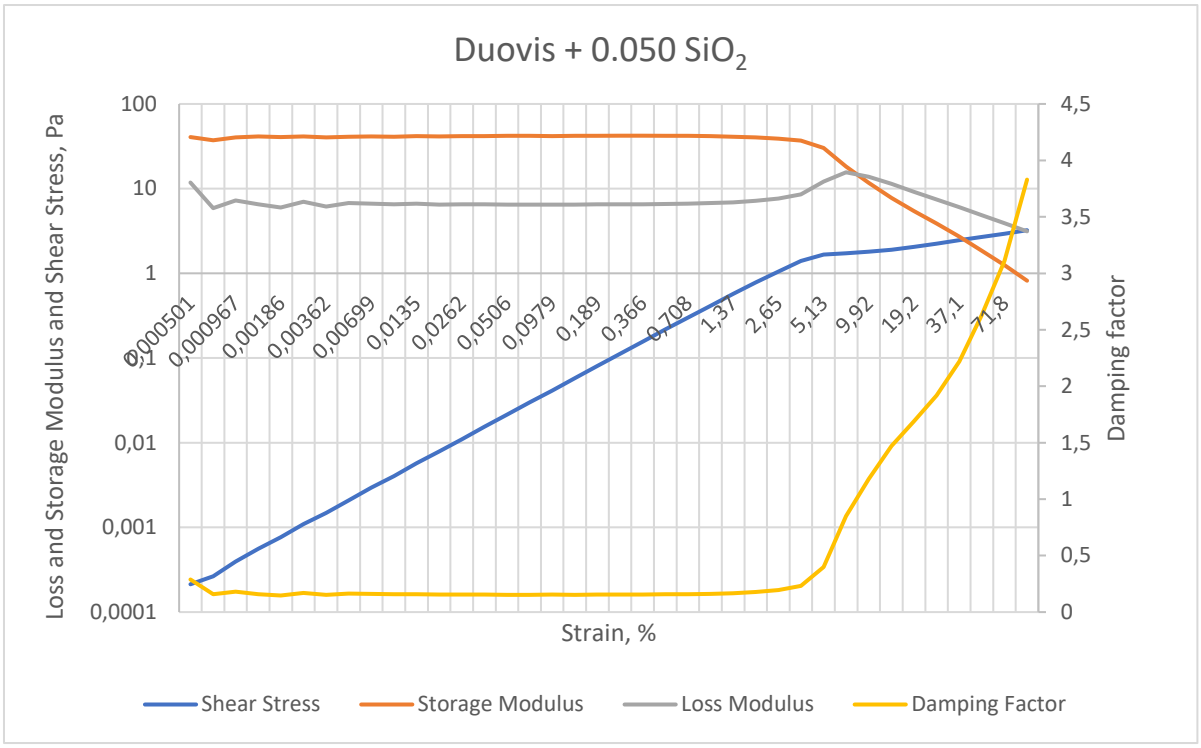

Figure 54 A diagram of amplitude sweep measurements for Ref Duovis + 0.050 SiO_2

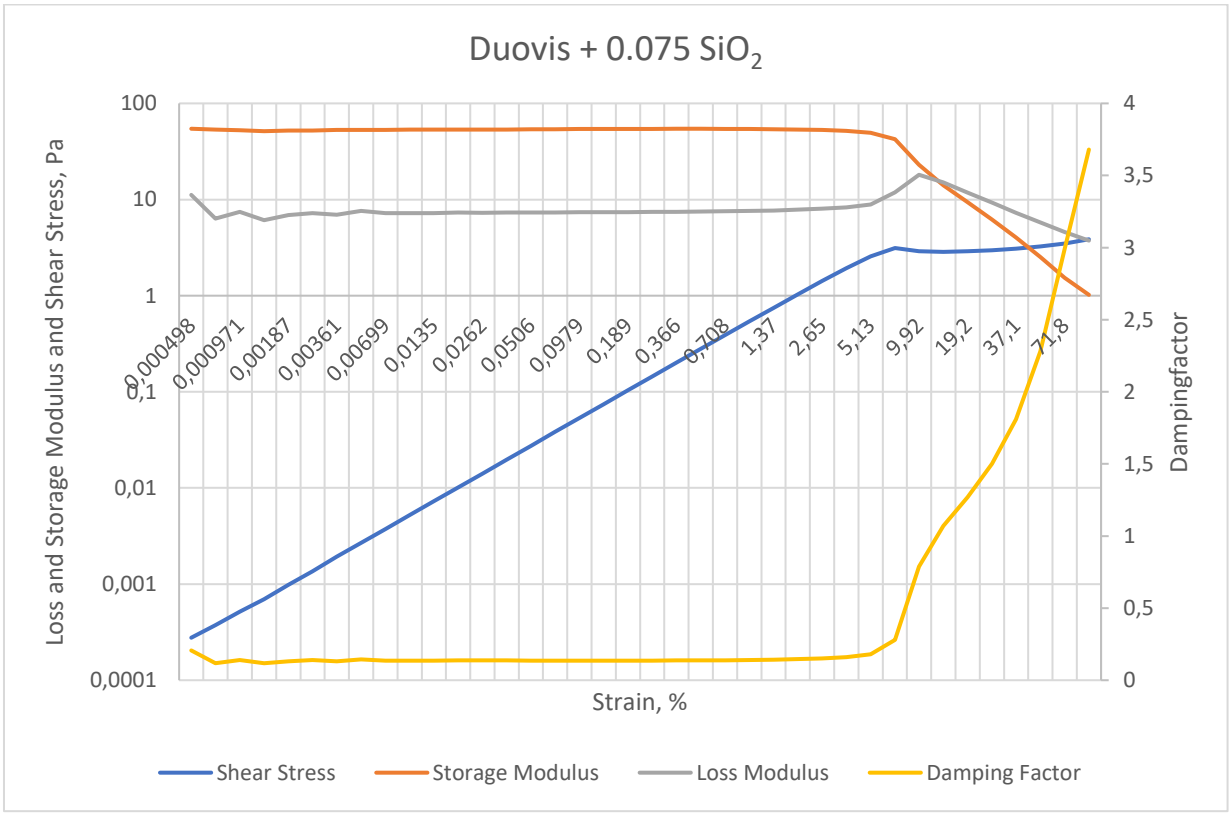

Figure 55 A diagram of amplitude sweep measurements for Ref Duovis + 0.075 SiO_2

APPENDIX B: SETUP FOR WELLPLAN AND WELLPATH

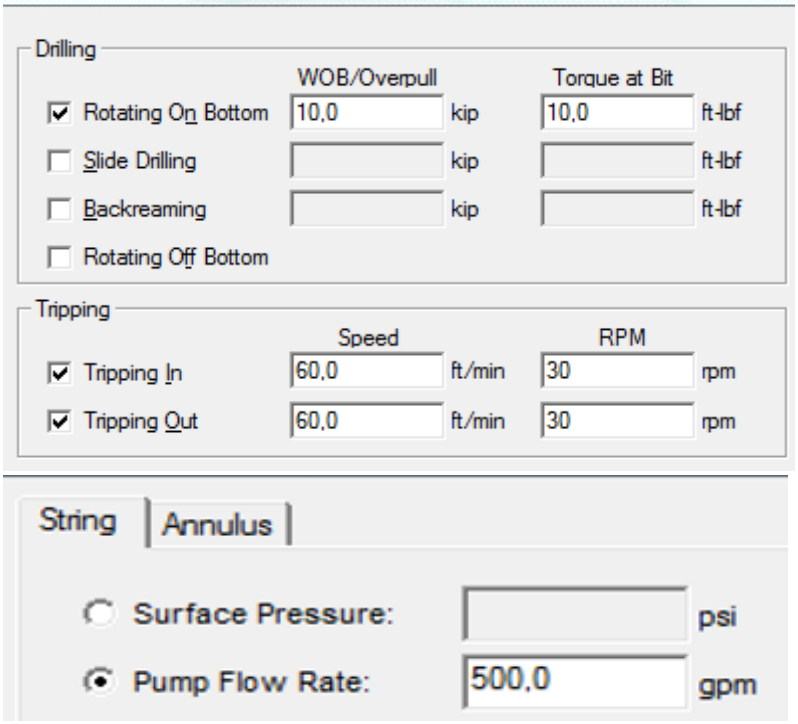

Figure 56 Pre-set parameters for the simulation setup

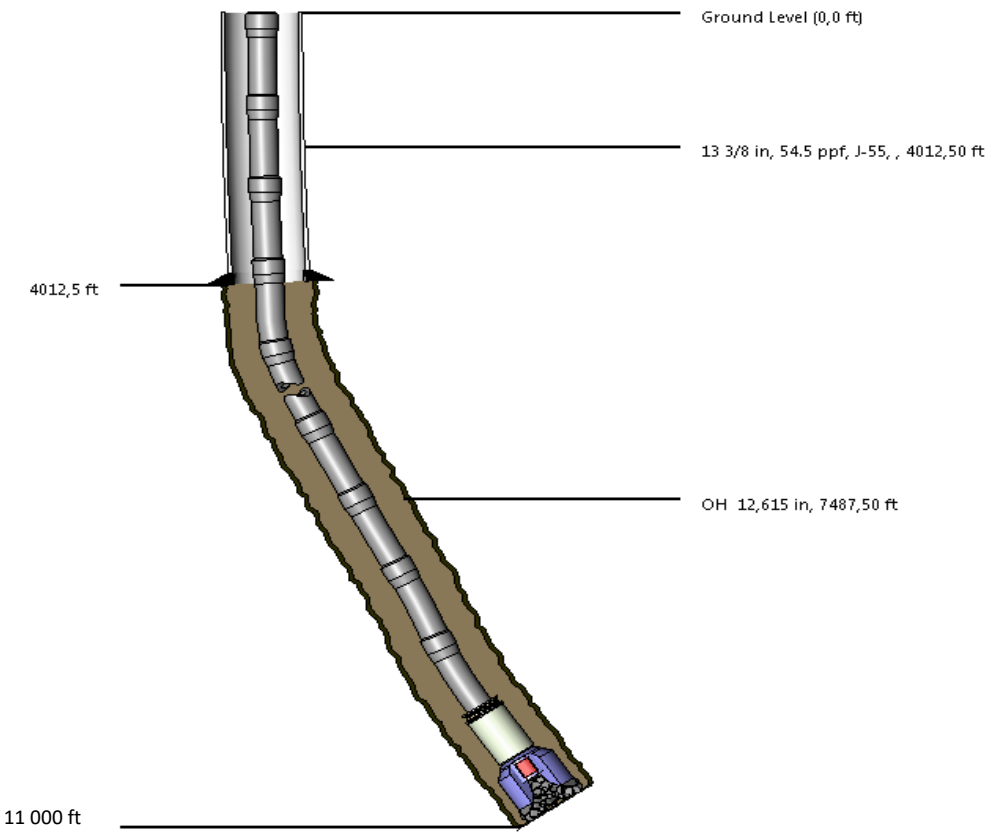

Figure 57 A graphical illustration of the well and drill string

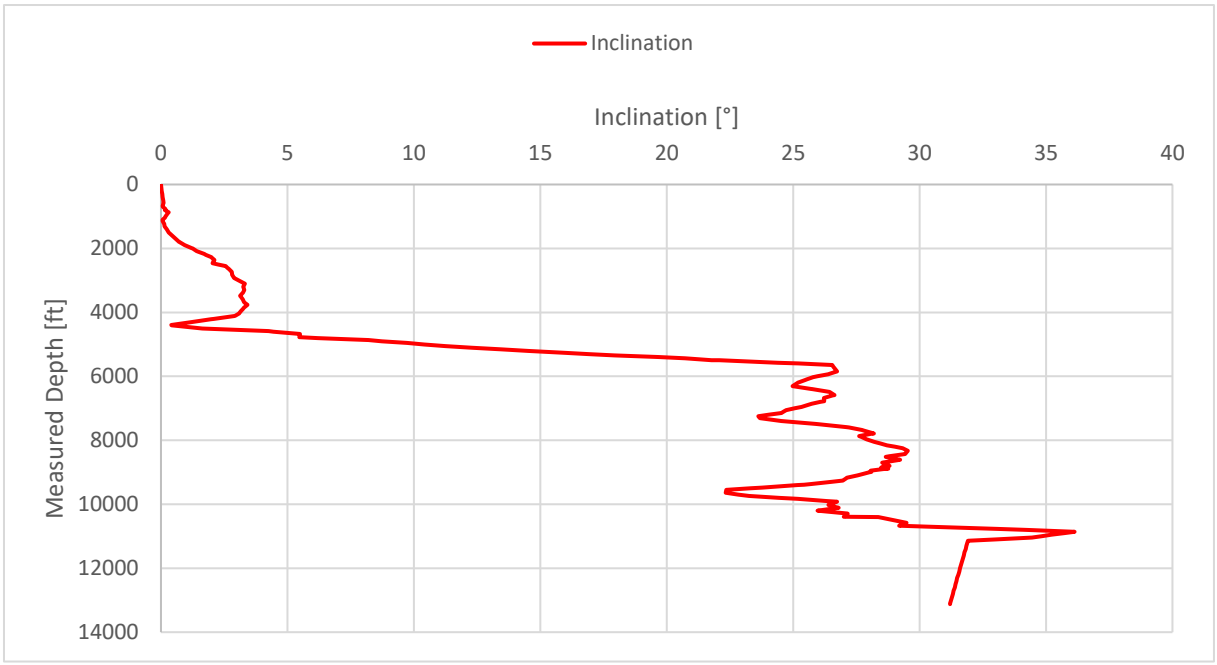

Figure 58 Inclination versus Measured Depth

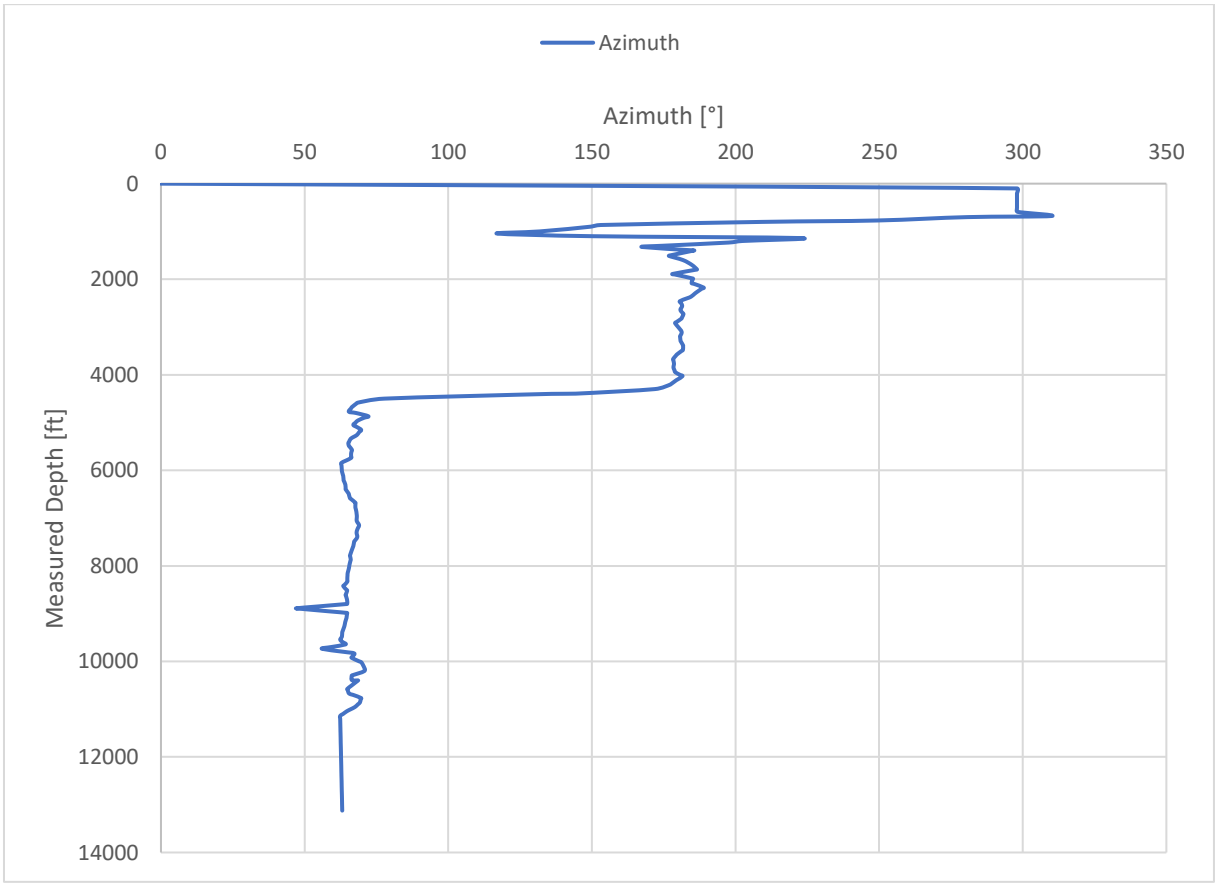

Figure 59 Azimuth versus Measured Depth

APPENDIX C: CORE FLOODING

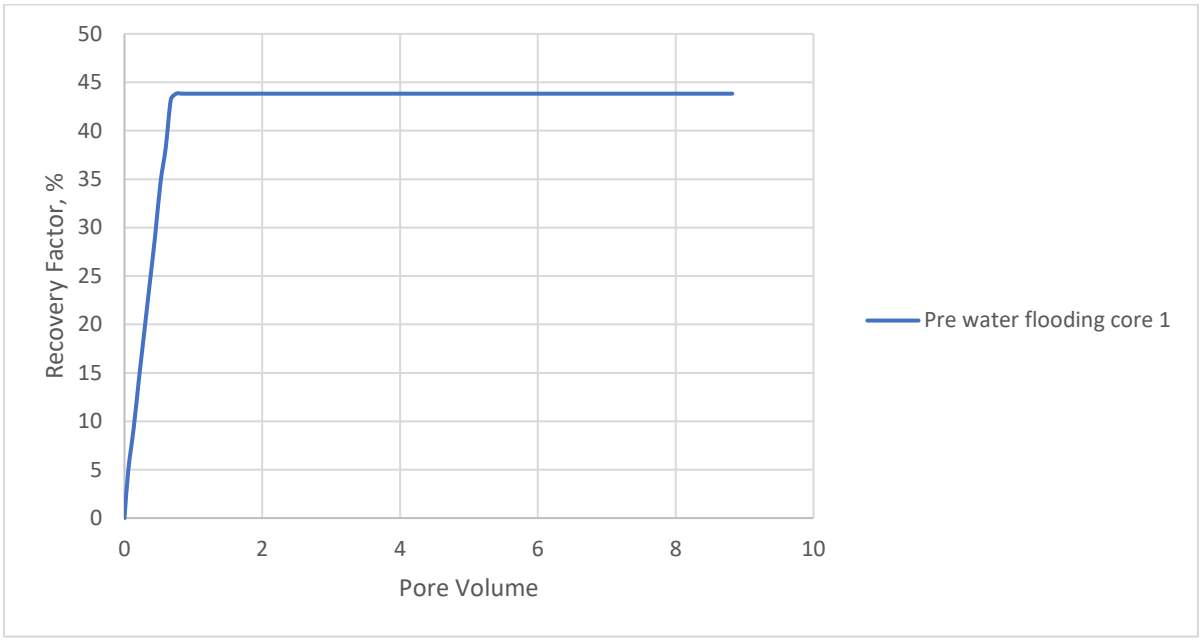

Figure 60 Recovery factor during pre-water flooding for core 1

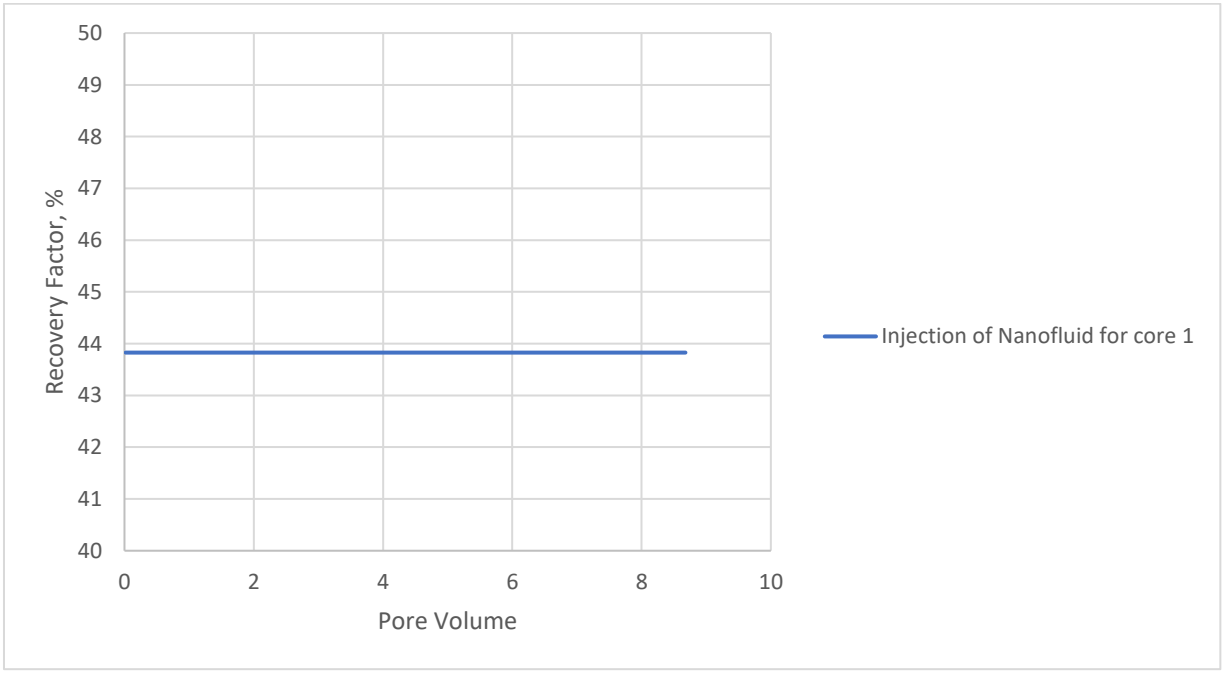

Figure 61 Recovery factor during injection of NF for core 1

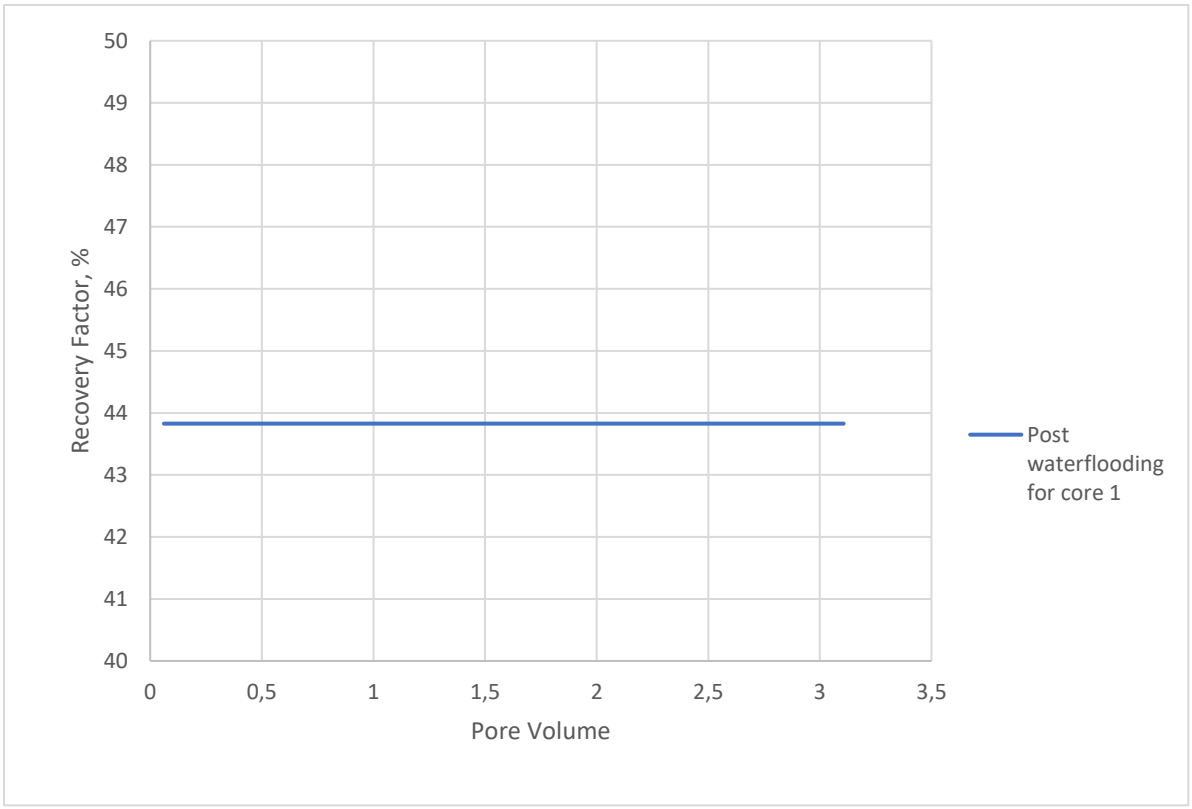

Figure 62 Recovery factor during post water flooding for core 1

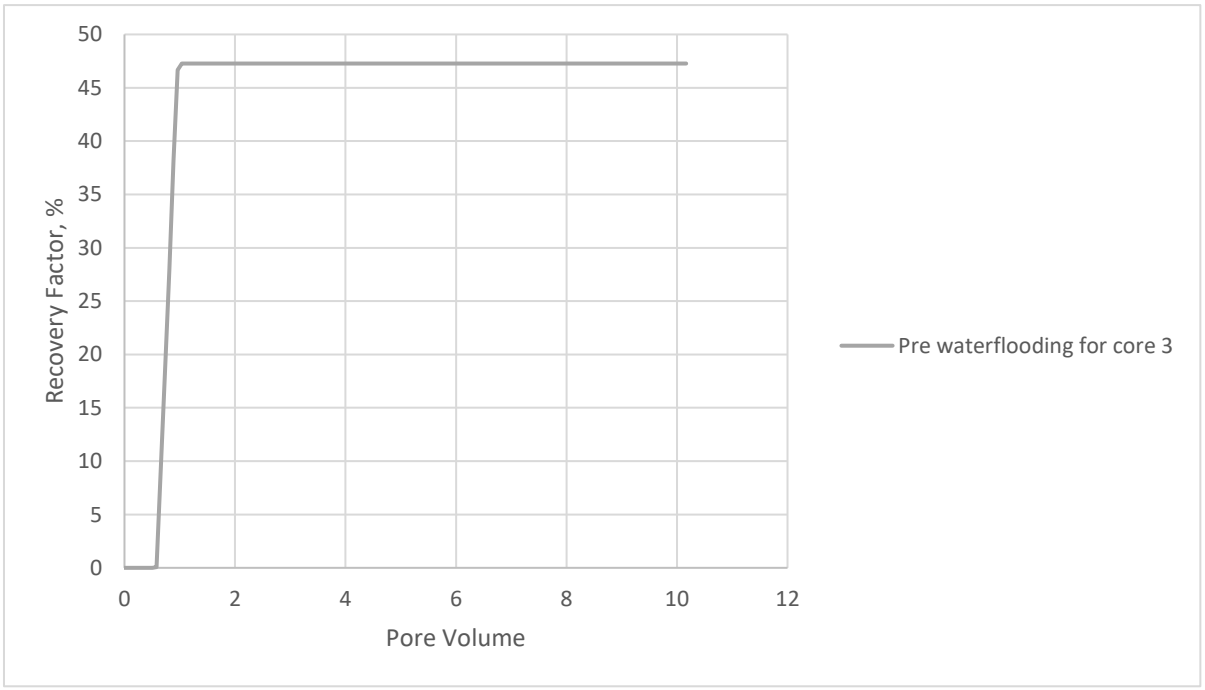

Figure 63 Recovery factor during pre-water flooding for core 3

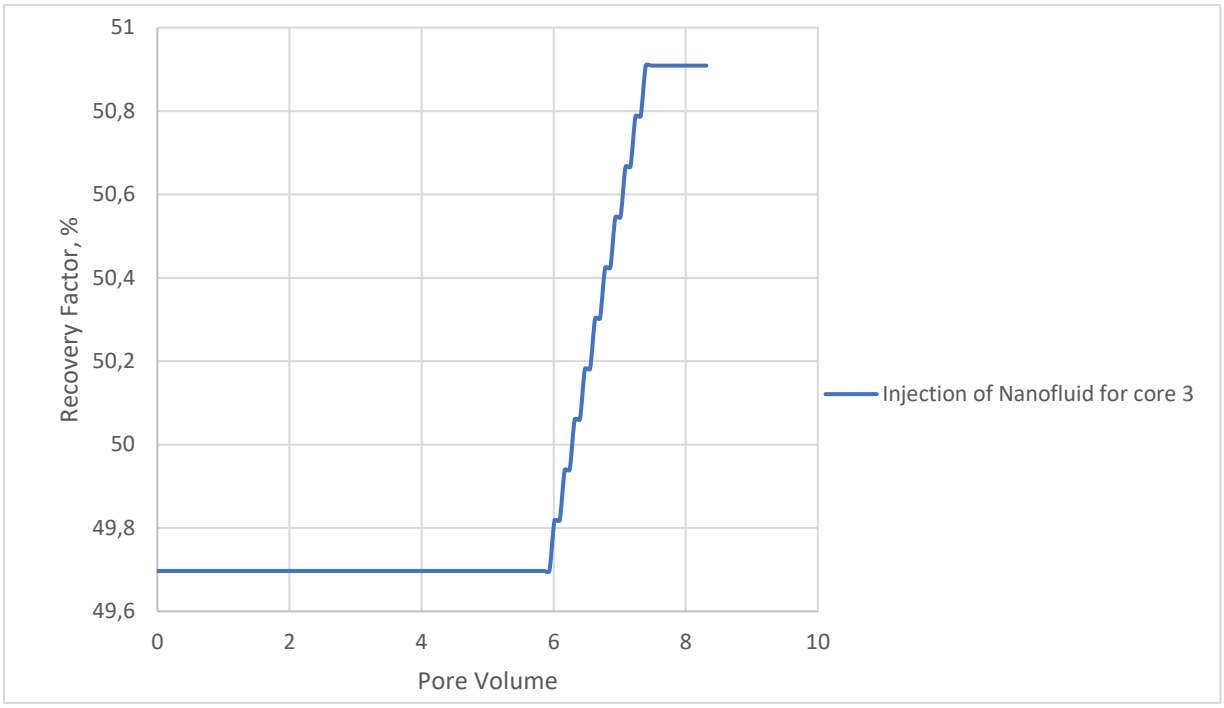

Figure 64 Recovery factor during injection of NF for core 3

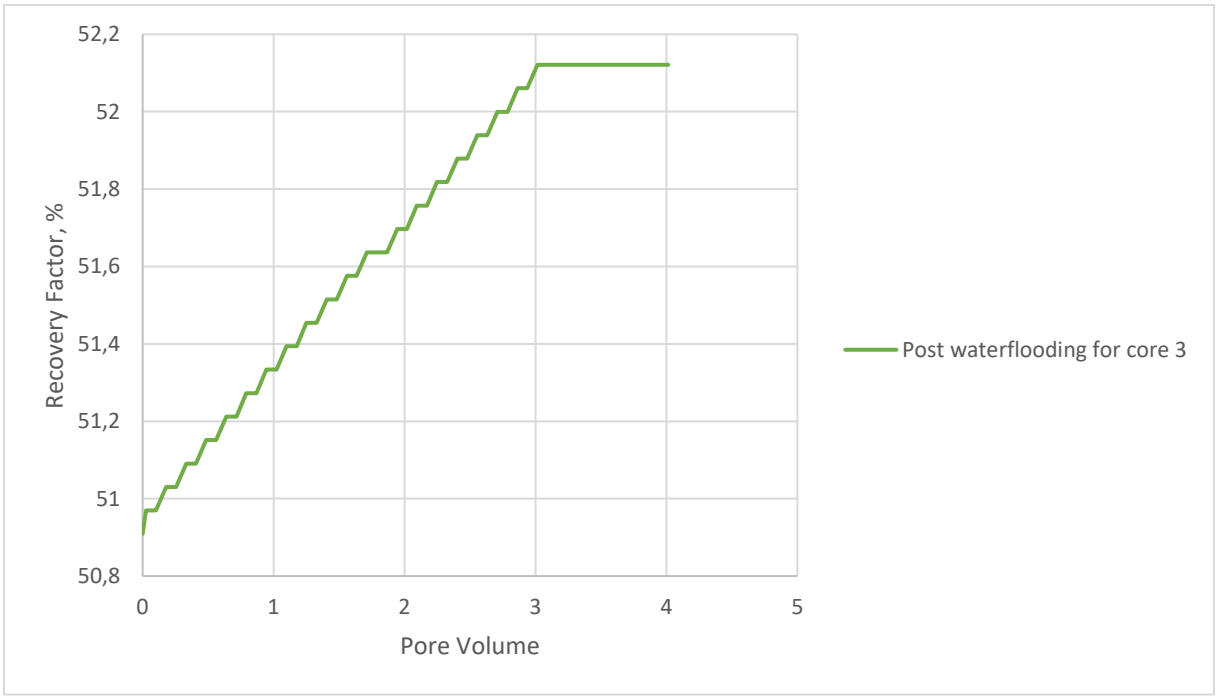

Figure 65 Recovery factor during post water flooding for core 3

APPENDIX D: CORRECTION FACTOR FOR TENSIOMETER

Parameter	Value
k	1,0246
density oil [g/ml]	0,73
density NF [g/ml]	1,025
r [cm]	0,0185
R [cm]	0,9549
U	11,9996

1) $\sigma = \sigma^* \cdot k \cdot F$

2) $F = \left[0{,}725 + sqrt\left(\frac{0{,}01452 \cdot \sigma^*}{\frac{U^2}{4} \cdot (\rho_2 - \rho_1)} + 0{,}04534 - \frac{1{,}679}{\frac{R}{r}}\right)\right] \cdot 1{,}07$

3) $U = 2 \cdot \pi \cdot (R_i + R_o) = 2 \cdot \pi \cdot (R + R) = 4 \cdot \pi \cdot R$

Figure 66 Equations for correction factor and the required parameters

Fluid System	σ*	F	σ
NF 0.15 wt.%	41,58	1,0582	45,0831199
NF 0.10 wt.%	40,78	1,0559	44,1227061
NF + 0.075 wt%	36,72	1,0444	39,2941687
NF + 0.050 wt%	40,18	1,0543	43,4043122
NF + 0.025 wt%	39,86	1,0534	43,0218425
Water + oil	42,28	1,0601	45,9258601

Table 20 A summary of the measured IFT values, and the corresponding corrected IFT

APPENDIX E: FANN VISCOMETER RESULTS

RPM	BF + 0.025g SiO2	BF + 0.050g SiO2	BF + 0.075g SiO2	Ref Duovis
600	29	30,5	29,5	28,5
300	23,5	24,5	23,5	22,5
200	21,5	22,5	21	19,5
100	17,5	18,5	16,5	16
60	15	16,5	14,5	14
30	13	14,5	12,5	12
6	10	10,5	9,5	9
3	8,5	9,5	8,5	8

Table 21 Data of viscometer for Duovis based DFs

RPM	BF + 0.025g SiO2	BF + 0.050g SiO2	BF + 0.075g SiO2	Ref CMC
600	14,6	15	14	17
300	9,7	10,7	9	12
200	7,9	8,3	8	10
100	6,3	6,1	5,5	8
60	5,1	5,6	4	6
30	3,8	4	3	4
6	2,7	3,2	2	3
3	2,1	2,8	1,5	2,8

Table 22 Data of viscometer for CMC based DFs

APPENDIX F: PHOTOS OF CORE FLOODING EXPERIMENTAL SETUP

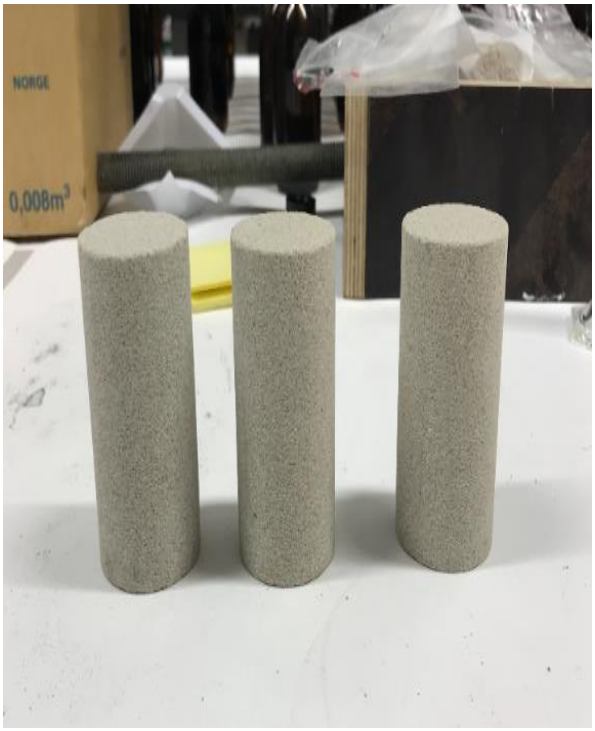

Figure 67 Three Berea Sandstone Core Plugs

Figure 68 A core within the corresponding core - sleeve

Figure 69 A Vacuum Pump

Figure 70 A camera to keep records of any oil production

Figure 71 The Setup for core flooding at IRIS

Figure 72 The core holder with the core inside of it

REFERENCES

[1] N. Petroleum, «Effective Resource Management in Mature Areas,» [Internett]. Available: https://www.norskpetroleum.no/en/developments-and-operations/resource-management-in-mature-areas/. [Funnet 6 April 2018].

[2] T. Smithson, «Schlumberger: HPHT Wells,» [Internett]. Available: https://www.slb.com/-/media/Files/resources/oilfield_review/defining_series/Defining-HPHT.pdf?la=en&hash=3FF8F894C76522C77D31DAF3B136B24371E7CCDC. [Funnet 18 April 2018].

[3] E. Boysen og N. Muir, Nanotechnology for Dummies, John Wiley & Sons, 2011.

[4] Schlumberger, «Primary Recovery,» [Internett]. Available: http://www.glossary.oilfield.slb.com/Terms/p/primary_recovery.aspx. [Funnet 13 April 2018].

[5] Schlumberger, «Secondary Recovery,» [Internett]. Available: http://www.glossary.oilfield.slb.com/Terms/s/secondary_recovery.aspx. [Funnet 13 April 2018].

[6] E. Gov., «Enhanced Oil Recovery,» [Internett]. Available: https://www.energy.gov/fe/science-innovation/oil-gas-research/enhanced-oil-recovery. [Funnet 15 February 2018].

[7] NPD, «NPD: Norwegian Continental Shelf,» [Internett]. Available: http://www.npd.no/en/Publications/Norwegian-Continental-Shelf/No-1-2017/Immobile-oil/. [Funnet 18 March 2018].

[8] «Petrowiki,» SPE, [Internett]. Available: http://petrowiki.org/Functions_of_drilling_fluid. [Funnet 2 March 2018].

[9] Petrowiki, «Drilling Fluids Types,» [Internett]. Available: http://petrowiki.org/Drilling_fluid_types. [Funnet 20 April 2018].

[10] Petrowiki, «Differential Pressure Pipe Sticking,» [Internett]. Available: http://petrowiki.org/Differential-pressure_pipe_sticking.. [Funnet 5 May 2018].

[11] Petrowiki, «Drilling Problems and Solutions,» [Internett]. Available: http://petrowiki.org/PEH:Drilling_Problems_and_Solutions. [Funnet 19 April 2018].

[12] U. i. Stavanger, Øvinger i Bore - og Brønnvæsker, Stavanger, 2015.

[13] O. Skjeggestad, Boreslamsteknologi, Alma Mater, 1989.

[14] Medium, «At what scale does complexity thrive, and why?,» [Internett]. Available: https://medium.com/@chuckfuller_49362/at-what-scales-does-complexity-thrive-and-why-2a9d0d9e349e.

[15] Nanogov., «What is Nanotechnology,» [Internett]. Available: http://www.nano.gov/nanotech-101/what/definition.

[16] A. Elgibaly, S. Saleh og M. Youssif, Silica nanofluid flooding for enhanced oil recovery in sandstone rocks, Egypt: Elsevier, 2016.

[17] N. Ogolo, O. Olafuyi og M. Onyekonwu, Silica nanofluid flooding for enhanced oil recovery in sandstone rocks, Nigeria: SPE, 2012.

[18] H. Yousefvand og A. Jafari, Enhanced Oil Recovery Using Polymer/nanosilica, Tehran: Elsevier, 2015.

[19] M. Tarek, Investigating Nano-Fluid Mixture Effects to Enhance Oil Recovery, Cairo: SPE, 2015.

[20] H. Ehtesabi, V. Taghikhani og H. Ghazanfari, Enhanced Heavy Oil Recovery in Sandstone Cores Using TiO2, Teheran: ACS Publications, 2013.

[21] O. Torsæter, L. Hendraningrat og S. Li, Improved Oil Recovery by Hydrophilic Silica Nanoparticles Suspension: 2 - Phase Flow Experimental Studies, IPTC, 2013.

[22] H. Bagherzadeh og A. Roustaei, Experimental investigation of SiO2 nanoparticles on enhanced oil, Tehran: Springer Link, 2015.

[23] A. Maghzi, S. Mohammadi, H. Ghazanfari og R. Kharrat, Monitoring wettability alteration by silica nanoparticles during water flooding, 2012.

[24] S. Iglauer, S. Wang, L. Maxim og S. Al-Anssari, Wettability alteration of oil-wet carbonate by silica nanofluid, Kensington: Elsevier, 2015.

[25] M. V. Ochoa, Analysis of Drilling Fluid Rheology and Tool Joint Effect to Reduce Errors in Hydraulics Calculations, Texas: PhD Dissertation, 2006.

[26] M. Belayneh, PET580 Advanced Well and Drilling Engineering compendium, UiS, 2018.

[27] T. Mezger, The Rheology Handbook, Hanover.

[28] S. Miska, A. Saasen og B. Bui, Viscoelastic Properties of Oil-Based Drilling Fluids, 2012.

[29] T. Sharman, «Characterization and Performance Study of OBM at Various Oil-Water Ratios,» Stavanger, MSc Uis, 2015.

[30] O. Torsæter og M. Abtahi, Experimental Reservoir Engineering - Laboratory Workbook.

[31] Schlumberger, «Permeability,» [Internett]. Available: http://www.glossary.oilfield.slb.com/Terms/p/permeability.aspx. [Funnet 13 April 2018].

[32] A. B. Zolotukhin og J. -. R. Ursin, Introduction to Petroleum Reservoir Engineering, Stavanger: Høyskoleforlaget, 1997.

[33] J. Forrest og F. Craig, The reservoir engineering aspects of waterflooding, Dallas: SPE, 1971.

[34] J. Fink , Petroleum Engineer`s Guide to Oil Field Chemicals and Fluids, Gulf Professional Publishing, 2011.

[35] A. Kutlic , I. Sobota og G. Bedekovic, Bentonite Processing Oplemenjivanje Bentonita, Zagreb, 2012.

[36] Schlumberger, «Duo - Vis,» [Internett]. Available: https://www.slb.com/-/media/Files/miswaco/ps-drilling-fluids/duo-vis.pdf?la=en&hash=63CD7F8B548B79D88492E0A261D36BABD2054480. [Funnet 30 March 2018].

[37] M. Manual, Drilling Fluids Engineering Manual, Polymer chemistry and Applications, 1998.

[38] M. Siqueira, G. Coelho, M. Moura og S. Hubinger, Evaluation of antimicrobial activity of silver nanoparticles for carboxymethylcellulose film applications in food packaging, Elsevier, 2014.

[39] «Sunray International: CMC,» [Internett]. Available: http://www.sunrayinternational.com/single_portfolio.php?p=67. [Funnet 14 March 2018].

[40] R. Caenn, H. Darley og G. Gray , Composition and properties of drilling and completion fluids, Gulf Professional Publishing, 2011.

[41] Inchem, «Potassium Chloride,» [Internett]. Available: http://www.inchem.org/documents/pims/pharm/potasscl.htm. [Funnet 23 February 2018].

[42] S. Farzad, Improved Waterfloding oil recovery from Carbonate reservoirs, Stavanger: PhD, Faculty of Science and Technology, University of Stavanger, 2012.

[43] Pubchem, «Decane,» [Internett]. Available: https://pubchem.ncbi.nlm.nih.gov/compound/15600#section=Top. [Funnet 28 April 018].

[44] R. Iler, The Chemistry of Silica, Wiley, 1979.

[45] S. Ayatollahi og M. Zerafat, Nanotechnology-assisted EOR techniques: New solutions to old challenges, Noordwijk: SPE, 2012.

[46] S. Van og B. Chon, Chemical flooding in heavy-oil reservoirs, Energies, 2016.

[47] X. Sun, Y. Zhang, G. Chen og Z. Gai, Application of Nanoparticles in Enhanced Oil Recovery: A Critical Review of Recent Progress, Qingdao: Energies, 2017.

[48] R. Shah, Application of nanoparticle saturated injectant gases for eor of heavy oils, SPE, 2009.

[49] P. Mcelfresh, C. Olugin og D. Ector, The application of nanoparticle dispersions to remove paraffin and, Los Angeles, 2012.

[50] R. Aveyard, B. Binks og J. Clint, Emulsions stabilized solely by colloidal particles, Hull: Elsevier, 2002.

[51] Wilson Center, «Opportunities and Challenges for Arctic oil and gas development,» [Internett]. Available: https://www.wilsoncenter.org/sites/default/files/Artic%20Report_F2.pdf. [Funnet 1 April 2018].

[52] L. Fernandez, E. Lara og E. Mitchell, Checklist, diversity and distribution of testate amoebae in Chile, Elsevier, 2015.

[53] I. Group, «CMC,» [Internett]. Available: http://www.irochemical.com/product/Mud-Drilling/CMC.htm. [Funnet 17 March 2018].